

APPENDIX G

**ADDITIONAL ANALYSIS AND VALIDATION OF THERMAL-MECHANICAL
EFFECTS ON FRACTURE PERMEABILITY
(RESPONSE TO RDTME 3.20, RDTME 3.21, AND GEN 1.01 (COMMENTS 83 AND 97))**

Note Regarding the Status of Supporting Technical Information

This document was prepared using the most current information available at the time of its development. This Technical Basis Document and its appendices providing Key Technical Issue Agreement responses that were prepared using preliminary or draft information reflect the status of the Yucca Mountain Project's scientific and design bases at the time of submittal. In some cases this involved the use of draft Analysis and Model Reports (AMRs) and other draft references whose contents may change with time. Information that evolves through subsequent revisions of the AMRs and other references will be reflected in the License Application (LA) as the approved analyses of record at the time of LA submittal. Consequently, the Project will not routinely update either this Technical Basis Document or its Key Technical Issue Agreement appendices to reflect changes in the supporting references prior to submittal of the LA.

APPENDIX G

ADDITIONAL ANALYSIS AND VALIDATION OF THERMAL-MECHANICAL EFFECTS ON FRACTURE PERMEABILITY (RESPONSE TO RDTME 3.20, RDTME 3.21, AND GEN 1.01 (COMMENTS 83 AND 97))

This appendix provides responses for Key Technical Issue (KTI) agreements Repository Design and Thermal-Mechanical Effects (RDTME) 3.20, RDTME 3.21, and General Agreement (GEN) 1.01 (Comments 83 and 97). These agreements are concerned with providing analyses related to thermal-mechanical effects on fracture permeability.

G.1 KEY TECHNICAL ISSUE AGREEMENTS

G.1.1 RDTME 3.20, RDTME 3.21, and GEN 1.01 (Comments 83 and 97)

Agreements RDTME 3.20 and RDTME 3.21 were reached during the U.S. Nuclear Regulatory Commission (NRC)/U.S. Department of Energy (DOE) Technical Exchange and Management Meeting on Repository Design and Thermal-Mechanical Effects (Reamer 2001a) February 6 to 8, 2001, in Las Vegas, Nevada. RDTME Subissues 1, 2, 3 and 4 were discussed at that meeting. RDTME 3.20 and RDTME 3.21 were discussed under Subissue 3, Thermal-Mechanical Effects on Underground Facility Design and Performance.

There are two items from agreement GEN 1.01 related to these KTI agreements. GEN 1.01 was reached during the NRC/DOE Technical Exchange and Management Meeting on Range of Thermal Operating Temperatures, held September 18 to 19, 2001. At that meeting, the NRC provided additional comments (Comments 83 and 97) relating to RDTME 3.20, and the DOE provided an initial response to those comments (Reamer 2001b).

The wording of the agreements is as follows:

RDTME 3.20¹

Provide the sensitivity analyses including the effects of boundary conditions, coefficient of thermal expansion, fracture distributions, rock mass and fracture properties, and drift degradation (from Subissue 3, Component 3, Slide 39). The DOE will provide sensitivity analyses of thermal-mechanical effects on fracture permeability, including the effects of boundary conditions, coefficient of thermal expansion, fracture distributions, rock mass and fracture properties, and drift degradation. This will be provided consistent with site data and integrated with appropriate models in a future revision to the Coupled Thermal Hydrologic Mechanical Effects on Permeability, ANL-NBS-HS-000037, and is expected to be available to NRC in FY 2003.

¹Slide 39, referenced in the first sentence of this agreement, lists the following sensitivity analyses that were under consideration to evaluate thermal-mechanical effects on hydrologic properties (Bodvarsson et al. 2001): boundary conditions; coefficient of thermal expansion; fracture distributions; rock properties; and drift degradation. In agreement RDTME 3.20, the DOE agreed to provide these sensitivity analyses.

RDTME 3.21²

Provide the results of additional validation analysis of field tests (from Subissue 3, Component 3, Slide 39). The DOE will provide the results of additional validation analysis of field tests related to the thermal-mechanical effects on fracture permeability in a future revision to the Coupled Thermal Hydrologic Mechanical Effects on Permeability, ANL-NBS-HS-000037, and is expected to be available to NRC in FY 2003.

GEN 1.01 (Comment 83)³

More comments on the abstraction of uncertainty:

Page 4-58: It appears that the different conceptual models or analytical techniques are the biggest source of uncertainty, but it isn't discussed in the summary.

Page 4-62: "However, because the initial water and gas compositions are only known approximately, and their spatial distributions unknown, a quantitative evaluation of the uncertainties associated with the predictions are not feasible. Yet the range of predicted and measured compositions in the drift-scale test for waters that may potentially seep into drifts are not extremely great and the model results generally capture this range." These two sentences do not appear to be consistent. If a quantitative evaluation of uncertainties is not feasible, how can one have confidence in the predicted ranges?

Page 4-65: "This localized permeability reduction tends to cause some additional flow focusing, but the changes are considerably less than the initial range in permeability." This is another example of a problem area mentioned previously. In addition, local arguments such as this can't be made in an integrated system.

Page 4-86: "The HTOM case predicted a decrease of 6 orders of magnitude in permeability for most vertical fractures during the period from 55 yrs to more than 1,000 yrs after emplacement." It is not obvious how this amount of change would be included in the original distribution of permeability.

DOE Initial Response to GEN 1.01 (Comment 83)

See comment 106 for uncertainties in THC models. RDTME agreement 3.20 will address reconciliation of the differences in THM simulations using the discrete fracture model (3DEC) and the continuum model (TOUGH-FLAC). Preliminary evaluations indicate that the discrepancies may be associated with the manner in which displacements are treated in the two models.

²Slide 39, referenced in the first sentence of this agreement, lists additional validation analyses of field tests that were under consideration to evaluate thermal-mechanical effects on hydrologic properties (Bodvarsson et al. 2001): measured temperatures; additional fractures; and analysis of multipoint borehole extensometer data. In agreement RDTME 3.21, DOE agreed to provide these validation analyses.

³Page numbers refer to *FY01 Supplemental Science and Performance Analyses, Volume 1: Scientific Bases and Analyses* (BSC 2001a).

GEN 1.01 (Comment 97)⁴

Page 4-97: “There are apparent contradictory results at the drift wall: there is an increase in permeability in the distinct element analysis, but there is a decrease in permeability in the continuum analysis.” This appears to be the area of the problem that one should be most concerned about, due to the influence on seepage.”

DOE Initial Response to GEN 1.01 (Comment 97)

RDTME agreement 3.20 will address reconciliation of the differences in THM simulations using the discrete fracture model (3DEC) and the continuum model (TOUGH-FLAC). Preliminary evaluations indicate that the discrepancies may be associated with the manner in which displacements are treated in the two models.

G.1.2 Related Key Technical Issues

GEN 1.01 (Comment 106) is related in that it pertains to uncertainties in the thermal-hydrologic-chemical models. This agreement is to be addressed in a separate technical basis document dealing with unsaturated zone flow.

G.2 RELEVANCE TO REPOSITORY PERFORMANCE

The heat generated by the decay of radioactive waste results in elevated rock temperatures for thousands of years after waste emplacement. Depending on the thermal load, these temperatures are high enough to cause boiling conditions in the rock, resulting in water redistribution and altered flow paths. These temperatures will also cause thermal expansion of the rock, with the potential of opening or closing fractures and, thus, changing fracture permeability in the near field. Understanding the thermal-hydrologic-mechanical coupled processes is important for the performance of the repository because the thermally induced permeability changes potentially affect the spatial distribution of percolation flux in the vicinity of the drift and, hence, the seepage of water into the drift.

The potential impact of coupled thermal-hydrologic-mechanical processes on the seepage of water into a repository drift is assessed in *Abstraction of Drift Seepage* (BSC 2004a), which provides seepage-relevant parameters and their probability distribution for use in the total system performance assessment (TSPA). The analyses have shown that thermal-mechanical effects on hydrologic properties are so small that they can be neglected in the seepage abstraction (BSC 2004a, Section 8). The NRC was concerned that the analysis did not consider potential increase in the aperture of subhorizontal fractures in pillars between drifts (NRC 2002). The DOE agrees to complete sensitivity analyses and additional validation analyses of field tests to address the NRC concerns, thereby strengthening the technical basis for neglecting thermal-mechanical effects on fracture permeability. These issues relate to unsaturated zone flow and seepage in total system performance assessment (TSPA) models.

⁴Page number refers to *FY01 Supplemental Science and Performance Analyses, Volume 1: Scientific Bases and Analyses* (BSC 2001a).

G.3 RESPONSE

At the DOE/NRC Technical Exchange and Management Meeting on Repository Design and Thermal-Mechanical Effects in February 2001, several issues and concerns were discussed under Component 3 (Thermal Effects on Flow into Emplacement Drifts). These included: (1) the technical basis for parameters used to assess thermal-mechanical effects on hydrologic properties, (2) alternative conceptual models to assess effects of changes in rock mass hydrologic properties, (3) potential diversion of fluid flow from the pillar region toward the drift, and (4) consideration of drift collapse in seepage. To address these issues and concerns, it was agreed that the DOE should provide a sensitivity analysis, including the effects of boundary conditions, coefficient of thermal expansion, fracture distributions, rock properties, and drift degradation (RDTME 3.20). Furthermore, it was agreed that the DOE should provide additional validation analysis of thermal-mechanical effects on fracture permeability against field tests (RDTME 3.21). Since agreements RDTME 3.20 and RDTME 3.21 were made in February 2001, significant additional work has been performed and documented in other model reports that address issues related to RDTME 3.20 and RDTME 3.21.

The two items from agreement GEN 1.01 (Comments 83 and 97) are related to an apparent contradiction in the results of two thermal-hydrologic-mechanical analyses (a distinct element analysis and a continuum analysis) presented in *FY01 Supplemental Science and Performance Analyses, Volume 1: Scientific Bases and Analyses* (BSC 2001a, Section 4.3.7). The magnitude of the estimated permeability changes appeared to be quite different in the two analyses. As discussed below, the apparent contradictory results between the two analyses are partly caused by a misconception stemming from a comparison of two contour plots showing two different parameters. Furthermore, the apparent discrepancy is also partly caused by an unrealistic relationship between normal stress and permeability of fractures adopted in the distinct element analysis.

Detailed responses for RDTME 3.20, RDTME 3.21, GEN 1.01 (Comment 83), and GEN 1.01 (Comment 97) are given in Sections G.3.1, G.3.2, G.3.3, and G.3.4, respectively. The technical basis for these responses is provided in Section G.4.

G.3.1 RDTME 3.20: Sensitivity Analysis

Sensitivity analyses have been performed, and concerns about boundary conditions and flow diversion from the pillar region toward the drift have been resolved as a result of recent revisions and enhancements to the coupled thermal-hydrologic-mechanical-process analysis at Yucca Mountain (Sections G.4.1 and G.4.2).

A bounding analysis was conducted that brackets the potential impact of thermal-hydrologic-mechanical processes on permeability and the flow field. The bounding case is realized by adopting parameter values that maximize the effect of coupling. This includes a bounding estimate of the thermal expansion coefficient (leading to the maximum possible thermal stress) and a bounding estimate of a stress-versus-permeability function (leading to maximum possible permeability change). In addition, the results of thermal-hydrologic-mechanical analyses with maximum effect of coupling are compared to thermal-hydrologic analyses with no effect of thermal-hydrologic-mechanical coupling. Thus, the current analysis covers the entire sensitivity

range, from minimum to maximum effect of thermal-hydrologic-mechanical coupling. The appropriateness of the adopted conceptual fracture model and in situ rock properties have been tested and confirmed through extensive validation, in particular against measurements at the Drift Scale Test (DST) (BSC 2004b, Section 7). The impact of drift degradation on permeability has been analyzed for several scenarios, including bounding scenarios from an intact to a completely collapsed drift (BSC 2004b, Section 6.8). The bounding analysis shows that effects of thermal-mechanically-induced changes in permeability on the unsaturated zone flow field are small and observable only near the emplacement drifts. The predicted changes in permeability (1 to 2 orders of magnitude) are within the permeability range (4 orders of magnitude) already considered in the seepage analysis (BSC 2003a, Figure 6-4).

G.3.2 RDTME 3.21: Additional Validation Analysis of Field Tests

The additional agreed-upon validation has been conducted for recent revisions to and enhancements of the coupled thermal-hydrologic-mechanical process analysis at Yucca Mountain (BSC 2004b, Section 7) in a comprehensive manner (Section G.4.3). Validation in this report includes comparison to measured temperatures, displacements, and air-permeability changes at the DST, comparison to permeability changes around excavated drifts, comparison to observed side-wall fracturing in the ECRB Cross-Drift, and comparison to an alternative conceptual model. Further validation is provided through multiple lines of evidence from other similar heater tests, from geothermal fields, and by comparison to other models in an international code comparison project (DECOVALEX). The model and the analysis have also been published in several international journals, undergoing scientific peer-review of the adopted concepts. The comprehensive model validation provided in *Drift Scale THM Model* (BSC 2004b, Section 7) shows that the current coupled thermal-hydrologic-mechanical models developed for the repository at Yucca Mountain can capture relevant thermal-hydrologic-mechanical processes and that the underlying conceptual model is sound.

G.3.3 GEN 1.01 (Comment 83): Comparison of Distinct Element and Continuum Modeling Analysis

The 6-order-of-magnitude decrease in fracture permeability calculated from the earlier distinct element analysis (BSC 2001b, Section 6.3.3) is an artifact of an unsubstantiated assumed relationship between normal stress and fracture permeability (Section G.4.4). The relationship between normal stress and fracture permeability adopted for the distinct element analysis resulted in overstating the fracture permeability because it did not consider residual fracture permeability at high fracture normal stress. Current estimates, using an alternative continuum analysis with consideration of residual fracture permeability, shows that permeability will not decrease by more than 2 orders of magnitude and is unlikely to decrease by more than 1 order of magnitude (BSC 2004b, Sections 6 and 8). These model estimates are well established through model validation against permeability measurements at the DST. Using a consistent relationship of normal stress versus fracture permeability in both the distinct element analysis and continuum analysis, the magnitude of calculated changes in permeability would be similar. If the same residual permeability was assigned as input to both analyses, the same maximum decrease in permeability would be obtained in both analyses. For example, if a residual permeability correction factor of 0.1 is assigned to the normal stress versus fracture permeability function, the permeability cannot decrease below a factor of 0.1 of the original permeability in both analyses. A 6 order-of-

magnitude decrease in permeability would not be possible. Calculated changes in permeability in such analyses can be provided to the seepage models, where they can be factored in as changes in mean permeability into the original permeability distribution for evaluation of the impact on liquid flow distribution and drift seepage (BSC 2004a). However, as mentioned in Section G.3.1, the current estimates of thermal-mechanically-induced permeability changes (1 to 2 orders of magnitude) are within the permeability range (4 orders of magnitude) already considered in the seepage analysis (BSC 2003a, Figure 6-4).

G.3.4 GEN 1.01 (Comment 97): Comparison of Distinct Element and Continuum Modeling Analysis

The apparent contradictory result between the distinct element analysis and continuum analysis regarding calculated permeability at the drift wall is partly caused by a misconception stemming from a comparison of contour plots for two different parameters (see Section G.4.5). The apparent disagreement was observed by comparing the permeability ratio at 55 years in the distinct element analysis (BSC 2001a, Figure 4.3.7-1) with the permeability changes at 10 and 1,000 years in the continuum analysis (BSC 2001a, Figures 4.3.7-12 to 4.3.7-15). However, the comparison of these figures is not very clear, because the figures are at different scales and do not show the same parameters. One figure (BSC 2001a, Figure 4.3.7-1) shows an overall mean permeability change, while others (BSC 2001a, Figures 4.3.7-12 to 4.3.7-15) show changes partitioned as permeability in horizontal and vertical fractures. A closer examination of consistent output parameters (i.e., changes in horizontal and vertical fracture permeability) shows that, in fact, the distinct element and continuum analyses produce consistent results (Section G.4.5). On top of the drift, which is the most relevant area for drift seepage, both the distinct element analysis and the continuum analysis show that vertical permeability decreases, whereas horizontal permeability increases. A decreased vertical permeability just above the drift tends to reduce vertical gravity-driven liquid water flow and, thereby, tends to prevent water from reaching the top of the open drift, which, in turn, reduces the potential for seepage (BSC 2003a, Section 6.7). A simultaneous increased horizontal permeability just above the drift tends to facilitate diversion of liquid fluid flow around the drift (see Section G.4.5). Using the consistent relationship between normal stress and permeability of fractures in both the distinct element analysis and continuum analysis, the magnitude of calculated changes in permeability is similar. If the same residual permeability was assigned as input to both analyses, the same maximum decrease in permeability would be obtained in both analyses. For example, if a residual permeability correction factor of 0.1 is assigned to the normal stress versus fracture permeability function, the permeability cannot decrease below a factor of 0.1 of the original permeability in both analyses. A 6 order-of-magnitude decrease in permeability would not be possible. The only exception would be for a case in which a mechanical failure at the drift wall would form a loose rock block that could slide and create an additional local permeability change in the distinct element analysis.

The information in this report is responsive to agreements RDTME 3.20, RDTME 3.21, and GEN 1.01 (Comments 83 and 97) made between DOE and NRC. The report contains the information that DOE considers necessary for NRC review for closure of these agreements.

G.4 BASIS FOR THE RESPONSE

G.4.1 Revisions and Enhancement of Coupled Thermal-Hydrologic-Mechanical Modeling since 2001

Since agreements RDTME 3.20, RDTME 3.21, and GEN 1.01 were made in 2001, the analysis and understanding of coupled thermal-hydrologic-mechanical processes at Yucca Mountain have been substantially improved through new alternative modeling approaches, improved and extended predictive analyses, and extensive model validation. Model validations against the DST have been particularly important for making a bounding estimate of permeability changes at the Yucca Mountain repository induced by thermal-mechanical processes.

In *FY01 Supplemental Science and Performance Analyses, Volume 1: Scientific Bases and Analyses* (BSC 2001a), predictions of coupled thermal-hydrologic-mechanical processes and their impacts on permeability and flow fields were calculated both at drift scale (Section 4.3.7) and at mountain scale (Section 3.3.7). In this document, results from two alternative models were presented: (1) results from a distinct element analysis extracted from *Coupled Thermal-Hydrologic-Mechanical Effects on Permeability Analysis and Models Report* (BSC 2001b) and (2) results from an alternative fully coupled thermal-hydrologic-mechanical continuum analysis.

In the distinct element analysis, a fracture network that consisted of three fracture sets was modeled with orientations based on the fracture statistics from fracture surveys in the ESF. The analysis gave changes in fracture aperture caused by thermally induced changes in the stress field. The local changes in fracture permeability were estimated based on calculated changes in fracture apertures in the fracture network. While this analysis correctly predicted the regions around the drift where the permeability would increase or decrease, the magnitude of the relative change in permeability was generally overestimated. In particular, estimated decreases in permeability caused by thermal-mechanical-induced fracture closure were substantially overestimated, with decreases in permeability as high as 6 orders of magnitude. The distinct element model was validated against thermal and mechanical measurements in the DST and the large block test. However, no validation against observed changes in fracture permeability induced by thermal-mechanical processes was performed. At the time, data for only the first 18 months of heating in the DST were available for model validation. Furthermore, the distinct element model of the DST included only major fractures, and it was not possible to evaluate permeability changes in the hydraulically conducting fracture network between those major fractures.

The alternative fully coupled thermal-hydrologic-mechanical continuum analysis was presented for the first time in *FY01 Supplemental Science and Performance Analyses, Volume 1: Scientific Bases and Analyses* (BSC 2001a, Sections 3.3.7 and 4.3.7). It was based on a newly developed code, TOUGH-FLAC, for coupled thermal-hydrologic-mechanical analysis under multiphase flow conditions (Rutqvist, Wu et al. 2002). In this analysis, calculated changes in permeability were also based on changes in stress normal to three fracture sets. However, in this analysis, the relationship between normal stress and permeability of fractures was determined based on field experiments at Yucca Mountain. Several niche excavation experiments showed that permeability would increase by about 1 order of magnitude in a zone just above the excavation. Furthermore, results from air-permeability measurements at the DST showed that, during heating of the rock mass, the permeability decreased by about 1 order of magnitude as a result of thermally induced

coupled processes. The measured increase in permeability during excavation at the niche experiments and the measured decrease during heating at the DST permit constraining the relationship between fracture normal stress and fracture permeability. A lower bound for maximum permeability decrease (minimum value of k/k_i where k is permeability and k_i is the initial permeability) is provided by the fact that rock fractures do not close completely for water flow even at very high normal stress across the fracture. In numerous laboratory and field experiments, it has been shown that even when the fracture appears to be completely closed at high normal stress, a residual hydraulic aperture still allows water flow along the fracture (Rutqvist and Stephansson 2003, p.15). The results of the alternative coupled thermal-hydrologic-mechanical continuum analysis showed that thermal-mechanical-induced changes in permeability for both the drift scale and mountain scale were less than 2 orders of magnitude and that the impact of those changes on the flow field was small.

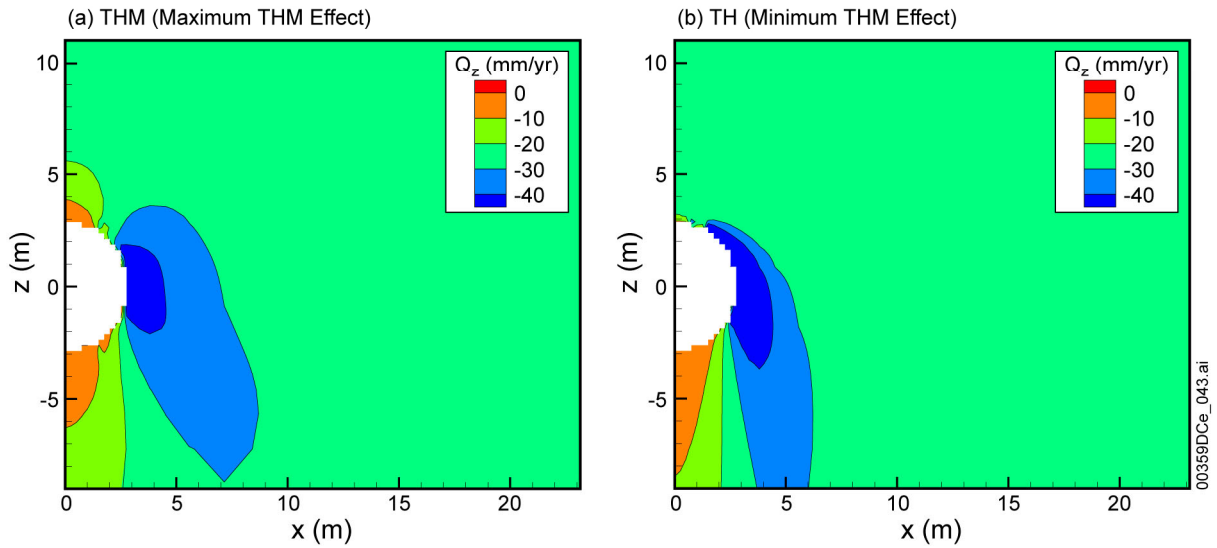
Based on *Coupled Thermal-Hydrologic-Mechanical Effects on Permeability Analysis and Models Report* (BSC 2001b) and *FY01 Supplemental Science and Performance Analyses, Volume I: Scientific Bases and Analyses* (BSC 2001a, Sections 3.3.7 and 4.3.7), the fully coupled thermal-hydrologic-mechanical continuum approach has been further developed and documented in *Drift Scale THM Model* (BSC 2004b) and *Mountain-Scale Coupled Processes (TH/THC/THM)* (BSC 2004c, Section 6.5).

Drift Scale THM Model (BSC 2004b) contains improved and extended analysis of coupled thermal-hydrologic-mechanical processes for a drift located both in the Topopah Spring Tuff middle nonlithophysal unit (Ttptmn) and the Topopah Spring Tuff lower lithophysal unit (Ttptll). Furthermore, a comprehensive model validation has been performed, specifically against measurements of coupled thermal-hydrologic-mechanical responses at the DST. The continuum drift-scale thermal-hydrologic-mechanical model is able to simulate thermal-hydrologic-mechanical responses at the DST, including temperature, water saturation, mechanical displacement, and changes in air permeability. A good agreement between simulated and measured changes in air permeability at the DST has been crucial for validation of the adopted relationship between fracture normal stress and permeability that is applied in the predictive analysis. In the predictive analysis, potential changes in fracture permeability at Yucca Mountain are bounded by adopting parameter values that maximize the effect of stress on permeability. Using the bounding estimates that maximize changes in permeability, the impact on the flow field is also evaluated. In addition, potential changes in rock permeability around a completely collapsed drift are evaluated in the *Drift Scale THM Model* (BSC 2004b, Section 6.8) based on recent results in the *Drift Degradation Analysis* (BSC 2004d). The *Mountain-Scale Coupled Processes (TH/THC/THM)* (BSC 2004c, Section 6.5) evaluates potential changes in mountain-scale hydrologic properties and their impact on mountain-scale flow distribution. This includes potential changes in hydraulic properties caused by shear along preexisting faults and fractures near the ground surface.

The above discussion is an overview of the work conducted since agreements RDTME 3.20, RDTME 3.21, and GEN 1.01 (Comments 83 and 97) were made in 2001. Sections G.4.2 to G.4.5 give the scientific basis for the responses to these agreements. The scientific basis is drawn from the available information in the above-mentioned revisions of the work related to coupled thermal-hydrologic-mechanical processes at the Yucca Mountain.

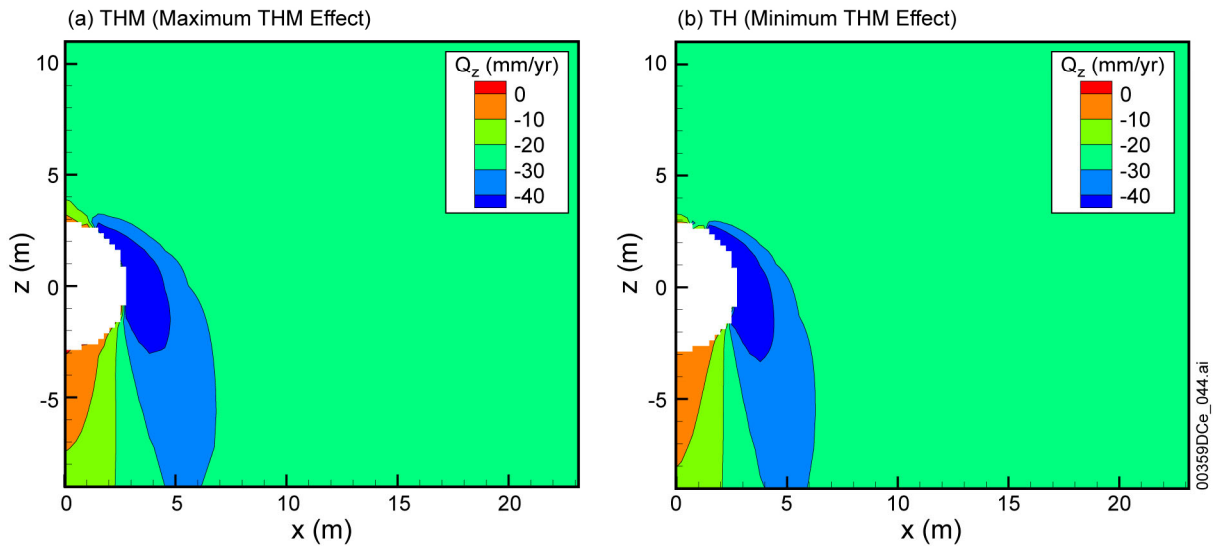
G.4.2 RDTME 3.20: Sensitivity Analysis

The sensitivity of the parameters mentioned in RDTME 3.20 have been addressed in more recent revisions and enhancements of coupled thermal-hydrologic-mechanical process analyses of Yucca Mountain. For estimating thermal-mechanical-induced permeability changes at Yucca Mountain, thermal-mechanical changes and the impact of those thermal-mechanical changes on the permeability and the fluid flow field need to be estimated. Thermal-mechanical changes are affected by temperature changes, coefficients of thermal expansion, rock mass strength, and rock mass modulus. A larger temperature change, a higher value of the coefficient of thermal expansion, and a higher modulus (stiffer rock mass) will give rise to a higher thermal stress. If the thermal stress is sufficiently high and the rock strength is low, mechanical failure occurs, giving rise to irreversible (permanent) mechanical changes. The analysis documented in *Drift-Scale THM Model* (BSC 2004b) shows that the most important parameter for predicting thermal-mechanical-induced changes in permeability is the normal stress versus permeability relationship for fractures (in particular for vertical fractures). The sensitivity range of some parameters is covered by bounding analyses that were conducted to bracket the potential impact of thermal-hydrologic-mechanical processes on permeability and the flow field. The bounding cases are realized by adopting parameter values that minimize and maximize the effect of coupling. This includes a bounding estimate of the thermal expansion coefficient (leading to the maximum possible thermal stress) and a bounding estimate of a stress versus permeability function (leading to maximum possible permeability change). In addition, the results of thermal-hydrologic-mechanical analyses with maximum effect of coupling are compared to thermal-hydrologic analyses with no effect of mechanical coupling (see example in Figures G-1 and G-2). Thus, the current analysis covers the entire sensitivity range, from minimum to maximum effect of the thermal-hydrologic-mechanical coupling. The examples in Figure G-1 and G-2 show that thermal-hydrologic-mechanical coupling has a small impact on the flow field but tends to reduce the vertical flow just above the drift. In RDTME 3.20, a sensitivity analysis was agreed upon that should include the following parameters: boundary conditions, coefficient of thermal expansion, fracture distribution, rock properties, and drift degradation. These parameters are discussed in Sections G.4.2.1 to G.4.2.5. In addition, the important fracture stress versus permeability relationship is discussed in Section G.4.2.6.



Source: BSC 2004b, Figures 6.5.5-5.

Figure G-1. Comparison of the Distribution of Vertical Percolation Flux (Q_z) at 10,000 Years for a Fully Coupled Thermal-Hydrologic-Mechanical Simulation That Maximizes the Effect of Thermal-Hydrologic-Mechanical Coupling and Thermal-Hydrologic Simulation That Minimizes the Effect of Thermal-Hydrologic-Mechanical Coupling (For a Repository Drift in the Tptpmn Unit)



Source: BSC 2004b, Figures 6.6.2-3.

Figure G-2. Comparison of the Distribution of Vertical Percolation Flux (Q_z) at 10,000 Years for a Fully Coupled Thermal-Hydrologic-Mechanical Simulation That Maximizes the Effect of Thermal-Hydrologic-Mechanical Coupling and Thermal-Hydrologic Simulation That Minimizes the Effect of Thermal-Hydrologic-Mechanical Coupling (For a Repository Drift in the Tptpll Unit)

G.4.2.1 Boundary Conditions

In the previous distinct element analysis (conducted in 2001), permeability changes were estimated in a 20-by-20-m region surrounding an emplacement drift (BSC 2001b, Figure 6.2-2

and 6.2-5). This region, the inner drift-scale model, was discretized into distinct element blocks defined by discrete fractures. This inner region was surrounded by a pillar-scale model, which was a continuum representation of the rock mass (BSC 2001b, Figure 6.2-2). For the lateral boundaries (vertical sides of the model) a zero-displacement restriction on normal displacements along these surfaces was applied. A zero-displacement restriction on normal displacement is a realistic representation of a repository environment, as given by repetitive symmetry conditions among neighboring emplacement drifts (BSC 2001b, Section 6.2.2.2). The stress and displacement calculated in the pillar-scale model were then used to assist in selecting appropriate boundary conditions for the inner drift-scale model. Results showed that a zero-displacement restriction on normal displacements along lateral boundaries (vertical sides of the model) of the inner drift-scale model was also appropriate. On top of the inner drift-scale model a constant vertical stress was applied, while the bottom of the model was fixed (zero displacement restriction).

At the NRC/DOE Technical Exchange and Management Meeting on Repository Design and Thermal-Mechanical Effects in February 2001, the NRC questioned why the distinct element model was set up to examine changes around the drift and not in the pillar. The NRC also commented that a drift-scale model was not adequate to capture thermal-mechanical effects on flow (a repository scale model is required). These concerns, as well as the concerns regarding the boundary conditions applied between the pillar-scale and inner region models, have been addressed through the revised and enhanced coupled thermal-hydrologic-mechanical analysis provided in *Drift-Scale THM Model* (BSC 2004b, Section 6) and *Mountain-Scale Coupled Processes (TH/THC/THM)* (BSC 2004c, Section 6.5). In the *Drift Scale THM Model* (BSC 2004b, Section 6), permeability changes and the impact of these changes on the flow field are evaluated both around drifts and in the pillar between drifts. Furthermore, the model extends vertically from the water table to the ground surface. Because the model extends from the drift to the pillar, vertically between the ground and the water table, issues related to transfer of boundary between different submodels in *Coupled Thermal-Hydrologic-Mechanical Effects on Permeability Analysis and Models Report* (BSC 2001b) have been eliminated in *Drift Scale THM Model* (BSC 2004b). The model domains used in the most current *Drift Scale THM Model* (BSC 2004b) are consistent with model domains used in *Drift Degradation Analysis* (BSC 2004d, Section 6) and *Drift-Scale Coupled Processes (DST and THC Seepage) Models* (BSC 2004e, Section 6).

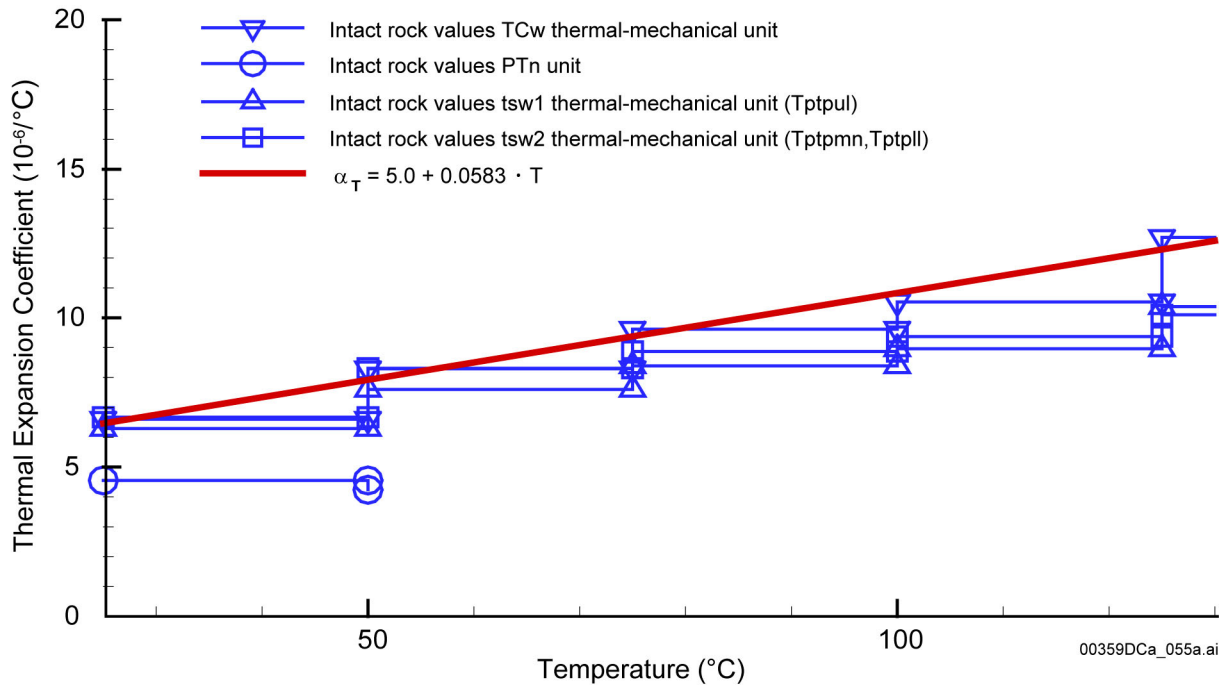
In the current *Drift Scale THM Model* (BSC 2004b, Section 6), the lateral boundaries (vertical sides of the model) have the appropriate zero displacement restriction on normal displacement. These boundary conditions represent a case in which the emplacement drifts are heated simultaneously, leading to a repetitive symmetric drift-scale model region. As noted in *Drift Scale THM Model* (BSC 2004b, Section 6.3, p. 56), the condition that emplacement of waste occurs at once in neighboring drifts provides a bounding estimate of the impact of thermal-hydrologic-mechanical processes because it leads to the highest possible heat load and, therefore, the highest possible thermal stress. In addition to the drift-scale thermal-hydrologic-mechanical model, a repository-scale thermal-hydrologic-mechanical analysis has been conducted and documented (BSC 2004b, Section 6.5). Since this is a repository-scale model, there are no issues related to selection of lateral boundary conditions at the drift scale. The mountain scale thermal-hydrologic-mechanical model provides an additional calculation of repository-wide

permeability changes and their impact on mountain-scale flow distribution. This calculation includes potential edge effects at the lateral edges of the repository.

G.4.2.2 Coefficient of Thermal Expansion

The coefficient of thermal expansion affects magnitudes of rock mass thermal expansion and thermal stress. A higher coefficient of thermal expansion will result in a larger thermal expansion and, generally, in a higher thermal stress. During heating of the rock mass surrounding a repository, thermal stress will develop preferentially in the horizontal direction, whereas little or no repository-wide thermal stress will develop in the vertical direction. Thermal stress does not develop in the vertical direction because of the free-moving ground surface. The increased thermal stress in the horizontal direction will tend to increase the horizontal in situ stresses. The increased horizontal stresses will act upon vertical fractures, which thereby tightens to a smaller aperture, leading to a decreased vertical permeability.

The thermal expansion coefficient adopted for *Drift Scale THM Model* (BSC 2004b, Section 6.4) was derived from laboratory measurements on intact rock samples (Figure G-3). The thermal expansion coefficient in the field could theoretically be equal to or lower than the intact value because of the presence of fractures. At the Single Heater Test, an in situ thermal expansion coefficient was determined to be slightly lower than the corresponding values for intact rock (CRWMS M&O 1999, pp. 9 to 10). However, the in situ thermal expansion coefficient determined at the Single Heater Test is not the appropriate coefficient of thermal expansion to be input into a numerical model, because it is not determined under a constant stress state. A correct value of the in situ coefficient of thermal expansion can only be determined by back-analysis using thermal-mechanical numerical models that simulate the evolution of stress and strain (including stress-induced closure of fractures) during the heating of the rock mass. Such coupled thermal-mechanical analyses were applied to predict multiple-point borehole extensometer (MPBX) displacements at the early part of the DST by Sobolik et al. (1999, p. 741) and in *Coupled Thermal-Hydrologic-Mechanical Effects on Permeability Analysis and Models Report* (BSC 2001b, pp. 21, 115 to 125). Those studies indicate that the displacements are well predicted if an intact-rock thermal expansion coefficient is used. Adopting a thermal expansion coefficient that closely represents the intact rock values can be considered a conservative estimate for the purpose of calculating the thermal impact on stress and permeability. The intact rock value is an upper bound of the possible in situ thermal expansion coefficient, which maximizes thermal-mechanical impact on permeability and flow distribution. Figure G-3 shows that the adopted function of temperature-dependent thermal expansion coefficient closely represents intact-rock thermal expansion coefficients for various rock units at Yucca Mountain.



Source: BSC 2004b, Figures 6.4-1.

Figure G-3. Temperature-Dependent Thermal Expansion Coefficient Adopted in the Revised Drift Scale Thermal-Hydrologic-Mechanical Model (BSC 2004b, Section 6.4) and the Mountain Scale Thermal-Hydrologic-Mechanical Model (BSC 2004c, Section 6.5)

A comprehensive validation against field measurements of rock mass thermal expansion (extensometer displacement) at the DST (BSC 2004b, Section 7) shows that the adopted temperature-dependent coefficient of thermal expansion is a correct representation of the in situ coefficient of thermal expansion at the DST. This confirms the appropriateness of using laboratory values for the in situ thermal expansion coefficient, which at the same time provide an upper bound that maximizes the thermal-mechanical impact on permeability. The lower bound would be a thermal expansion coefficient equal to 0, which is equivalent to a thermal-hydrologic analysis that minimizes the thermal-mechanical impact on permeability. The calculated flow fields for these two bounding cases are shown in Figures G-1 and G-2.

G.4.2.3 Fracture Distributions

The fracture distribution used in the distinct element analysis documented in *Coupled Thermal-Hydrologic-Mechanical Effects on Permeability Analysis and Models Report* (BSC 2001b) and in the continuum analysis documented in *Drift Scale THM Model* (BSC 2004b) are based on mapping of fractures along the Exploratory Studies Facility (ESF). The two main stratigraphic units in which the emplacement drifts will be located (Tptpmn and Tptpll) are both highly fractured, and the fractures are well connected. In these rock units, three dominant sets of fractures are oriented almost orthogonal to each other (CRWMS M&O 1998a, Section 7.4.5; BSC 2004d, Section 6.1.4.1). A mean fracture spacing of less than 0.4 m has been derived, using mappings of fractures with a trace length larger than 1 m (CRWMS M&O 1998a, Section 7.4.6). However, as pointed out in *Drift Degradation Analysis* (BSC 2004d, Section 6.3.3), 80% of the fractures have a trace length of less than 1 m, and, therefore, including small-scale fractures, the

fracture spacing should be less than 0.4 m. The concept of a well-connected fracture network for fluid flow is confirmed by air-permeability measurements conducted in boreholes with short (1 ft) packer intervals at several excavated niches (BSC 2003b, Section 6.1). In these tests, the permeability at each 0.3-m interval of the boreholes is several orders of magnitude larger than the matrix permeability, indicating that at least one hydraulic conductive fracture intersects (every 0.3 m) and is connected to a network of hydraulic conducting fractures. For such intensively fractured rock, the detailed fracture geometry will not impact the coupled thermal-hydrologic-mechanical behavior significantly, and, hence, a continuum model should be appropriate.

The appropriateness of the continuum approach to simulate flow through fractured rock at Yucca Mountain was demonstrated by Jackson et al. (2000) using synthetic and actual field data. The dual-permeability continuum model appropriately accounts for the difference in water retention between the fractures and matrix necessary to capture important fracture–matrix interaction processes (e.g., matrix imbibition). In the drift-scale coupled thermal-hydrologic-mechanical model, changes in the three-dimensional stress field are coupled to rock mass permeability through a cubic-block conceptual model (BSC 2004b, Figure 6.2-2b). Although the fracture orientation in the cubic-block model is roughly consistent with common fracture orientations at Yucca Mountain, it is a simplified representation of the in situ fracture network. For example, in some rock units, the subhorizontal fracture set may be less frequent, and there may also be randomly oriented fractures. Furthermore, trace distributions of fractures mapped along the ESF for the Ttpmn unit make them discontinuous in nature, with fractures frequently terminating against an intersecting fracture (BSC 2004d, Section 6.1.4.1). However, the conceptual model shown in *Drift Scale THM Model* (BSC 2004b, Figure 6.2-2b) is consistent with established hydrologic and thermal-hydrologic process models for the unsaturated zone. The hydrologic properties of those models are largely derived directly from in situ permeability measurements and through model calibration against in situ hydrologic data, such as liquid saturation profiles along vertical boreholes. Fracture density is used primarily for deriving parameters for fracture–matrix interaction behavior, such as interface area and connection length between fracture elements and matrix blocks in the underlying conceptual model. Using this underlying conceptual model, hydraulic properties such as the water retention curve are calibrated against field measurements. Thus, for deriving hydrologic properties and for analysis of hydrologic and thermal-hydrologic processes in the unsaturated zone, detailed information on distributions of fracture length, orientation, and aperture is not explicitly incorporated, except for a generic value of mean fracture spacing in each rock unit.

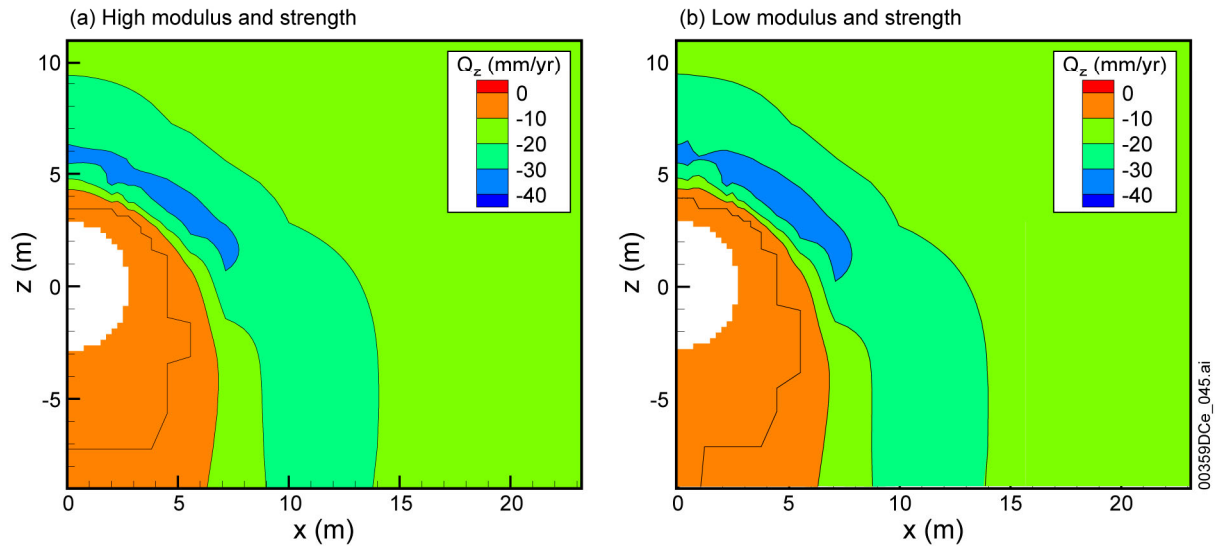
The underlying conceptual model for stress versus permeability coupling shown in the drift-scale coupled thermal-hydrologic-mechanical model is justified as being consistent with the established hydrologic models of the unsaturated zone. Analogous to the derivation of hydrologic properties, the resulting hydromechanical properties are not critically dependent on the exact underlying conceptual model. This is because the relationship is calibrated for the underlying conceptual model and, thus, is only valid for the underlying conceptual model. Similarly, the calibrated hydrologic properties are only valid when using the underlying conceptual model. It is, therefore, important that the same underlying conceptual model be used for both model calibration and predictions. The appropriateness of the continuum model and the underlying conceptual model of orthogonal fracture sets have been extensively validated against field experiments in *Drift Scale THM Model* (BSC 2004b, Section 7).

The analysis in the *Drift Scale THM Model* (BSC 2004b, Section 6) was conducted with initially homogeneous rock properties for each stratigraphic unit, based on calibrated mean hydrologic properties and a conservative fracture normal stress versus permeability relationship. A heterogeneous fracture distribution will result in an initially heterogeneous permeability field, which, in turn, would result in heterogeneous changes in permeability. However, the overall results from niche excavation experiments show that, while mechanically induced changes in mean permeability are about 1 order of magnitude, the standard deviation of the heterogeneous permeability field changes much less (BSC 2003b, Table 6.1.2-1). This indicates that the main impact of thermal-hydrologic-mechanical processes is a change in the mean permeability, even for an initially heterogeneous permeability field. Therefore, it is appropriate to apply the mean permeability changes calculated to a seepage analysis that considers either the homogeneous or heterogeneous permeability field. The impact of a heterogeneous permeability field on seepage is investigated in *Seepage Model for PA Including Drift Collapse* (BSC 2003a, Section 6.6).

G.4.2.4 Rock Mass and Fracture Properties

The mechanical rock properties include elastic properties (e.g., Young's modulus) and strength properties (e.g., cohesion and internal friction angle). The elastic properties impact the magnitude of thermal stresses due to heating. The thermal stresses, in turn, impact the stress-induced closure of fractures and associated reduction in permeability. Furthermore, if the thermal stresses are sufficiently large, failure could occur in the walls of an open emplacement drift.

The elastic properties of a fractured rock mass (e.g., the deformation modulus) are a function of intact rock properties and the degree of fracturing. As mentioned above, the repository units are highly fractured volcanic tuff and, consequently, the Young's modulus is considerably lower than its values for intact rock. The Young's modulus for the Tptpmn repository unit is estimated to be 50% of its intact rock value. This is in agreement with several in situ tests at Yucca Mountain and consistent with the literature (BSC 2004b, Section 6.4). Using this value, thermal stresses are not sufficient to cause any mechanical failure at the drift wall for an emplacement drift in the Tptpmn unit (BSC 2004b, Section 6.10.2). For the Tptpll unit, rock properties are also impacted by the presence of lithophysae, and the modulus and strength properties of the Tptpll unit are generally lower than those of the Tptpmn unit. Because of the low strengths of the Tptpll unit, there is a possibility of failure in the rock walls, and a complete drift collapse may be possible as a result of long-term rock-strength degradation and earthquakes (BSC 2004d). For this unit, the mechanical properties ranging from poor quality to good quality have been accounted for in *Drift Scale THM Model* (BSC 2004b, Sections 6.6 and 6.7). These properties were derived from and are consistent with those used in *Drift Degradation Analysis* (BSC 2004d). Furthermore, the adopted strength properties were validated against observed sidewall fracturing at the ECRB Cross-Drift (BSC 2004b, Section 7.6). Figure G-4 shows that the resulting flow field is not very sensitive to the mechanical rock mass properties. This is expected since the effect of thermal-hydrologic-mechanical coupling is small anyway.



Source: BSC 2004b, Figures 6.6.2-2a and 6.7.3-1a.

Figure G-4. Comparison of the Distribution of Vertical Percolation Flux (Q_z) at 1,000 Years for a Good-Quality Rock (High Modulus and Strength) and Poor-Quality Rock (Low Modulus and Strength).

G.4.2.5 Drift Degradation

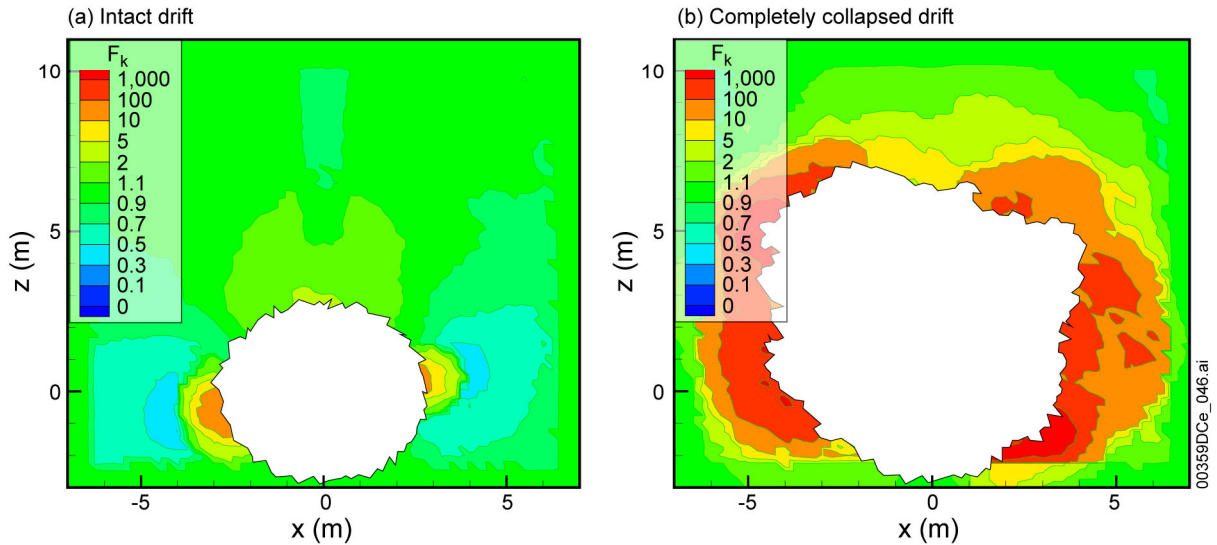
Drift Degradation Analysis (BSC 2004d, Section 6.4.1) indicates that an emplacement drift located in the Tptpl unit could be severely damaged and even completely collapse as a result of a strong seismic event or long-term strength degradation of the drift-wall rock. A drift collapse may change the capillarity around the drift and, thereby, impact the potential for seepage of water into the drift. Drift seepage can be impacted by the change in shape or size of the drift and by changes in hydraulic properties (permeability and capillarity) in the host rock surrounding the collapsed drift. In *Drift Scale THM Model* (BSC 2004b, Section 6.8), changes in hydrologic properties around a collapsed drift were estimated. The analysis was conducted using outputs from the mechanical analysis described in *Drift Degradation Analysis* (BSC 2004d, Section 6.4.1).

Changes in hydrologic properties were evaluated for the following scenarios:

- Excavation without drift degradation and seismic impact
- Drift degradation with 100% cohesion loss (complete drift collapse)
- 1,000,000-year earthquake event (complete drift collapse)
- 2,000-year earthquake event (minor damage).

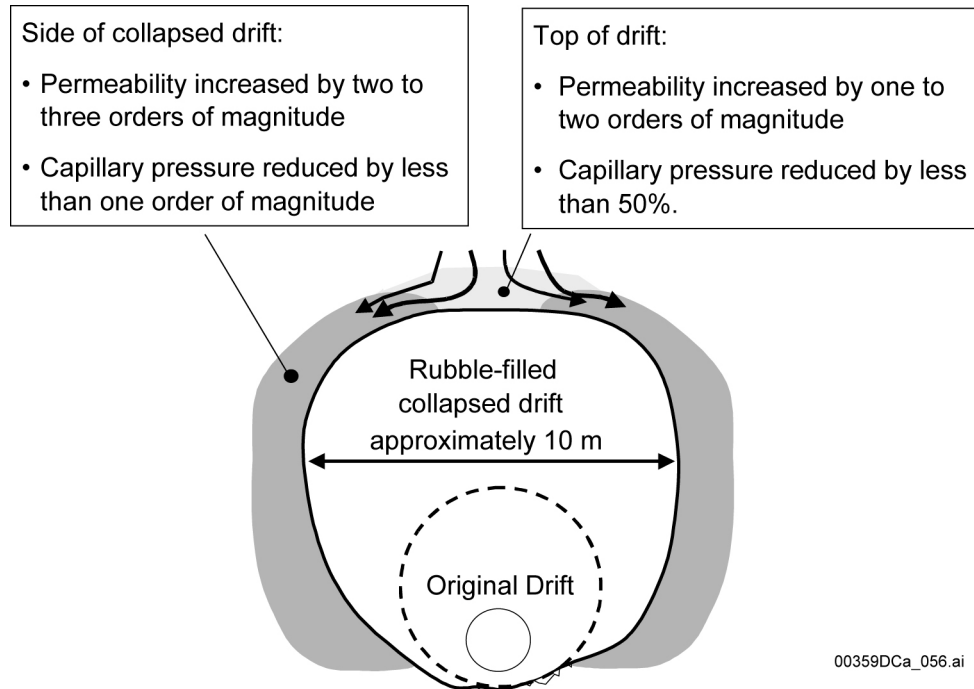
The two scenarios leading to a complete drift collapse were considered worst-case scenarios of drift degradation and seismic effects. The 2,000-year earthquake scenario represents the threshold earthquake event over the 10,000-year licensing period, for which minor damage was predicted (BSC 2004d, Section 6.4.1). Figure G-5 shows calculated permeability changes for the bounding scenarios of an intact drift and a completely collapsed drift. The permeability changes, as expected, are larger around a completely collapsed drift, especially on the side of the drift.

Figure G-6 presents a conceptual summary of the estimated changes in hydrologic properties around a completely collapsed drift. The changes shown in the figure reflect a complete collapse caused by either seismic loading or 100% cohesive loss. It is estimated that permeability could increase by about 1 to 2 orders of magnitude and that capillary pressure could decrease to a factor of about 0.5 of initial values just above the drift, whereas larger changes are predicted to occur on either side of the drift. The larger changes predicted to occur on both sides of the drift are caused by a zone of loosening blocks partly detaching from each other, creating larger fracture openings. It appears that the rock blocks in this zone would be almost completely loose but are prevented from complete detachment and caving into the drift by support from the rubble inside the drift.



Source: BSC 2004b, Figures 6.8.1-3b and 6.8.2-2b.

Figure G-5. Comparison of the Permeability Correction Factor ($F_k = k/k_i$) Relative to Preexcavation Values for the Bounding Scenarios of an Intact Drift and a Completely Collapsed Drift



Source: BSC 2004b, Figure 6.8.5-1.

Figure G-6. Summary of Estimated Changes in Hydrologic Properties around a Completely Collapsed Drift

The increasing permeability around the drift can lead to a larger redistribution of the flow field than would be the case for a stable drift. The larger changes on the sides of the drift are not as relevant for drift seepage as the changes at the top of the drift (above the waste package). In general, the increase in permeability on top of the drift and the larger increase on the sides of the drift would facilitate diversion of water flow around the drift and, thereby, reduce the potential for water seeping into the drift. While most of the results (BSC 2004b, Sections 6.8.1 to 6.8.4) show permeability changes averaged over the horizontal and the vertical directions, typically the increase in horizontal permeability at the drift crown is larger than the increase in vertical permeability on the sides. As discussed earlier, such anisotropic behavior would tend to increase the likelihood of flow diversion around the drift compared to what would happen under isotropic conditions. On the other hand, increasing drift size while simultaneously reducing capillarity could weaken the capillarity and, thereby, increase the likelihood for drift seepage.

G.4.2.6 Fracture Stress versus Permeability Relationship

The model predictions of thermal-mechanical permeability changes are dependent on an accurate relationship between stress and fracture permeability. An upper bound of maximum permeability correction factor and a lower bound of minimum permeability correction factor bracket the range of predicted changes in fracture permeability. The upper bound is important for the prediction of a possible permeability increase caused by unloading in the excavation disturbed zone of an emplacement drift. The lower limit is important for the prediction of the maximum possible reduction in permeability caused by thermal stresses.

Near the drift wall, the analysis shows that permeability can increase about 1 order of magnitude in a direction parallel to the drift wall (BSC 2004b, Figure 6.5.1-1). This magnitude of change is dictated by the upper bound of the fracture normal stress versus permeability function, which has been calibrated against in situ tests in both the Tptpmn and Tptpll unit (BSC 2004b, Figure 6.4-2). The fact that mean permeability increases about 1 order of magnitude near the drift in the Tptpmn unit and less than 1 order of magnitude in the Tptpll unit is well established from observed permeability changes at excavated niches. *In Situ Field Testing of Processes* (BSC 2003b, Table 6.1.2-1) shows that the geometric mean of the ratios of postexcavation and preexcavation permeabilities varies between 9.42 to 25.38 for three niches in the Tptpmn unit, whereas the geometric mean of the ratios of postexcavation and preexcavation permeabilities is 2.37 for one niche in the Tptpll unit (BSC 2003b, Table 6.1.2-2). Thus, the upper bound of the fracture stress–permeability function is established from these field data.

In the longer term, at 1,000 to 10,000 years, the analysis shows that permeability decreases significantly in an area extending hundreds of meters above and below the drift (BSC 2004b, Figure 6.5.4-1). The model simulation shows that the permeability decreases most in the vertical direction, by closure of vertical fractures. Such closure of vertical fractures has been confirmed by calculations in *Coupled Thermal-Hydrologic-Mechanical Effects on Permeability Analysis and Models Report* (BSC 2001b, Section 7), using the alternative distinct-element model. Permeability decreases of up to 6 orders of magnitude were calculated (BSC 2001b, Section 6.3.3). The 6 order-of-magnitude decrease in fracture permeability calculated from the earlier distinct element analysis (BSC 2001b, Section 6.3.3) is an artifact of an unsubstantiated assumed relationship between normal stress and fracture permeability (Section G.4.4). The relationship between normal stress and fracture permeability adopted for the distinct element analysis resulted in overstating the fracture permeability because it did not consider residual fracture permeability at high fracture normal stress. The calculated lower limit of permeability decrease in the current continuum analysis—a factor of 0.03 in the Tptpmn unit and 0.6 in the Tptpll unit (BSC 2004b, Figures 6.5.4-3c and 6.6.1-5a)—is strongly dependent on the assigned residual fracture permeability. This residual permeability is a parameter constrained by the maximum observed decrease in permeability at the DST and the Single Heater Test. The fact that the parameter is constrained from the maximum observable change at the DST and the Single Heater Test indicates that predicted change in permeability provides a bounding worst case of thermal-hydrologic-mechanical-induced permeability changes at the repository.

There are currently no in situ tests available to estimate residual permeability within the Tptpll unit. However, considering the trend of relatively smaller changes in permeability for initially larger permeability values observed at the niche excavation experiments (BSC 2003b, Section 6.1.2.3), the impact of thermal-hydrologic-mechanical processes on fluid flow is likely to be smaller in the Tptpll unit than in the Tptpmn unit. This trend is also captured in the modeling results, which show a relatively smaller change in permeability for the Tptpmn unit than for the Tptpll unit (BSC 2004b, Sections 6.5 and 6.6).

G.4.3 RDTME 3.21: Additional Validation Analysis of Field Tests

Specifically, RDTME 3.21 states that DOE will provide the results of additional validation analysis of field tests related to thermal-mechanical effects on fracture permeability. In addition, validation analyses of field tests were under consideration by DOE to evaluate

thermal-mechanical effects on hydrologic properties (Bodvarsson et al. 2001), including measured temperatures, additional fractures, and analysis of multipoint borehole extensometer data. The suggested validation analysis for additional fractures is concerned with the distinct element analysis of the DST (BSC 2001b, Section 7), which included only widely spaced, major fractures in the rock mass. In contrast, the recent continuum analysis (BSC 2004b, Section 7) also implicitly accounts for small-scale fractures in an equivalent continuum. Thus, these two analyses represent two extremes, one simulating the rock as a sparsely fractured medium and one as a highly fractured medium. The two analyses were compared for thermal displacements and showed consistent results (BSC 2004b, Section 7.7).

The additional validation agreed upon in RDTME 3.21 has been conducted in recent revisions and enhancements of the coupled thermal-hydrologic-mechanical process analysis at Yucca Mountain. *Drift Scale THM Model* (BSC 2004b, Section 7) provides comprehensive validation for coupled thermal-hydrologic-mechanical processes. This validation is summarized in Sections G.4.3.1 to G.4.3.9.

G.4.3.1 Specifics of the Drift-Scale Thermal-Hydrologic-Mechanical Model Validation

The most important part of the validation of the drift-scale thermal-hydrologic-mechanical model is simulation of the DST, with comparison of calculated results to measurements. A basic requirement is that the drift-scale thermal-hydrologic-mechanical model should be able to capture the general and most relevant thermal-hydrologic-mechanical responses in the field. Disparity between measurements and simulations should not be widespread but local and isolated events that do not distract from the overall agreement of calculated and measured thermal-hydrologic-mechanical responses.

The drift-scale thermal-hydrologic-mechanical model is a continuum model consistent with the overlapping-continuum (matrix and fracture continuum) approach applied in *Drift-Scale Coupled Processes (DST and TH seepage) Models Report* (BSC 2003c, Section 6.2.1). The validity of the conceptual model for simulating thermal-hydrologic processes has been demonstrated through model validations against various in situ tests (BSC 2003c, Section 7). Hence, the drift-scale thermal-hydrologic-mechanical model needs to validate the conceptual model for thermal-mechanical and hydrologic-mechanical processes, including impact of thermal-mechanical processes on permeability. Special emphasis is placed on the validation for hydrologic-mechanical processes, which are key processes for the drift-scale thermal-hydrologic-mechanical model.

The validation of the drift scale thermal-hydrologic-mechanical model against the DST is conducted in the following steps:

1. Check that the simulated temperature field is in reasonable agreement with the observed temperature field to ensure that the thermal-hydrologic-mechanical model is properly implemented in terms of thermal behavior.
2. Check that simulated rock mass displacements capture the general trends and average magnitudes of observed displacements (validation of thermal-mechanical processes).

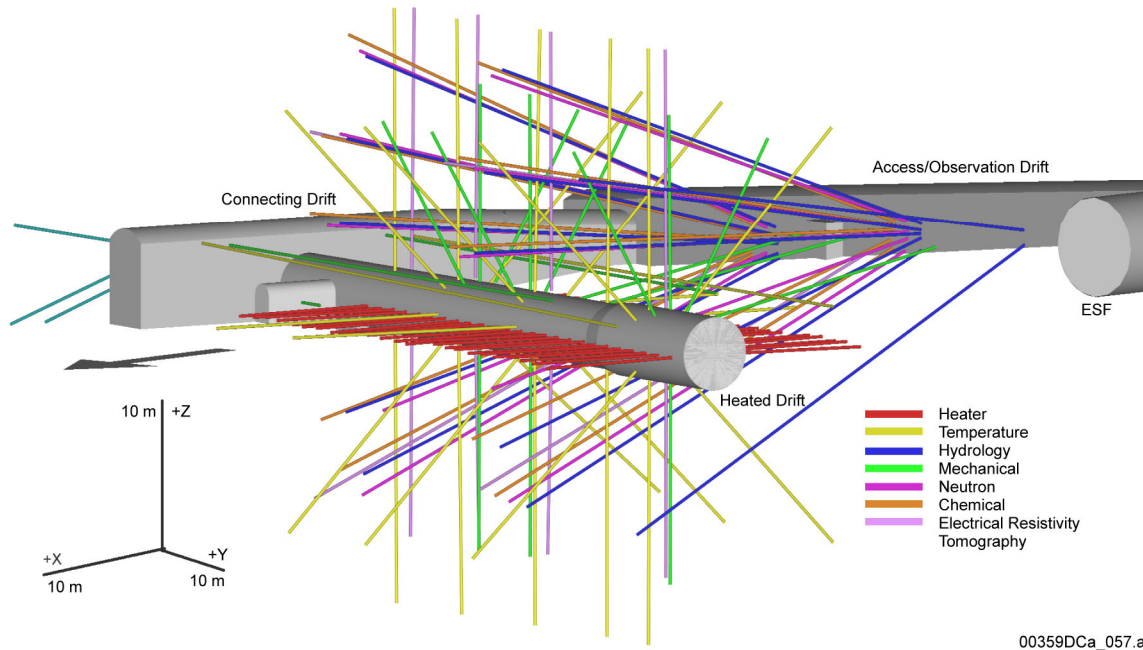
3. Check that the simulated changes in air permeability capture the general trends and magnitudes observed in the field (validation of thermal-hydrologic-mechanical processes).

For thermal-mechanical processes, the average magnitudes of relative displacement and the trends of displacement evolution should be captured in the numerical model. During heating, the average magnitudes of relative displacement measured between two points depended on the average thermal expansion coefficient for the rock mass between the two measurement points. The average thermal expansion coefficient is also important for prediction of the thermal stresses during heating. A representation of the average thermal expansion coefficient as $\pm 50\%$ of in situ values is deemed sufficient and achievable. It is sufficient because $\pm 50\%$ variation in thermal expansion corresponds to very small rock strain with an absolute displacement variation on the order of 1 mm over a 1-m rock section. Previous experiences at similar in situ experiments have shown that the thermal-expansion of fractured rock generally can be well predicted within $\pm 50\%$ of measured values. This indicates that the predicted average displacements for the rock mass as a whole should be within 50% of averaged measured values. Moreover, as discussed in Section G.4.3.4.2, the measured displacements at the DST generally span over $\pm 50\%$ for various but equivalently located monitoring points. For thermal-hydrologic-mechanical processes, the validation criterion is to find the general qualitative agreement with air-permeability measurements and trends during the heating phase. The predicted changes in air permeability are in the correct direction and correct within an order of magnitude; that is, $\log(k/k_i)$ simulated and measured values differ by less than 1. Observed trends (e.g., k/k_i decreases followed by increases, or the reverse) are matched by model predictions.

The validation of the drift-scale thermal-hydrologic-mechanical model against the DST was complemented with validation against the niche tests to check that the conceptual model for stress versus permeability coupling is appropriate over a larger permeability range. Further support for the drift-scale thermal-hydrologic-mechanical model was provided by evidence from other heater tests, from comparison to an alternative conceptual model, and publication in peer-reviewed journals.

G.4.3.2 Drift Scale Test

The DST is a large-scale, long-term thermal test designed to investigate coupled thermal-mechanical-hydrologic-chemical behavior in a fractured, welded tuff rock mass (CRWMS M&O 1998b). The test block is located in one of the alcoves of the ESF in the Ttptmn unit. Figure G-7 shows a three-dimensional perspective of the DST, showing electrical heaters and many of the approximately 150 instrumented boreholes for measuring thermal, hydrologic, mechanical, and chemical processes. The DST test block centers around the heated drift, which is 47.5 m long. Heating is provided by nine floor canister heaters within the heated drift and 50 rod heaters referred to as wing heaters placed into horizontal boreholes emanating from the heated drift. Each wing heater is composed of two equal-length segments (4.44 m) separated by 0.66 m. The distance between the heated drift wall and the tip of the first wing heater segments is 1.66 m. Dimensions of the heated drift and canister heaters are similar to the current design of waste emplacement drifts. The heaters of the DST were activated on December 3, 1997. The heating phase continued for approximately 4 years until January 14, 2002. Currently, the DST is in a planned 4-year period of monitoring the natural cooling process.



00359DCa_057.ai

Source: BSC 2002, Figure 6.3-2.

Figure G-7. Three-Dimensional Perspective of the As-Built Borehole Configuration of the Drift Scale Test

Measurements in the DST include laboratory and field characterization of the test block prior to the activation of heaters, passive monitoring and active testing during the heating and subsequent cooling phases, and planned postcooling laboratory and field characterization activities similar to those conducted prior to activation of heaters. Preheat laboratory characterization included measurements of thermal properties, hydrologic properties, mechanical properties, mineral-petrology studies, and pore-water chemical and isotopic analysis from rock cores. Preheat field characterization of the thermal test block involved rock mass classification, fracture mapping, video logging of the boreholes, geophysical measurements, and air-permeability testing.

Measurements during the heating and cooling phases of the DST are divided into two categories: the continuous passive monitoring data and the active testing data, which are taken periodically. The DST test block has been instrumented with thousands of sensors to monitor the thermal, mechanical, hydrologic, and chemical processes on at least an hourly basis. In Figure G-7, the instrumented boreholes are color-coded according to their functions. For the purposes validation of a coupled thermal-hydrologic-mechanical model, the focus is on boreholes designed to measure thermal (yellow), hydrologic (blue), and mechanical (green) behavior. Radial arrays of 20-m-long boreholes emanating from the heated drift monitor the temperature evolution, as do longitudinal boreholes parallel to and extending over most of the length of the heated drift. Temperature sensors in each borehole are installed at approximately 30-cm intervals. Most boreholes labeled as hydrologic originate from the observation drift. These are clusters of 40-m-long boreholes forming vertical fans that bracket the heated drift and the wing heaters. These boreholes are used for periodic active testing of air-permeability changes to track the time

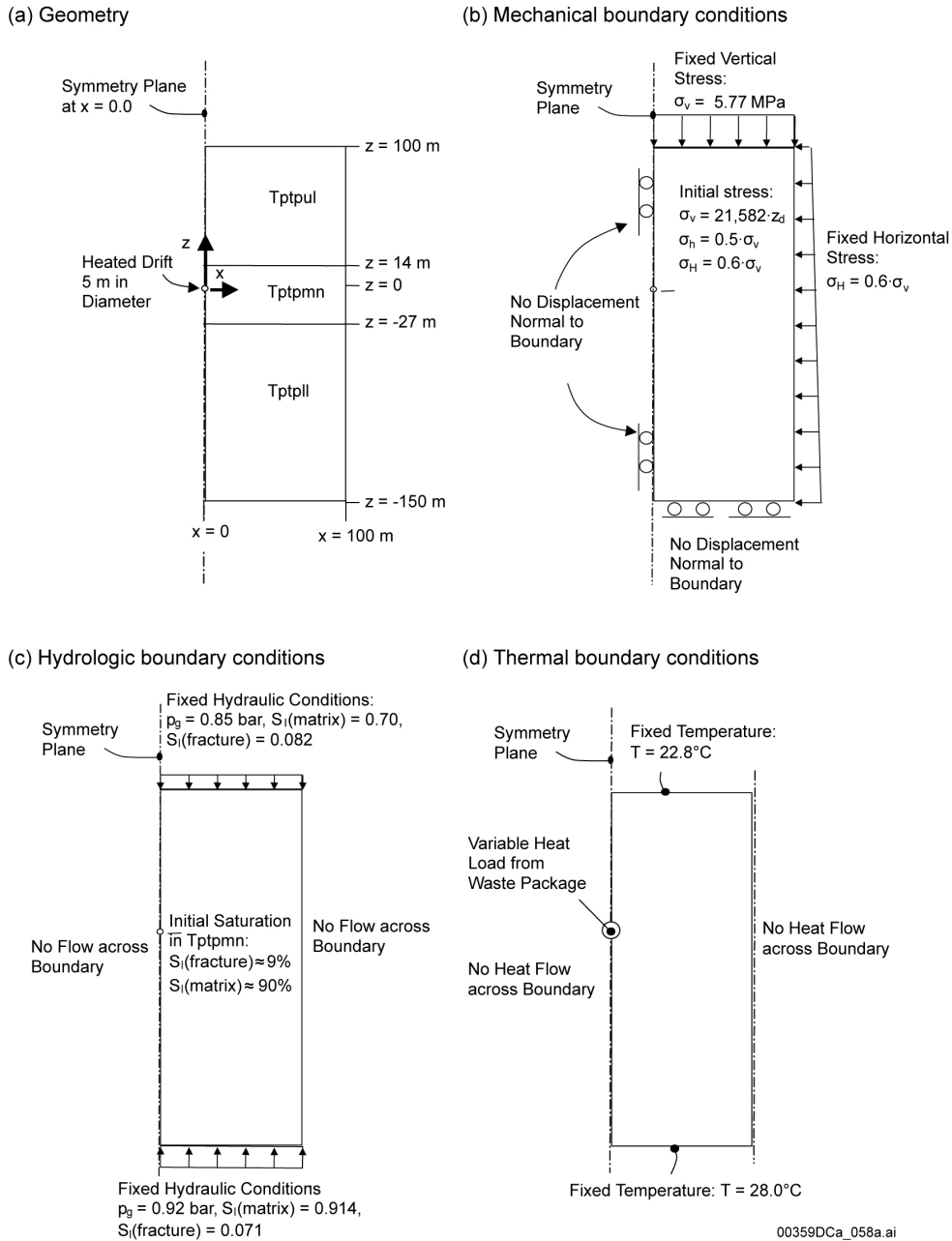
evolution and spatial distribution of drying and condensation zones in the test block. Deformation of the rock mass is being monitored with an array of MPBX systems. In the radial MPBX boreholes, there are four anchors attached to the borehole wall at a distance of about 1, 2, 4, and 15 m from the drift wall. The displacements of each anchor, relative to the drift wall, are continuously monitored.

The DST design and geometry are described in *Drift Scale Test Design and Forecast Results* (CRWMS M&O 1997a) and *Drift Scale Test As-Built Report* (CRWMS M&O 1998b). The results of preheat characterization of the test block are contained in *Ambient Characterization of the Drift Scale Test Block* (CRWMS M&O 1997b). DST measurements for the 4-year heating period are given in *Thermal Testing Measurements Report* (BSC 2002). This report elaborates on the testing methods, gives representative results, and discusses measurement uncertainties. The comparison of simulated and measured DST results below primarily uses data described in that report.

G.4.3.3 Drift Scale Test Model Domain

The DST model domain is a two-dimensional representation of the DST in a section crossing the heated drift perpendicular to its axis (Figure G-8a). The two-dimensional model is half-symmetric with a vertical symmetry plane along the center axis of the heated drift. The model domain extends vertically 250 m from the top of the Tptpul stratigraphic unit ($z = 100$ m) down to the bottom of the Tptpll stratigraphic unit ($z = -150$ m). The stratigraphy of the geologic units is extracted from nearby borehole USW SD-9. The lateral model boundary is placed at a distance of 100 m from the center of the heated drift. Model components include three geologic units (Tptpul, Tptpmn, and Tptpll), the heated drift, the concrete invert, and wing heaters. The heated drift is represented by a gridblock that is assigned a large permeability and heat conductivity to allow for advective, conductive, and radiative transport of heat. An extra grid element is added to simulate loss of heat and vapor through the bulkhead at the end of the heated drift.

The mechanical, hydraulic, and thermal boundary conditions and initial conditions are presented in Figure G-8. The initial vertical stress is estimated using an average density of $2,200 \text{ kg/m}^3$ for the overlying rock units, leading to a vertical stress of about 5.8 MPa at the depth of the heated drift (267.5 m). The magnitude of maximum and minimum principal compressive horizontal stresses is a factor of 0.6 and 0.5 of the vertical stress, with the maximum stress oriented normal to the drift axis (CRWMS M&O 1997c, Table 3-2, pp. 3 to 23). The stress normal to the top boundary (representing the stress produced from the overlying rock mass) and the left lateral boundary (representing the remote maximum principal compressive stress) are fixed throughout the simulation. The top and bottom model boundary conditions are identical to the ones used in the *Thermal Tests Thermal-Hydrological Analyses/Model Report* (BSC 2001c, Section 6.1.2). The fixed hydraulic and thermal boundary conditions on the top and bottom of the model were obtained from an independent thermal-hydrologic simulation of a one-dimensional model domain extending from the ground surface to the water table (BSC 2001c, Section 6.1.2).



Source: BSC 2004b, Figure 7.3-1.

NOTE: P_g = gas pressure, S_l = liquid saturation, z_d = depth below ground surface.

Figure G-8. Two-Dimensional Representation of the Drift Scale Test in a Section Crossing the Heated Drift Perpendicular to Its Axis Presented with (a) Geometry; (b) Mechanical; (c) Hydrologic; and (d) Thermal Boundary Conditions

The total heating power applied to the DST model domain reflects average values of the actual heating power. Average values were calculated for various time periods in *Drift-Scale Coupled Processes (DST and TH Seepage) Models* (BSC 2003c, Table 7.3.4-1). The periods of identical average power output, as applied to the model, are given separately for the drift heaters and the

wing heaters. The heat power for the two-dimensional model was calculated from the total heat power in Table G-1, divided by 47.5 m (the length of the heat source along the heated drift). In addition, the heat power for the drift heater in the half-symmetric model is divided by two, and the power of the wing heaters are distributed with 43.1% to the inner wing heaters and 56.9% to the outer wing heaters.

Table G-1. Total Average Heater Power at Various Times of Heating in the Drift Scale Test

Time	Drift Heater Power (kW)	Wing Heater Power (kW)
12/03/1997 to 05/31/1999	52.1	132.1
06/01/1999 to 03/02/2000	50.0	125.1
03/02/2000 to 05/02/2000	47.9	120.4
05/02/2000 to 08/15/2000	45.8	114.6
08/15/2000 to 03/31/2001	43.3	106.4
04/01/2001 to 05/02/2001	43.4	106.7
05/02/2001 to 08/22/2001	41.4	101.6
08/22/2001 to 09/30/2001	39.4	96.3
10/01/2001 to 01/14/2002	39.4	96.8

Source: BSC 2003c, Table 7.3.4-1.

The properties utilized in the DST model domain are summarized in Table G-2. Thermal-hydrologic properties are taken from the site-specific rock-property set DKM-TT99, which is also used in the DST thermal-hydrologic model in *Drift-Scale Coupled Processes (DST and TH Seepage) Models* (BSC 2003c, Table 4.1.2). The elastic properties, which represent the bulk rock mass (including the effect of fractures), have been estimated using an empirical method based on the Geological Strength Index (GSI) (BSC 2004b, Section 6.4). The adopted rock mass Young's modulus is about 50% lower than the Young's modulus of intact rock determined on core samples from the site.

Table G-2. Summary of Thermal-Mechanical and Hydrologic-Mechanical Parameters and Properties of the Rock Mass Developed for the Drift Scale Test Model Domain

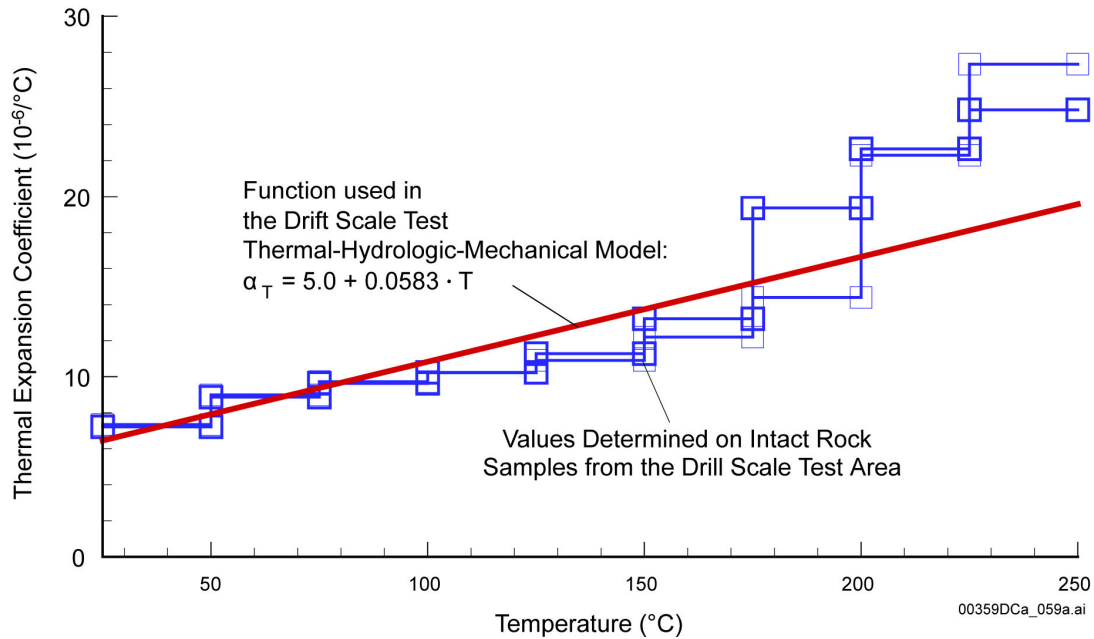
Parameter	Unit	Geologic Unit		
		Ttpul (tsw33)	Ttpmn (tsw34)	Ttpll (tsw35)
Initial Hydraulic Aperture	b_i (μm)	167	52	153
Parameters b_{max} and α for the Stress-Aperture Function	b_{max} (μm)	200	200	200
	α (1/MPa)	0.52	0.52	0.52
Thermal Expansion Coefficient	α_T ($10^{-6}/^\circ\text{C}$)	$5.0+0.0583 \times T$	$5.0+0.0583 \times T$	$5.0+0.0583 \times T$

Source: BSC 2004b, Table 7.3-2.

NOTE: T = Temperature in degrees Celsius.

The thermal-mechanical and hydrologic-mechanical properties of the rock mass were developed in *Drift Scale THM Model* (BSC 2004b, Section 6.4). The parameters for these properties are given in Table G-2. In Figure G-9, the function for a temperature-dependent thermal expansion

coefficient is compared to measured thermal expansion coefficients on intact rock samples from the DST block. The adopted thermal expansion coefficient is close to the site-specific values of the intact-rock thermal expansion coefficient (Figure G-9) for a temperature up to 200°C. Values close to the intact-rock thermal expansion coefficient were adopted in *Drift Scale THM Model* (BSC 2004b, Section 6.4) based on thermal-mechanical simulation results by Sobolik et al. (1999, p. 741) and in *Coupled Thermal-Hydrologic-Mechanical Effects on Permeability Analysis and Models Report* (BSC 2001b, pp. 21, 115 to 125), which showed that measured thermal-mechanical responses are well predicted by assigning the rock mass an intact-rock thermal expansion coefficient.



Source: BSC 2004b, Figure 7.3-2.

NOTE: Laboratory values were determined on core samples from the DST block during two cycles of heat-up.

Figure G-9. Temperature-Dependent Thermal Expansion Coefficient Used in the DST Model Domain and Comparison to Laboratory-Determined Values on Intact Rock

G.4.3.4 Drift Scale Test Validation Results

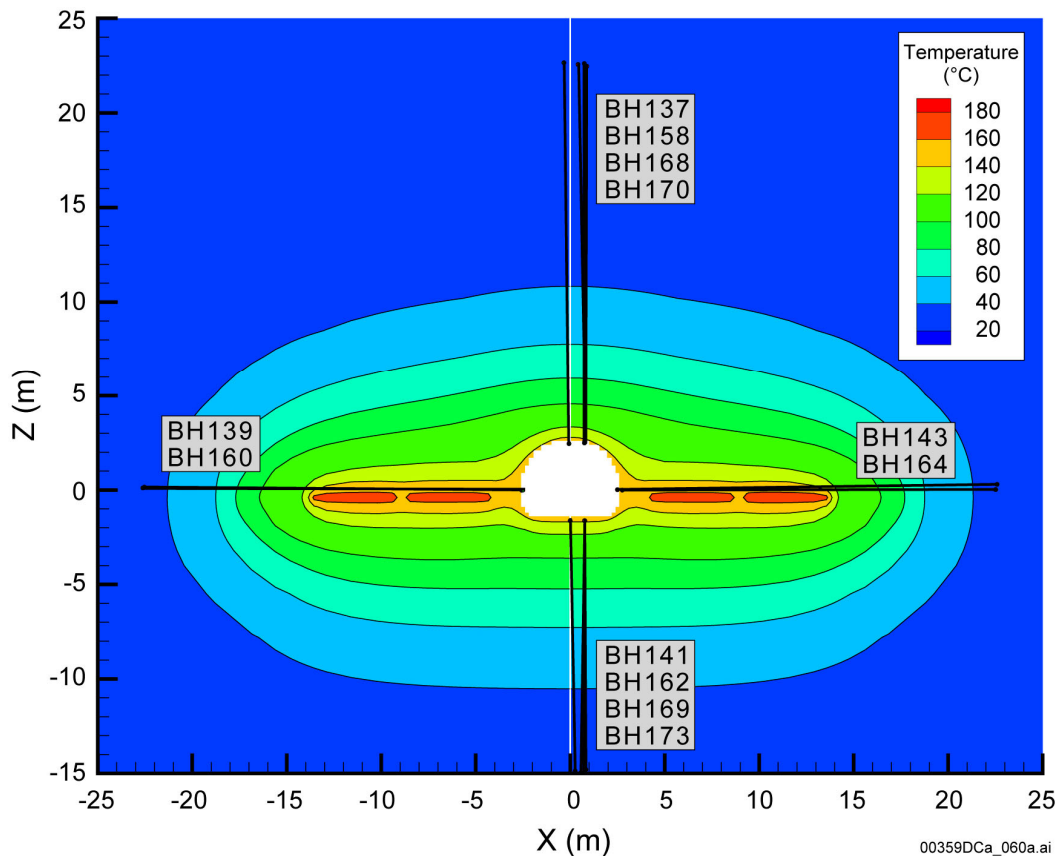
The drift-scale thermal-hydrologic-mechanical model is validated for measurements taken during the 49.5-month heating phase of the DST. The results are presented by comparing the calculated thermal-hydrologic-mechanical responses to measurements, which have been grouped into equivalent categories based on their location relative to the heated drift. Such grouping of the field data is conducted to display typical trends of the field data and their variability.

G.4.3.4.1 Modeling of Temperature Field

For the purpose of validating the drift-scale thermal-hydrologic-mechanical model for thermal-mechanical and hydrologic-mechanical processes, the calculated temperature field must be in reasonable agreement with measured temperature. This is essential because the temperature field is the driving force behind both thermal-mechanical and thermal-hydrologic-mechanical processes. In modeling the DST, an accurate agreement between the calculated and measured

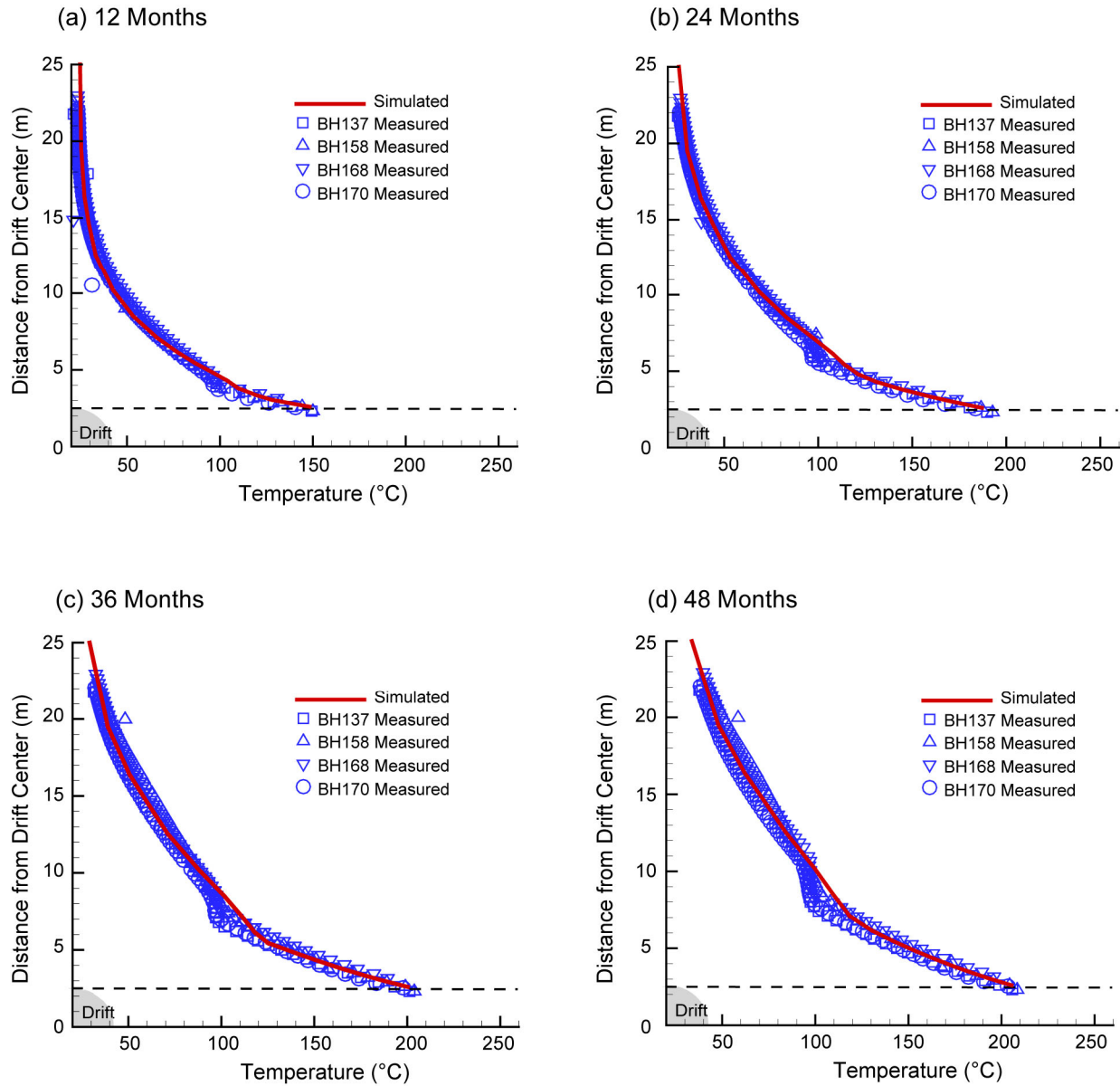
temperature was obtained if heat loss through the bulkhead was simulated. A bulkhead heat-loss coefficient of 0.4375 W/K was determined by calibrating the model for a drift-wall temperature of 150°C at 12 months (Wang 2003, p. 60). Without considering the heat loss through the bulkhead, the temperature at the drift wall would be overestimated, and, consequently, thermal-mechanical forces and displacements would also be overestimated.

Figure G-10 shows calculated temperature after 12 months of heating and the location of thermal boreholes used for validation of the temperature calculation. Figures G-11 and G-12 show the comparison of measured and simulated temperature profiles. The measured temperature includes data from four borehole arrays located at y of approximately 12, 23, 32, and 39 m along the heated drift. These borehole arrays are located well inside the axial extensions of the heated drift and wing heaters. In Figures G-11 and G-12, the calculated temperatures are well within the range of measured values. Furthermore, it can be concluded from Figures G-11 and G-12 that the two-dimensional and half-symmetric model approximation is justified and accurate for predicting temperatures in boreholes located well within the extension of the heated drift.



Source: BSC 2004b, Figure 7.4.1-1.

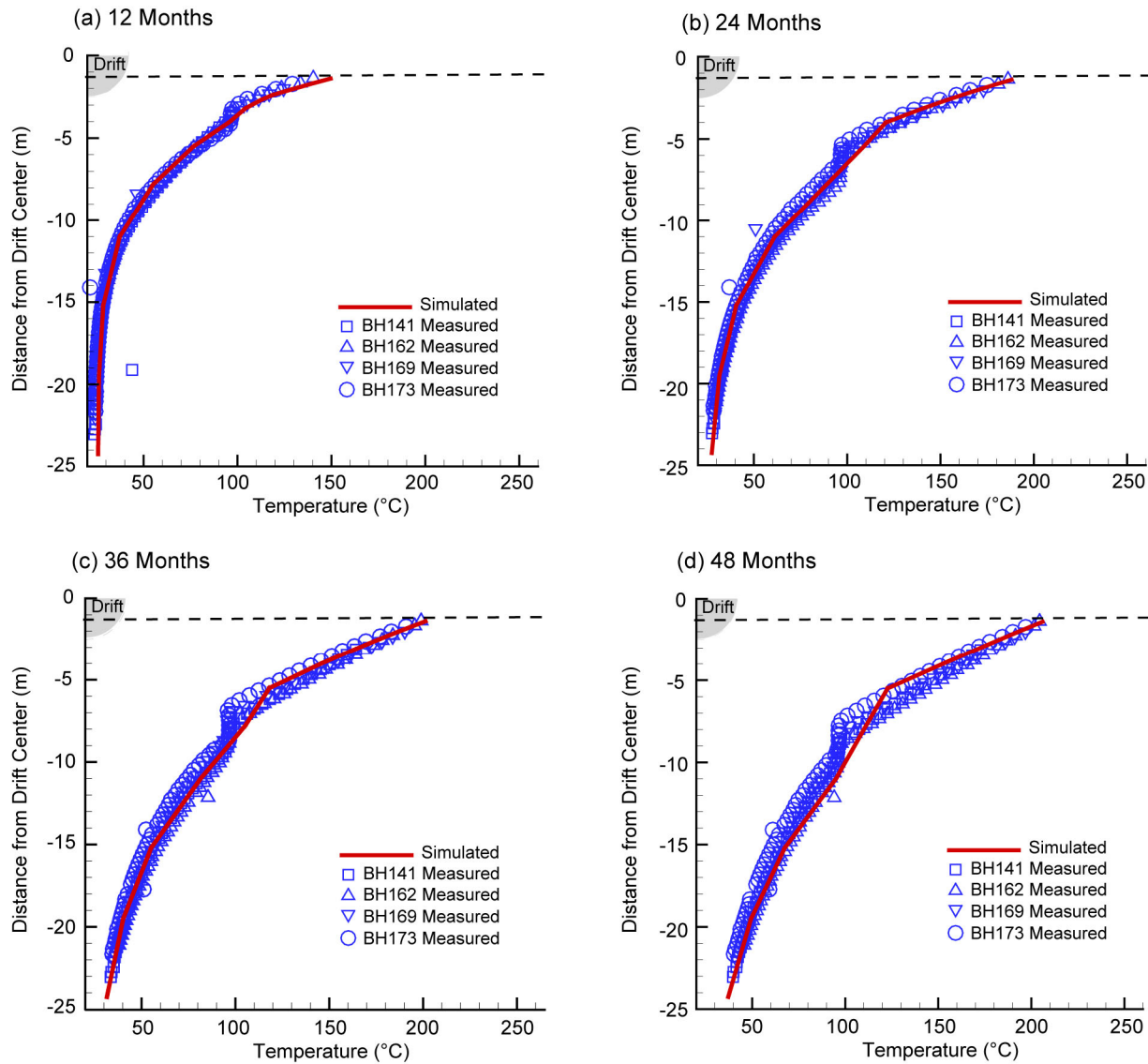
Figure G-10. Calculated Temperature Distribution after 12 Months of Heating and Location of Thermal Boreholes for Comparison of Simulated and Measured Temperature Profiles



00359DCa_061a.ai

Source: BSC 2004b, Figure 7.4.1-2.

Figure G-11. Measured and Simulated Temperature Profiles along Vertically Up Boreholes at the Drift Crown



00359DCa_062a.ai

Source: BSC 2004b, Figure 7.4.1-3.

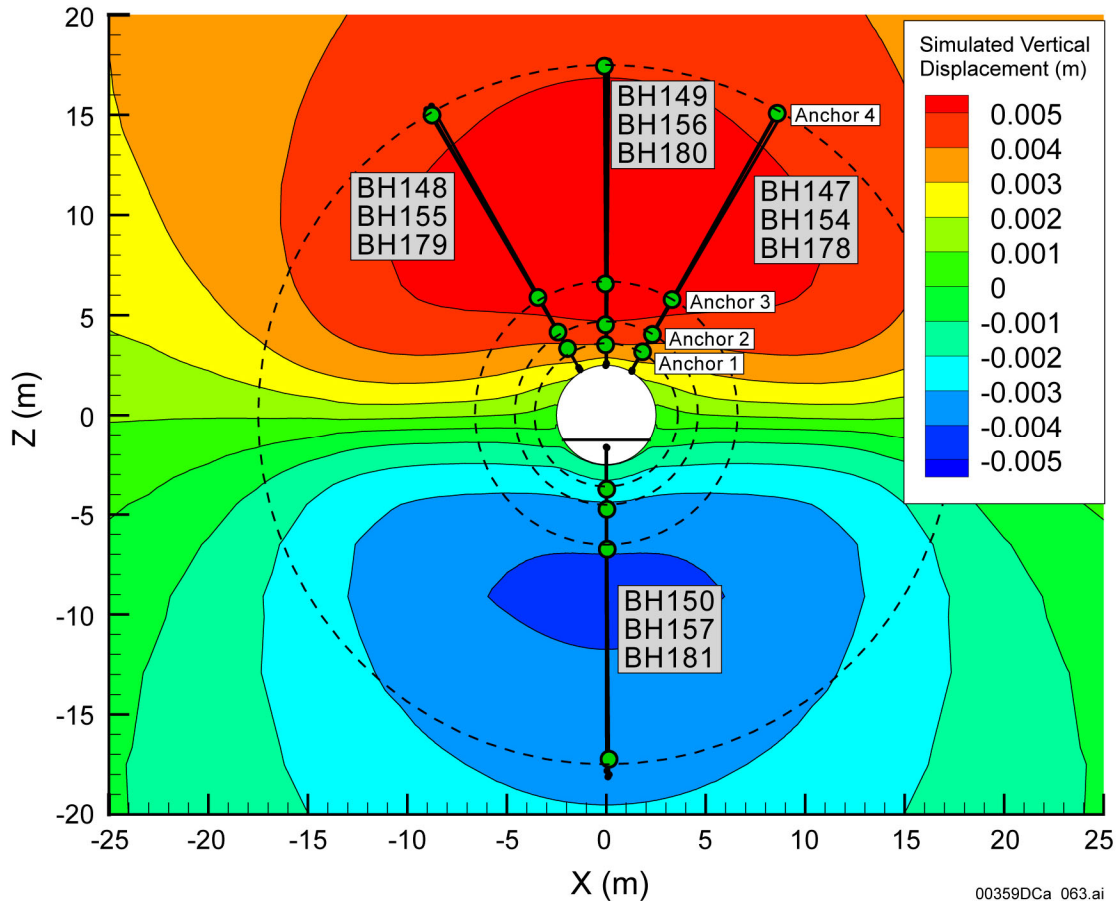
Figure G-12. Measured and Simulated Temperature Profiles along Vertically Down Boreholes Extending Downward from the Drift Floor

G.4.3.4.2 Validation for Thermal-Mechanical Processes

The thermal-mechanical part of the drift-scale thermal-hydrologic-mechanical model is validated by comparing calculated and measured displacements in radial MPBX boreholes. Such comparison validates the drift-scale thermal-hydrologic-mechanical model for the thermal expansion process, as well as for the values of the thermal expansion coefficient.

Figure G-13 shows calculated displacements relative to the drift axis and the locations of radial MPBX boreholes and their anchors, which are used for validation of the calculated thermal expansion. Measured data include displacements from MPBX borehole arrays located at y of approximately 41.1, 21.0, and 13.7 m. These arrays are within the axial extensions of the heated

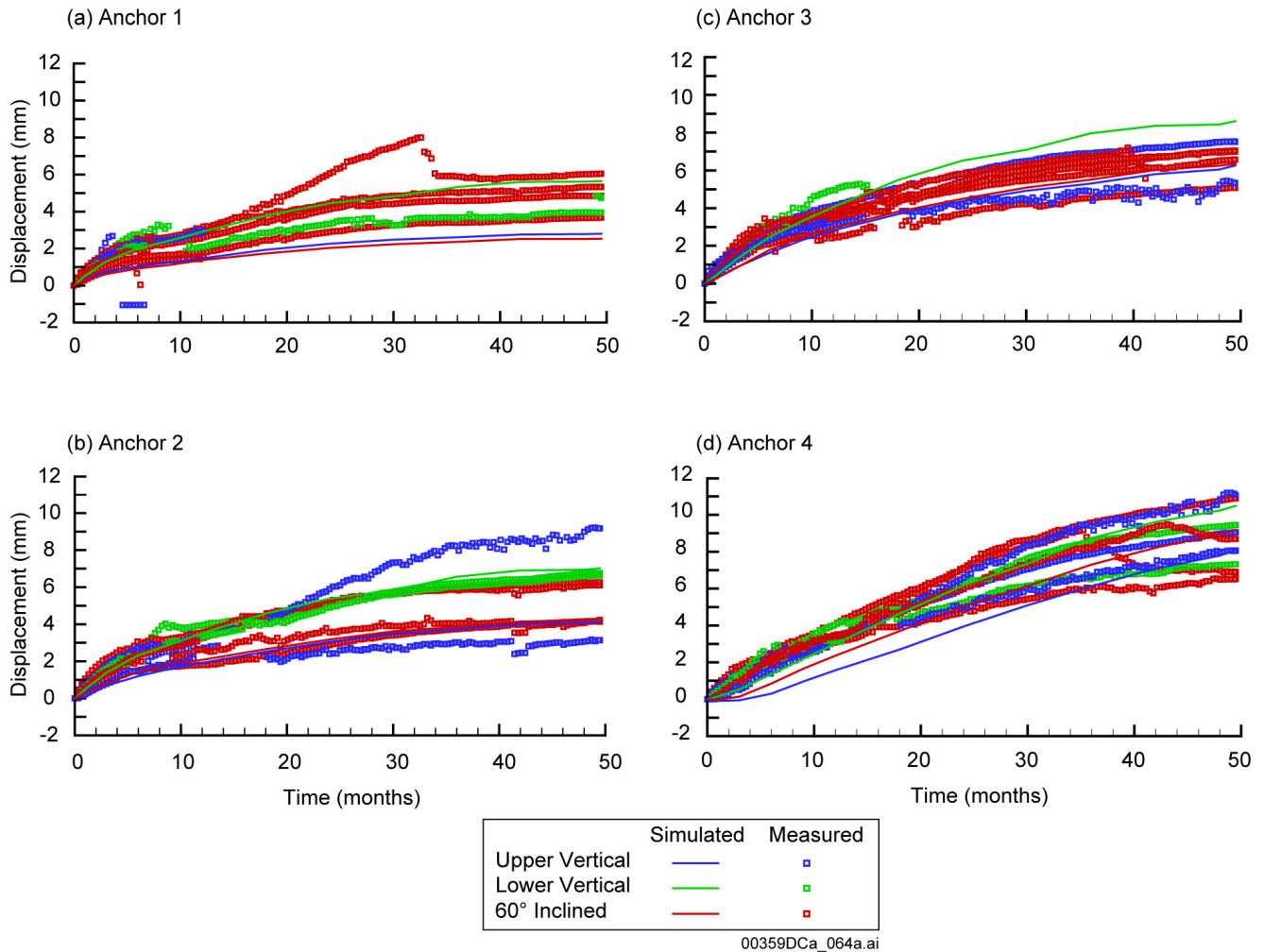
drift, with the array at y of approximately 41.1 m being farthest out, located about 4.6 m from the edge of the heated area. In general, the measured displacements show a larger spread than temperature measurements. This reflects the fact that mechanical displacements are more sensitive to local heterogeneities in the rock mass, such as fractures. In addition, there are a few anchors in which the measured data are erratic, unreasonable, or missing and are, therefore, excluded from this analysis. The quality of displacement measured in the various anchors is documented in *Thermal Testing Measurements Report* (BSC 2002, Section 6.3.3.1.1).



Source: BSC 2004b, Figure 7.4.2-1.

Figure G-13. Simulated Vertical Displacement after 12 Months of Heating and Location of Mechanical Multiple-Point Borehole Extensometer Boreholes for Comparison with Measured Displacement

The measured displacements at various points in the rock mass are grouped according to their radial distances from the drift wall. That is, measurements taken at Anchors 1, 2, 3, and 4, respectively located at 1, 2, 4, and 15 m from the drift wall, were compiled into four groups without regard to their angular direction and axial location along the heated drift. The measured and simulated displacements for each group are compared in Figure G-14. With the exception of the very early time, the simulated displacements are within the range of measured displacement. The agreement is best for Anchors 2 and 3, whereas the calculated displacement in Anchor 1 is a lower-bound prediction. In Anchor 4, the displacement is predicted to be slightly lower during the first half of the heating period, with good agreement at the end of the heating period.



Source: BSC 2004b, Figure 7.4.2-2.

NOTE: Measured values are from boreholes shown in Figure G-13.

Figure G-14. Measured and Simulated Evolution of Displacement in Multiple-Point Borehole Extensometer Boreholes

A quantitative evaluation of model predictions is provided by statistical measures according to Wagner et al. (2001). Three statistical measures were considered in the quantitative evaluations: root-mean-square difference, mean difference, and normalized-absolute-mean difference. The three statistical measures are functions of simulated ($V_{sim,i}$) and measured ($V_{meas,i}$) variables that, in this case, are the simulated and measured displacements.

The root-mean-square difference for a specific time is described as:

$$RMSD = \left[\frac{\sum_{i=1}^N (V_{sim,i} - V_{meas,i})^2}{N} \right]^{1/2} \tag{Eq. G-1}$$

Root-mean-square difference is a classic statistical measure that has a bias toward larger differences between measured and simulated responses. A smaller root-mean-square difference, indicates better agreement between simulated and measured responses. N is the number of measurements for a specific time.

The mean difference for a specific time is described as:

$$MD = \frac{\sum_{i=1}^N [V_{sim,i} - V_{meas,i}]}{N} \quad (\text{Eq. G-2})$$

A positive mean difference indicates a general overestimation of the measured variable, whereas the converse applies for a negative mean difference.

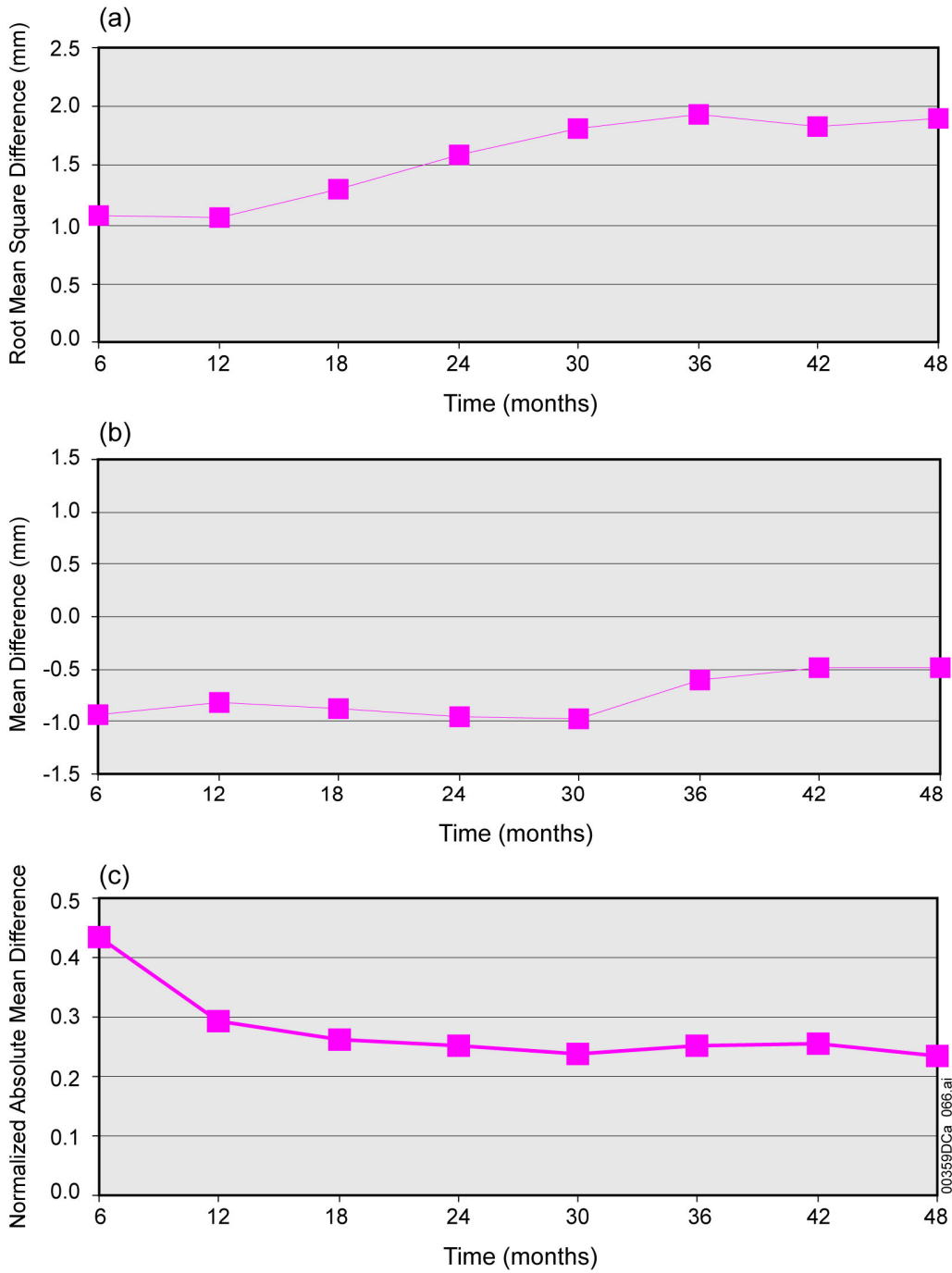
The normalized-absolute-mean difference for a specific time is described as:

$$NAMD = \sum_{i=1}^N \left| \frac{V_{sim,i} - V_{meas,i}}{V_{meas,i}^0} \right| \cdot \frac{1}{N} \quad (\text{Eq. G-3})$$

where $V_{meas,i}^0$ is measured displacement. Normalized-absolute-mean difference provides a percentage of the absolute difference between measured and simulated variables relative to the measured variable.

Figure G-15 presents the root-mean-square difference, mean difference, and normalized-absolute-mean difference for the simulated and measured displacements shown in Figure G-14. In Figure G-15a, the root-mean-square difference increases from about 1 mm at 6 months to about 2 mm at the end of the heating. Root-mean-square difference increases with time because of the increasing variability in measured displacement. The mean difference shows that the overall displacement field during the first 30 months is underestimated by about 1 mm, a number that is reduced to about 0.5 mm at the end of the heating period, Figure G-15b. The normalized-absolute-mean difference is about 45% at 6 months but is gradually reduced to less than 25% after 24 months of heating, Figure G-15c. Thus, as a whole, the displacements are well predicted at the DST and are clearly within the validation criterion of $\pm 50\%$ discussed in Section G.4.3.1.

The general agreement in the magnitude of displacement during the heating period confirms the findings by Sobolik et al. (1999, p. 741) and *Coupled Thermal-Hydrologic-Mechanical Effects on Permeability Analysis and Models Report* (BSC 2001b, pp. 21, 115 to 125), indicating that the intact-rock thermal expansion coefficient is an appropriate representation of the in situ thermal expansion coefficient at the DST. Also, the Single Heater Test was simulated using the intact-rock thermal expansion coefficient and showed generally good agreement with measured results (CRWMS M&O 1999, pp. 9 to 10).



Source: BSC 2004b, Figure 7.4.2-3.

NOTE: Statistical analyses leading to the curves presented in this figure are described in *Drift Scale THM Model* (BSC 2004b, Attachment II).

Figure G-15. Statistical Measures for Displacement Comparative Analysis

The finding that the intact-rock thermal expansion coefficient is appropriate seems to contradict results from separate determinations of a rock mass thermal expansion coefficient at the Single Heater Test and DST (CRWMS M&O 1999, pp. 9 to 11; BSC 2002, p. 6.3-35). In that case, the in situ thermal expansion coefficient was back-calculated directly from measured deformations and temperature changes along certain extensometers at the Single Heater Test and DST. The in situ thermal expansion coefficient determined by this method was about 50% lower than the intact-rock thermal expansion coefficient. This difference was attributed to some of the displacements being accommodated by closure of fractures. Two other causes contributed to this apparent contradiction between the results:

1. The in situ back-analyzed thermal expansion coefficients at the Single Heater Test and DST were determined from measurements in horizontal boreholes, whereas the comparison of measured and simulated displacements in *Drift Scale THM Model* (BSC 2004b, Section 7) was conducted for vertical or subvertical boreholes. The in situ thermal expansion coefficient along horizontal boreholes may be lower because vertical fractures are most abundant at the site.
2. The in situ back-analyzed thermal expansion coefficient at the Single Heater Test and DST is impacted by simultaneous increases in temperature and thermal stress and may, therefore, be different from the basic thermal expansion coefficient that is part of the input to a numerical model. The basic thermal expansion coefficient is a measure of the expansion of the rock for a temperature increase under constant stress. If the thermal expansion coefficient is determined under an increasing thermal stress, some of the rock expansion will be prevented, and the basic thermal expansion coefficient would be underestimated.

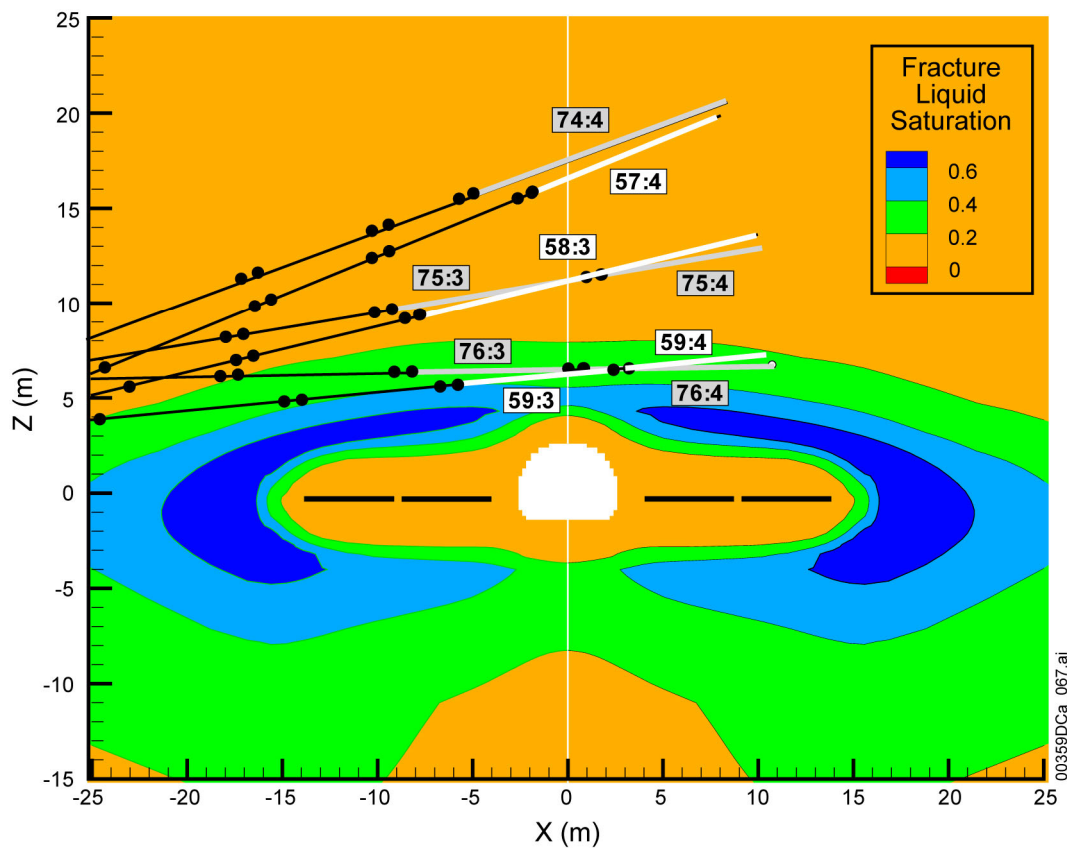
Nevertheless, the in situ back-analyzed thermal expansion is expected to provide a lower bound for the basic in situ thermal expansion coefficient, whereas the intact-rock thermal expansion coefficient is expected to provide an upper bound. In the vertical direction at the DST, the intact-rock thermal expansion coefficient is appropriate.

G.4.3.4.3 Validation for Thermal-Hydrologic-Mechanical Processes

The drift-scale thermal-hydrologic-mechanical model is validated for thermal-hydrologic-mechanical processes by comparing calculated against measured changes in absolute air permeability. The measured change in air permeability reflects two simultaneous processes: thermal-mechanical-induced changes in intrinsic permeability and thermal-hydrologic-induced changes in relative permeability for airflow. Thermal-mechanical-induced changes in intrinsic permeability result from thermal stresses associated with the heating of the rock mass. Thermal stresses act upon existing fractures, changing their aperture, which, in turn, may either increase or decrease the intrinsic fracture permeability. Thermal-hydrologic-induced changes are associated with thermally driven changes of moisture content in fractures. Wetting and drying in fractures (i.e., increase and decrease of liquid saturation) gives rise to changes in relative permeability for airflow.

Figure G-16 presents the simulated fracture liquid saturation after 12 months of heating and the location of boreholes for air-permeability measurement. The figure shows that a dryout zone has

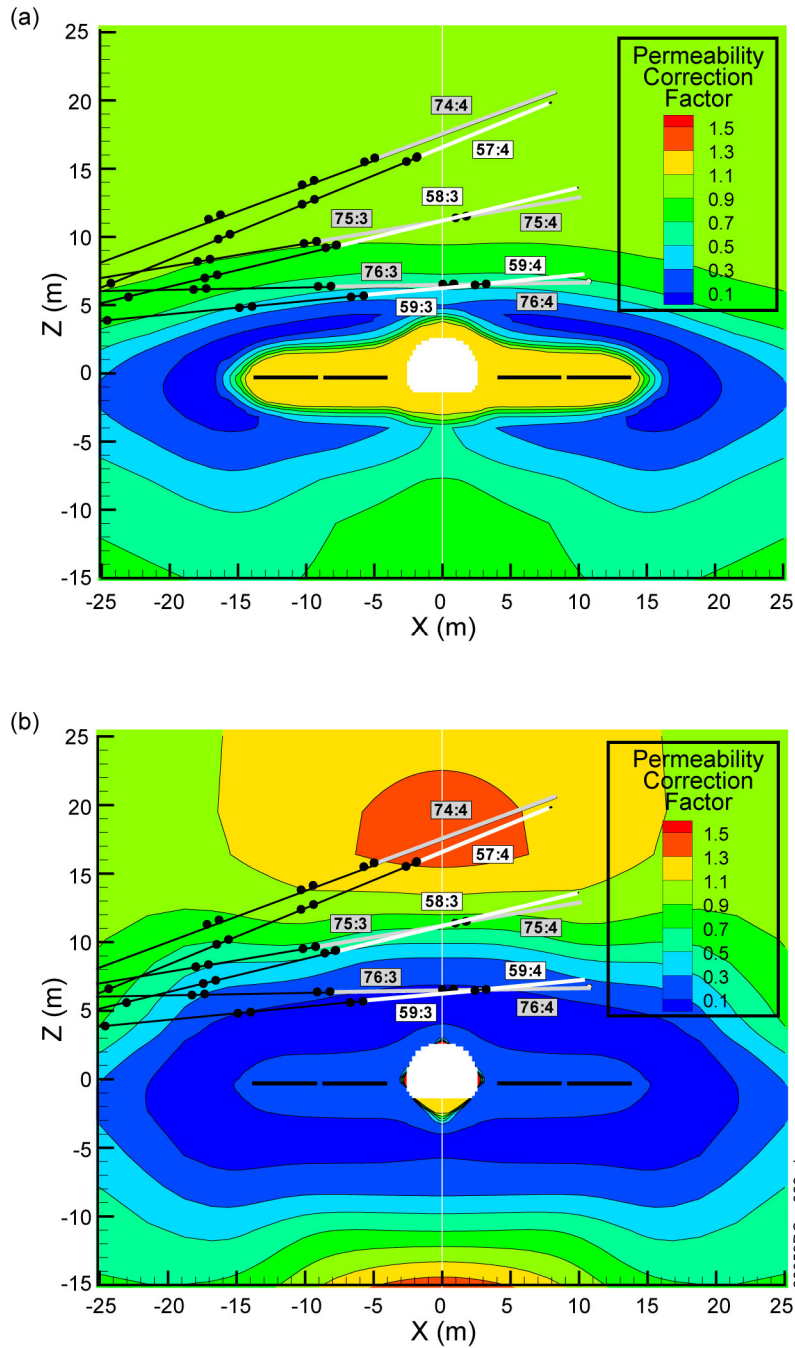
formed around the heated drift and wing heaters. Just outside the dryout zone, a zone of higher-than-ambient saturation forms because the produced vapor condenses in cooler areas. The dryout zone and the condensation zone move away from the heated drift over time. This movement is controlled by the flow of vapor away from the heat source along the thermal gradient and a reversed liquid flow along the pressure gradient toward the inner, dryer regions. In addition, there is a gravity-driven liquid flow that tends to drain the condensation zone above the heated drift. Air-permeability measurements performed in the condensate zone should exhibit a decrease in air permeability. Corresponding moisture-induced changes in relative permeability caused by the wetting and drying of fractures are shown in Figure G-17a. This figure shows that the increased fracture liquid saturation in the condensate zone causes a reduction in relative permeability to about 30% of its original value. In the dryout zone, the relative permeability has increased slightly from its original value because fractures in this zone are completely dry.



Source: BSC 2004b, Figure 7.4.3-1.

NOTE: Initial fracture liquid saturation is approximately 0.09.

Figure G-16. Simulated Distribution of Fracture Liquid Saturation after 12 Months of Heating and Location of Borehole Sections Where Simulated and Measured Air Permeability Is Compared



Source: BSC 2004b, Figure 7.4.3-2.

NOTE: (a) Changes in relative air permeability are caused by thermal-hydrologic-induced moisture redistribution. (b) Change in absolute air permeability is caused by the combined effect of moisture redistribution and stress-induced changes in intrinsic permeability. Numbers (e.g., 74:4, 57:4) label borehole sections for air-injection tests that are used for model validation.

Figure G-17. Simulated Changes in Air Permeability at the Drift Scale Test after 12 Months of Heating Expressed in Terms of Permeability Correction Factor Relative to Preheating Permeability

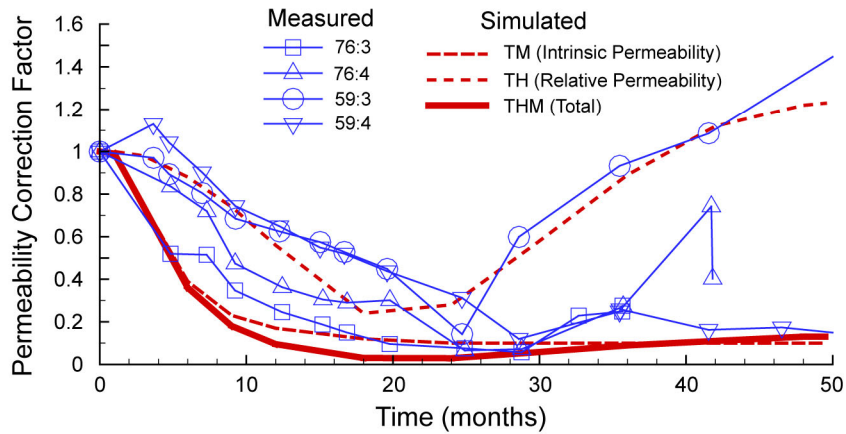
Figure G-17b shows the total permeability changes, combining thermal-hydrologic-induced relative permeability changes with thermal-mechanical-induced changes in intrinsic permeability. The figure shows that thermal-mechanical effects cause the permeability to decrease around the drift and wing heaters, including the inner dryout zone and the outer condensate zone. In the condensate zone, the permeability has decreased to about 10% of its original value. In Figure G-17b, a zone of increased permeability appears above the heated drift at about $z = 20$ m. This zone of increased permeability is caused entirely by thermal-mechanical effects, which are caused by open vertical fractures. Vertical fractures open in this area because of a reduction in horizontal stresses. This reduction causes the redistribution of horizontal stresses toward the heated drift to balance high thermal stresses near the heat source.

The calculated permeability changes are compared to air-permeability measurements in Figure G-18. The comparisons between calculated and measured responses are made at three locations about 6, 12, and 18 m above the center of the drift. At $z = 6$ m, four borehole sections; 76:3, 76:4, 59:3, and 59:4 are located symmetrically around $x = 0$ m (see Figure G-17). In these sections, the air permeability first decreases with time to reach a minimum at about 24 months. Thereafter, the permeability increases slightly in three of four borehole sections and increases dramatically in the fourth (Figure G-18a). The figure compares measured changes in air permeability at the four borehole sections with calculated changes in permeability. The solid line indicates the calculated changes in air permeability, which are the product of the intrinsic permeability (thermal-mechanical effect) and gas relative permeability (thermal-hydrologic effect). The figure shows that the solid line representing the combined thermal-hydrologic and thermal-mechanical effects matches three of four measurements best. In the fourth section, 59:3, the measured changes appear to match a pure thermal-hydrologic response the best.

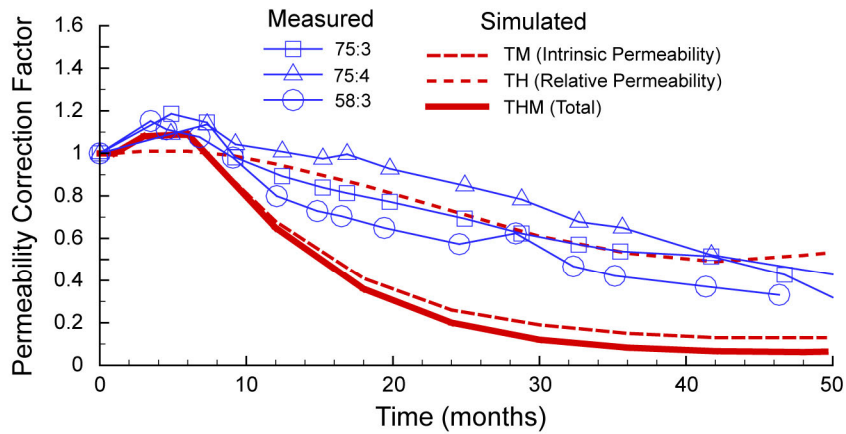
At about $z = 12$ m, borehole sections 75:3, 75:4, and 58:3 are located symmetrically around $x = 0$ m and between $z = 10$ and 14 m. Measured responses in these three boreholes are consistent, with an initial increase in air permeability during the first 9 months, followed by a gradual decrease until the end of heating (Figure G-18b). The decrease in permeability can be interpreted either as a change in intrinsic permeability (thermal-mechanical), or as a change in relative permeability (thermal-hydrologic), or a combination of the two (thermal-hydrologic-mechanical). However, the initial increase during the first 9 months can only be explained as a thermal-mechanical response. Although the trend of decreasing permeability from 9 to 50 months is captured in the simulation, the simulated changes in permeability are stronger than the measured ones. As will be discussed in more detail in the last paragraph of this section, this shows that the stress-versus-permeability function used in the numerical modeling provides a bounding case of a maximized impact of stress on permeability.

For the measurements located farthest from the drift, 74:4 and 57:4 at z of approximately 18 m, there is an increase in air permeability caused by thermal-mechanical-induced changes in intrinsic permeability (thermal-mechanical in Figure G-18c). At this location, far from the heated drift, no effect from thermal-hydrologic-induced changes appears until about 36 months, when a slight wetting starts to take place.

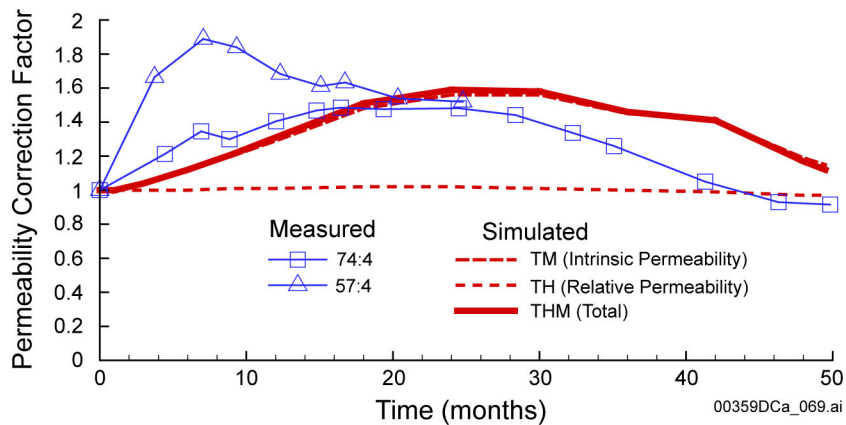
(a) Group located at z approximately 6 m



(b) Group located at z approximately 12 m



(c) Group located at z approximately 18 m



Source: BSC 2004b, Figure 7.4.3-3.

NOTE: $b_{max} = 200 \mu\text{m}$; $\alpha = 0.52 \text{ MPa}^{-1}$.

Figure G-18. Measured and Simulated Evolution of Permeability Correction Factors for Three Groups Located at Various Distances above the Heated Drift

The results in Figure G-18 are calculated with the parameters of b_{max} equal to 200 μm and α equal to 0.52 MPa^{-1} , as developed in *Drift Scale THM Model* (BSC 2004b, Section 6.4). The overall simulated changes in air permeability using those parameters are in agreement with the measured change, and the validation criterion discussed in Section G.4.3.1 is met. That is, the predicted changes in air permeability are in the correct direction and correct within an order of magnitude: $\log(k/k_i)$ simulated and measured values differ by less than 1. Observed trends (e.g., k/k_i decreases followed by increases, or the reverse) are matched by model predictions. The predicted thermal-hydrologic-mechanical responses are, on average, stronger than the measured ones, and, hence, the stress-aperture function defined by the a b_{max} value of 200 μm and a α value of 0.52 MPa^{-1} can be considered a bounding set of parameters that maximize the effects of stress on permeability. As a sensitivity case, a second simulation is conducted with a more moderate stress-aperture function defined by a b_{max} value of 150 μm and a α value of 0.6 MPa^{-1} . The results of this simulation show a better agreement with the average observed hydrologic-mechanical behavior at the DST (Figure G-19).

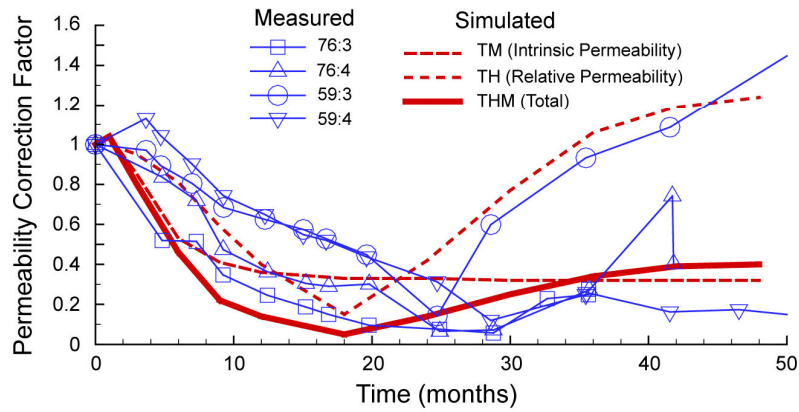
G.4.3.5 Validation against Niche Excavation Tests

An additional validation of the drift-scale thermal-hydrologic-mechanical model was conducted against observed permeability changes adjacent to underground excavations at Yucca Mountain. The permeability changes were observed using air-permeability measurements before and after excavation of three excavated niches located in the Tptpmn unit and one niche located in the Tptpll unit. These tests were conducted to study permeability changes near a drift wall caused by excavation effects (i.e., mechanical unloading of the rock mass near the drift wall, causing fracture opening and consequent permeability increase). In the Tptpmn unit, the air permeability was measured before and after excavation in 0.3 m packer-isolated sections along three boreholes located about 0.65 m above the niches (BSC 2003b, Section 6.1). The boreholes located at about 0.65 m above the drift are denoted UM (upper middle), UL (upper left), and UR (upper right). These boreholes are located at the same elevation (about 0.65 m above the drift), with UM located above the centerline of the drift and UR and UL located about 1 m to the right and left of the centerline, respectively. One data point of the permeability-change ratio was extracted from this data set (BSC 2004b, Section 6.4) to determine the parameters b_{max} and α . The validation performed in this section investigates the validity of the stress-permeability model and the stress-aperture function over a range of initial permeability values. These calculated changes in permeability were derived using an Excel spreadsheet, as described in *Drift Scale THM Model* (BSC 2004b, Attachment III).

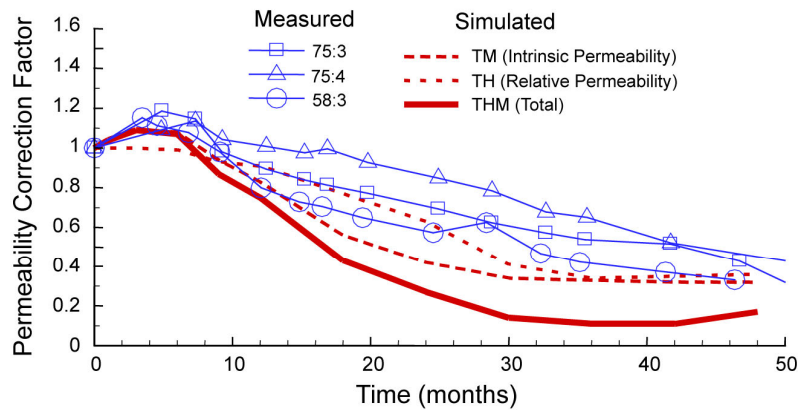
In this study, the niche excavations were modeled using the FLAC3D V2.0 code to calculate changes in the stress field. A model of the niches is described by Rutqvist (2002, p. 14). Based on the calculated stress field, the excavation permeability correction factors $F_{k_{xe}}$, $F_{k_{ye}}$, $F_{k_{ze}}$ in the x, y, and z direction are calculated (BSC 2004b, Attachment III). Figure G-20 compares calculated and measured preexcavation to postexcavation ratios for the four niches. The calculated values are within the scatter of the measurements, and the calculation appears to represent an average hydrologic-mechanical behavior at the niches. Furthermore, the calculation correctly captures the observed trend that, in general, permeability changes more in initially lower-permeability sections. A scatter of the measured data in Figure G-20 of orders of magnitude is not surprising, considering that a very short packer spacing of 0.3 m was used. The

drift-scale hydraulic properties are derived from the mean values of such packer tests, and, therefore, the validation of the numerical model should be toward the mean permeability changes.

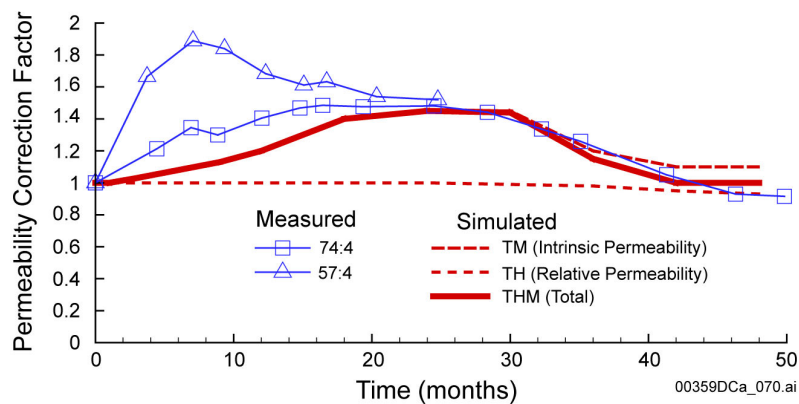
(a) Group located at z approximately 6 m



(b) Group located at z approximately 12 m



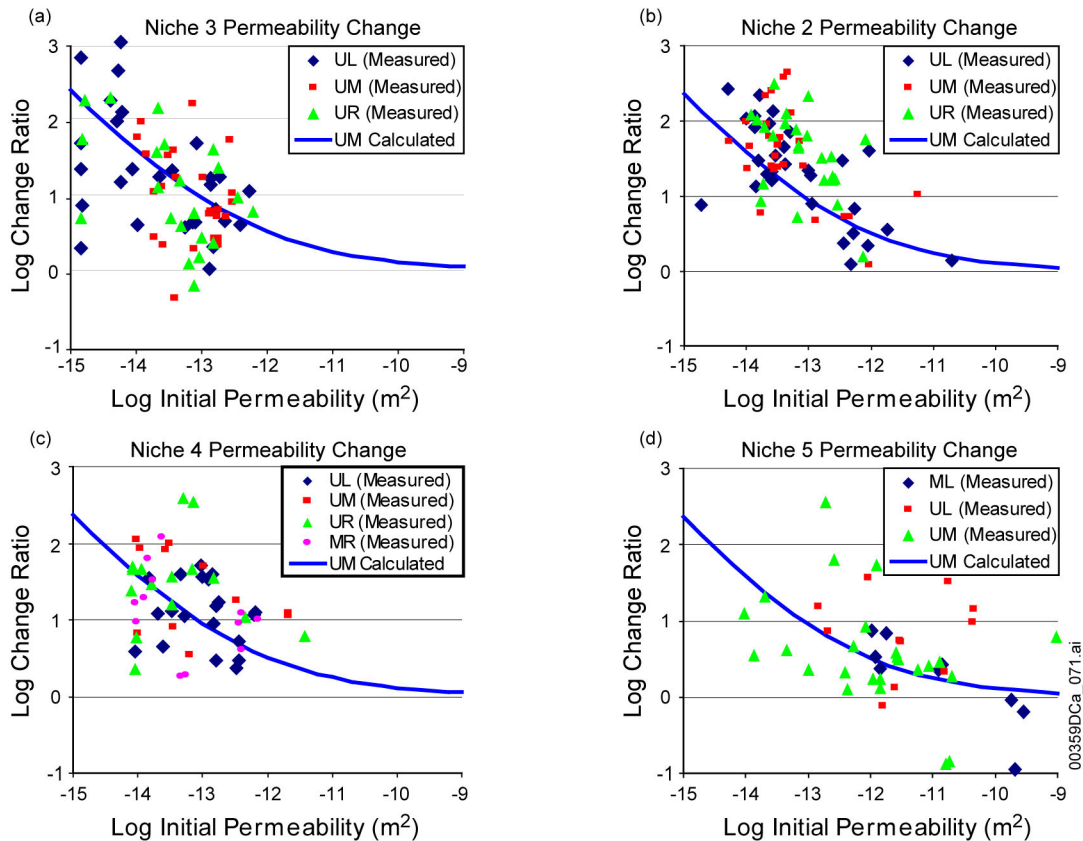
(c) Group located at z approximately 18 m



Source: BSC 2004b, Figure 7.4.3-4.

NOTE: $b_{max} = 150 \mu\text{m}$; $\alpha = 0.6 \text{ MPa}^{-1}$.

Figure G-19. Measured and Simulated Evolution of Permeability Correction Factors for Three Groups Located at Various Distances above the Heated Drift

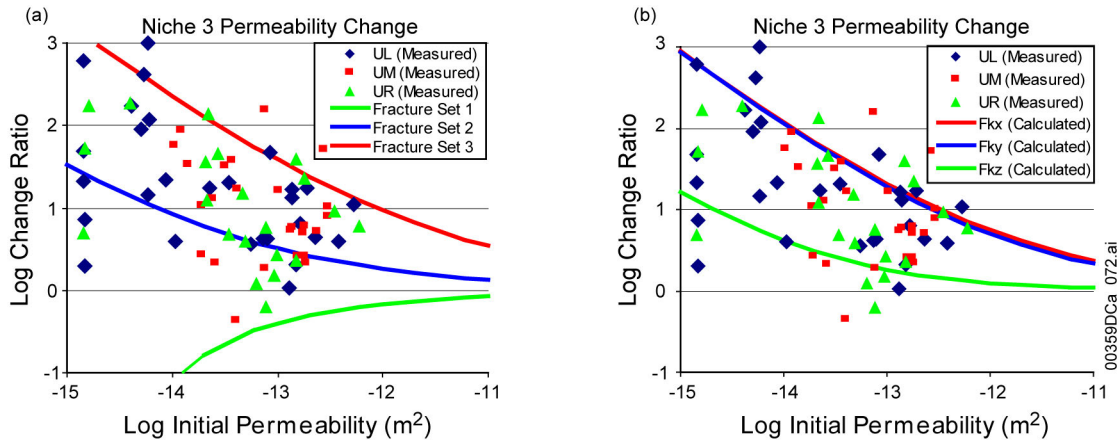


Source: BSC 2004b, Figure 7.5-1.

NOTE: UM is located above the drift along the centerline of the drift. UL and UR are located at the same elevation but about 1 m to the left and right of the centerline, respectively. Calculation is conducted with $b_{max} = 200 \mu\text{m}$ and $\alpha = 0.52 \text{ MPa}^{-1}$. The calculation of the lines for UM calculated is described in *Drift Scale THM Model* (BSC 2004b, Attachment III).

Figure G-20. Measured and Calculated Permeability Change Ratio at Niche 2, Niche 3, and Niche 4 in the Tptpmn Unit and Niche 5 in the Tptpl Unit

The variability in preexcavation to postexcavation ratios at a fixed initial permeability can be explained by mechanical responses in fractures belonging to different fracture sets (Figure G-21a). The largest permeability increases can occur as a result of opening of fractures in Set 3, which is a horizontal fracture set. Such large permeability increases could occur for the extreme case of a borehole interval connected only to horizontal fractures. Another extreme is the case in which the borehole is connected to a fracture of Set 2, in which the fractures are vertical, striking along the drift. Theoretically, this could give a significant reduction in permeability. However, the network at the Tptpmn and Tptpl units are highly fractured, and, therefore, a strong reduction in permeability caused by fracture closure in one fracture set only is unlikely. Although fractures in Set 2 would be close to their residual value, it is likely that they are connected to vertical fractures that are kept open. Fracture Set 1 is oriented perpendicular to the borehole axis and is, therefore, the most likely to intersect the borehole. Figure G-21b illustrates the calculated permeability changes in different directions (x, y, and z) and shows that permeability increases in all three directions, with most of the changes occurring in the horizontal permeability.



Source: BSC 2004b, Figure 7.5-2.

NOTE: Calculation is conducted with $b_{max} = 200 \mu\text{m}$ and $\alpha = 0.52 \text{ MPa}^{-1}$. The calculations resulting in the three lines (blue, red, and green) in (a) and (b) are described in *Drift Scale THM Model* (BSC 2004b, Attachment III).

Figure G-21. Measured and Simulated Permeability-Change Ratio at Niche 3: (a) Comparison to Simulated Permeability-Change Ratio in the Three Fracture Sets and (b) Comparison to Permeability Correction Factors in x, y, and z Direction

In summary, the good agreement between calculated mean value and trends in both the Tptpmn unit (Figures G-20a to G-20c) and Tptpll unit (Figure G-20d) shows that the stress-permeability model of the drift-scale thermal-hydrologic-mechanical model is applicable for both Tptpmn and Tptpll units over their entire range of initial permeability values. The model is also able to explain the local variability of permeability-change factors as the impact of fracture orientation for fractures intersecting the borehole (Figure G-22). For the air-permeability test conducted in the Tptpll unit, some extreme permeability changes occur (even at high initial permeability) that cannot be captured in the model. The presence of lithophysae may have impacted the measurements. In general, the measurements conducted at 1-ft borehole length are difficult in the Tptpll unit, since it contains lithophysal cavities that can be larger than 1 ft in diameter.

G.4.3.6 Validation against Observations of Sidewall Fracturing in the Enhanced Characterization of the Repository Block Cross-Drift

This section presents the validation of the mechanical model and the in situ strength properties of lithophysal rock against observations of minor damage in the sidewalls of the ESF main drift and ECRB Cross-Drift (BSC 2004d, Section 7.7.5.3). The lithophysal rock properties were extracted from *Drift Degradation Analysis* (BSC 2004d, Attachment V, Table V-9). Also, the mechanical properties of the lithophysal units were divided into several categories ranging from poor-quality (Category 1) to good-quality (Category 5) lithophysal rock, and the mechanical properties for Category 1 and 5 lithophysal rock are provided (BSC 2004d, Table 7.6-1).

G.4.3.6.1 Validation Method

The validation is checked against field observations of Tptpll and Tptpul units and against an alternative model of the drift degradation analysis. The mechanical properties derived for the poor-quality lithophysal rock are verified by comparison of predicted yielding to minor damage

observed in the sidewalls of the ESF main drift and ECRB Cross-Drift (BSC 2004d, Section 7.7.5.3). The consistency of this analysis with field observations and the alternative model provides confidence in the mechanical model and the mechanical properties derived for the poor-quality lithophysal rock.

G.4.3.6.2 Summary of Field Observations

Tunnels in rock units at Yucca Mountain are stable after excavation, regardless of depth or rock quality. However, some damage, in the form of wall-parallel fractures (opening of existing fracture fabric) at the springline, the point of highest shearing stress, can be observed in the sidewalls of the tunnels at greater depth in the Tptpll (BSC 2004d, Section 7.7.5.3). Figure G-22 shows formation and opening of wall-parallel fractures observed in 12-in.-diameter boreholes drilled for geomechanical sampling in the sidewalls of the ESF main drift and ECRB Cross-Drift at the tunnel springline. The wall-parallel fractures are typical of stress-induced yield in tunnels. The boreholes drilled in the relatively poor-quality Tptpll at depths of 300 to 350 m show sidewall fracturing to depths of approximately 0.5 to 0.6 m. On the other hand, holes drilled into relatively high quality Tptpul at depths of approximately 200 to 250 m show no fracturing (BSC 2004d, Section 7.7.5.3). The observed fracturing in the Tptpll and its depth into the drift wall and the observed lack of fracturing in the shallower Tptpul can be utilized to estimate the in situ rock mass strength properties and for model validation.



Source: BSC 2004d, Figure 170.

NOTE: Top photo shows sidewall fracturing and opening of preexisting wall-parallel fractures in a 12-in.-diameter horizontal borehole drilled in the springline of the ESF in poor quality Tptpl (approximately Category 1). Overburden depth is approximately 325 m. Depth of fracturing is approximately 1.5 to 2 ft. The bottom photo shows a horizontal, 12-in.-diameter borehole drilled in the springline in good quality Tptpul (approximately Category 5) in the ESF showing no sidewall damage. The depth of overburden is approximately 250 m.

Figure G-22. Observed Rock Mass Conditions at the Tunnel Springline in Lithophysal Rock in the Exploratory Studies Facility

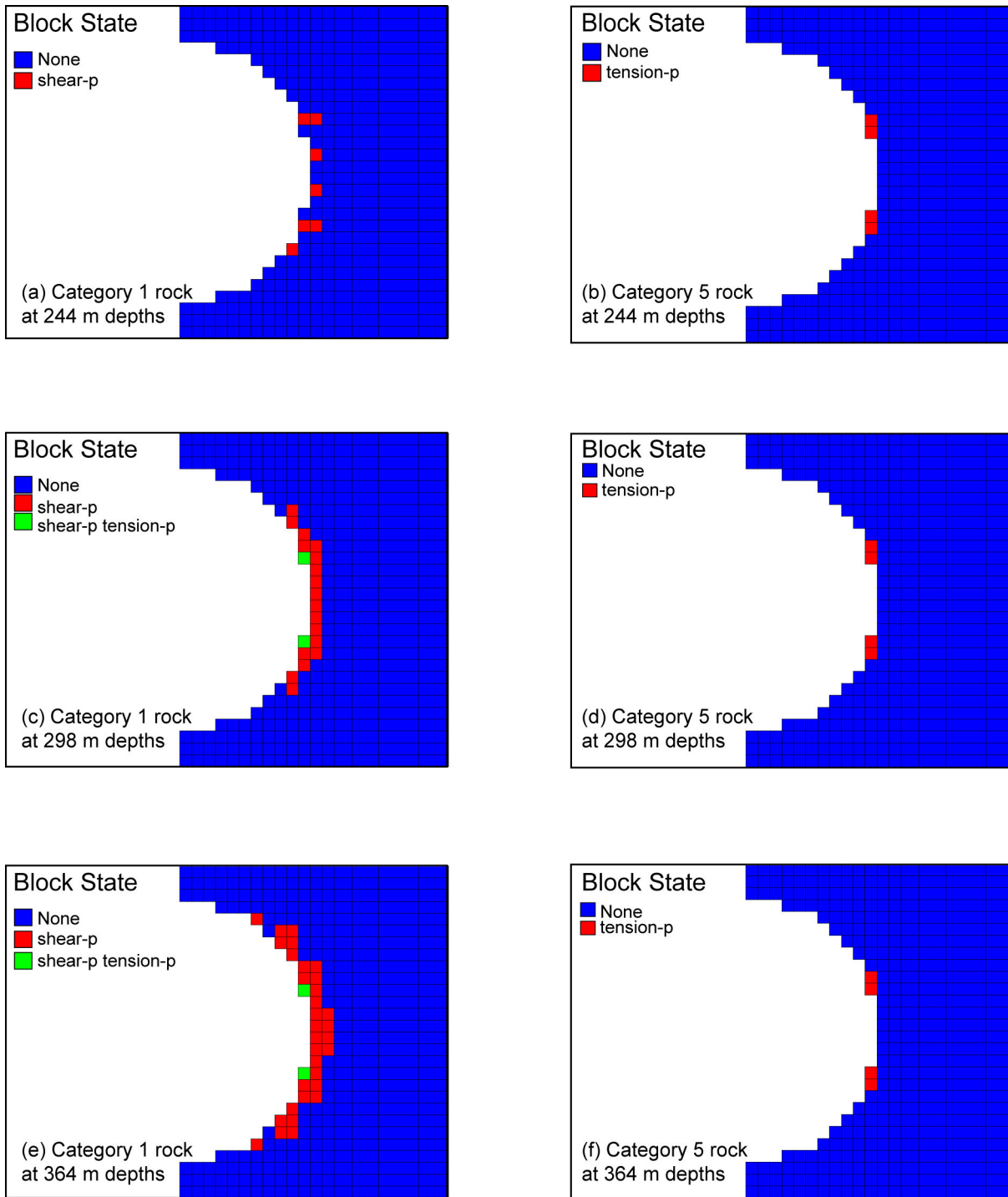
G.4.3.6.3 Calculation Results for Tptpl and Tptpul Units

Similar to an analysis made in *Drift Degradation Analysis* (BSC 2004d, Section 7.7.5.3), a parametric study of rock yield depth was conducted using FLAC3D for Category 1 (poor quality lithophysal rock) and Category 5 (good quality lithophysal rock). The analysis was conducted for an imposed overburden depth of between 244 and 364 m. A Mohr-Coulomb material model was used with material parameters for poor and good quality lithophysal rock given in Table G-3. As shown in Figure G-23, the model reproduces the approximate depth of observed underground sidewall damage for strength Category 1. The model results indicate that the rock adjacent to the drift wall yields in a state of uniaxial compression, because the minimum stress at or near the drift wall is zero or small (since the radial stress component is zero). The models also show that, for the range of potential lithophysal rock properties, there is no drift-wall yield at the depth of the Tptpul from strength Category 1. Some of the yield seen in Figure G-23 (e.g., for Category 5 above and below the springline) may be caused by the discretization of the circular drift shape, using square elements.

Table G-3. Mechanical Properties Used for Model Validation against Observations of Sidewall Fracturing in the Enhanced Characterization of the Repository Block Cross-Drift

Mechanical Property	Category 1	Category 5
Young's Modulus E (GPa)	1.9	19.7
Bulk Modulus (GPa)	1.07	10.95
Shear Modulus (GPa)	0.80	8.21
Cohesion (MPa)	2.33	7.00
Friction Angle (Degrees)	40	40
Tensile strength (MPa)	0.8	0.8

Source: Bulk modulus, shear modulus, cohesion, and friction angle are from BSC 2004d, Attachment V, Table V-9. Tensile strength is from BSC 2004d, Figure 166.



00359DCa_074.ai

Source: BSC 2004b, Figure 7.6.3-1.

NOTE: For Category 1 rock, the yield zone at the sidewall extends about 0.25 to 0.5 m (1 to 2 ft) into the sidewall when the depth increases from 298 to 364 m. Fracturing was observed to extend about 1 to 2 ft into the sidewall in a section of the ECRB Cross-Drift located in poor quality rock at a depth of 325 m.

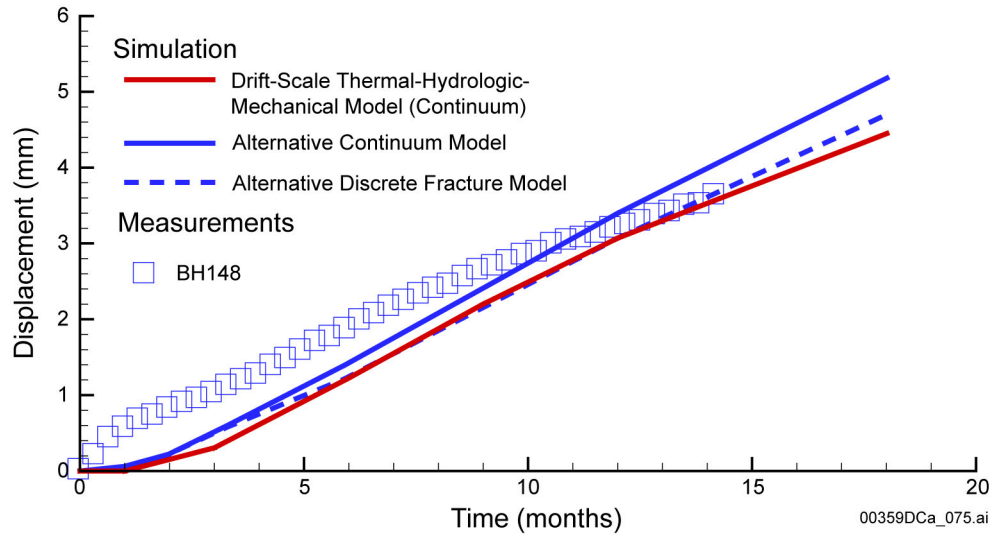
Figure G-23. Extent of Yield Zone for a Drift Located at 244, 298, and 364 m for Category 1 Rock and Category 5 Rock

G.4.3.6.4 Comparison with Alternative Model of Drift Degradation Analysis

The results of this analysis are consistent with simulation results presented in *Drift Degradation Analysis* (BSC 2004d, Section 7.7.5.3), using an alternative modeling approach. In *Drift Degradation Analysis* (BSC 2004d), the fracturing in the side wall was simulated using the distinct element model UDEC, which is conceptually different from the continuum approach used in this study. In both models (the distinct element model and the continuum model), inelastic deformations and yielding take place on the side of the drift and not on the top of the drift. Furthermore, both models predict a yielding of about 0.5 m at the springline (compare Figure G-23 with BSC 2004d, Section 7.7.5.3, Figures 171 and 172).

G.4.3.7 Comparison to an Alternative Conceptual Model

An additional validation of the drift-scale thermal-hydrologic-mechanical model is conducted by comparing this model to the results of a previous analysis of the DST. In *Coupled Thermal-Hydrologic-Mechanical Effects on Permeability Analysis and Models Report* (BSC 2001b, Section 6.4.2), the first 18 months of the DST was simulated by two separate three-dimensional analyses, one using a continuum-based model and one using a discrete-fracture model. In both simulations, the thermal expansion coefficient was set to $9.73^{\circ}\text{C}^{-1}$. In Figure G-24, the simulated results are compared to a separate simulation using the drift-scale thermal-hydrologic-mechanical model for displacement at Anchor 4 in borehole 148. In this analysis, the drift-scale thermal-hydrologic-mechanical model was applied using an equivalent value of the thermal expansion coefficient ($9.73^{\circ}\text{C}^{-1}$). It can be concluded that the three separate models analyzing the DST—the two continuum-based models and one discrete-element model—provided similar results in magnitude and trend, even taking into account differences in model discretization. The good agreement between the drift-scale thermal-hydrologic-mechanical model and the alternative discrete-fracture approach shown in Figure G-24 is typical for comparisons made at several anchors around the DST. The good agreement between the independent numerical models provides great confidence for the validation of the thermal-mechanical part of the drift-scale thermal-hydrologic-mechanical model. Moreover, the results in Figure G-24 support a continuum approach being sufficient to model the thermal expansion of the rock mass.



Source: BSC 2004b, Figure 7.7-1.

NOTE: The simulation results of the alternative discrete fracture model and alternative continuum model have been extracted from *Coupled Thermal-Hydrologic-Mechanical Effects on Permeability Analysis and Models Report* (BSC 2001b, Figure 6.4.2-12, p. 121). These simulation results are compared to simulation results using the drift-scale thermal-hydrologic-mechanical model.

Figure G-24. Simulated and Measured Evolution of Displacements at Anchor 4 in Multiple-Point Borehole Extensometer Borehole 148

G.4.3.8 Multiple Lines of Evidence

The impact of thermal-hydrologic-mechanical processes (e.g., excavation and heating) on the performance of the repository has been assessed through field studies at a variety of underground sites. These studies indicate that the effects of excavation on rock stability tend to be highly site-specific, depending on rock physical properties, the presence and orientation of faults and fractures, and the local stress regime. Excavation often leads to localized increases in permeability. Heating generally results in an increase in stress and a reduction in permeability due to thermal expansion. The general results of a number of thermal-hydrologic-mechanical experiments conducted at the Nevada Test Site and other fractured rock sites are described below for multiple lines of evidence in support of the drift-scale thermal-hydrologic-mechanical model.

G.4.3.8.1 Nevada Test Site Thermal-Hydrologic-Mechanical Experiments

Four thermal-mechanical/thermal-hydrologic-mechanical experiments relating to high-level radioactive waste research were conducted at the G-tunnel in Rainier Mesa. These tests included a single borehole heater test, a small-diameter heater test, a heated block test, and a prototype engineered barrier system field test. One objective of the heated block test was to measure rock mass mechanical and thermal-mechanical properties of ash-flow tuff under controlled thermal- and stress-loading conditions. The block was subjected to maximum temperatures ranging from 76°C to 130°C and equal biaxial stresses with magnitudes up to 10.6 MPa (Zimmerman et al. 1986). The effective modulus of deformation ranged from 0.4 to 0.83 times the intact rock measurements, depending on the number of joints included and their apertures. A

slight dependence of modulus on stress was indicated, but no significant temperature effects on modulus were identified.

A second objective of the heated block test was to determine the effects of excavation, stress, and temperature changes on the permeability of a single joint. The permeability of a single near-vertical fracture was measured using three vertical boreholes in a linear array. The largest changes in permeability were associated with excavation of the block, when the apparent permeability increased from 76 to 758 microdarcies. Subsequent compressive loading decreased the permeability but did not completely reverse the unloading conditions, and the apparent permeability ranged from 252 to 332 microdarcies over a stress range of 3.1 to 10.6 MPa (Hardin and Chesnut 1997, pp. 4 to 6). Increased temperature under biaxial confinement decreased the fracture aperture, lowering the apparent permeability from 234 to 89 microdarcies during heating caused by rock thermal expansion. These observations are consistent (i.e., of the same order of magnitude) with the thermal-hydrologic-mechanical modeling and field studies described earlier. That is, fracture permeability increases about 1 order of magnitude as a result of unloading during excavation and decreases by less than 1 order of magnitude during heating.

G.4.3.8.2 Underground Testing at Stripa Mine

A time-scaled heater test was performed at Stripa Mine to investigate the long-term thermal-mechanical response to thermal loading (Chan et al. 1980). Analysis showed that, in the full-scale and time-scale heater tests, heat flow conformed to linear conduction theory and was not affected by fractures or other discontinuities. Thermoelastic deformation of the rock mass was nonlinear and less than expected. Early in the tests, measured displacements were much less than predicted by linear thermoelasticity. Later, the displacements increased uniformly but in fixed proportions to predicted levels. This was likely a result of the closing of fractures in response to thermal expansion. Fracture closure was confirmed by observation of diminished water inflow to the heater and instrument boreholes (Nelson et al. 1981, p. xi) and by increased compressional wave velocity during heating (Paulsson et al. 1980, p. 4). The closing of fractures (and resulting changes in fracture permeability due to thermal input) is consistent with the results of the studies described in this appendix.

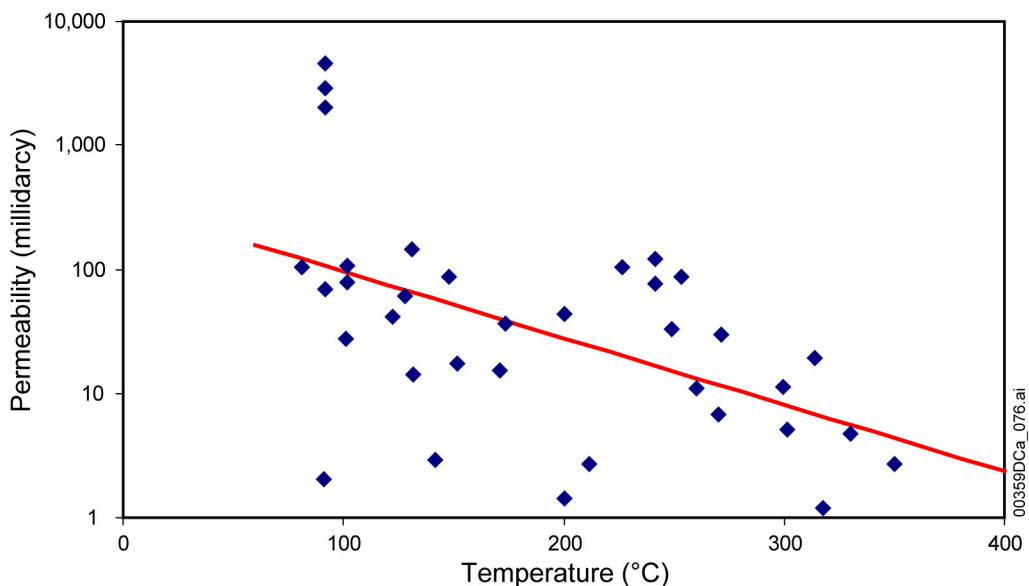
G.4.3.8.3 DECOVALEX Findings at Fanay-Augères and Kamaishi Mine Heater Tests

The results in the *Drift Scale THM Model* (BSC 2004b) can also be compared to findings in the international cooperative project DECOVALEX (DEvelopment of COupled Models and their VALidation against EXperiments in nuclear waste isolation). Model validation against in situ tests, such as Fanay-Augères (Rejeb 1996) and Kamaishi Mine (Rutqvist, Börgesson et al. 2001), demonstrates that the temperature field can be predicted with confidence because it is mainly governed by heat conduction through rock masses, with little influence from discrete fractures. Rock mass deformation measured along extensometers between anchors placed several meters apart can also be predicted reasonably well in trends and magnitudes. This is because the bulk thermal expansion of the rock is dominated by the thermal expansion of the matrix rock, while fractures have a secondary effect that appears as a reduction of the rock-mass thermal expansion coefficient. It can also be concluded from these two heater tests that the general thermal expansion of the rock mass is essentially elastic for measurements conducted over several meters of fractured rock. However, although the bulk thermal expansion of the rock mass is essentially

elastic and reversible, the displacement and aperture changes measured over individual fractures are generally irreversible. That is, there is a remaining change in fracture aperture after the rock mass has cooled to ambient conditions. Furthermore, it is generally much more difficult to predict the responses of individual fractures than to predict the overall rock mass thermal expansion. This might be important for predicting changes in hydraulic permeability, which critically depend on the changes of fractures apertures.

G.4.3.8.4 Geothermal Reservoir Temperature-Permeability Correlation

In addition to field studies of coupled thermal-hydrologic-mechanical processes that provide direct evidence of how the repository would perform, corroborative results for coupled thermal-hydrologic-mechanical effects may be found in the geothermal literature. A survey of geothermal reservoir properties worldwide (Björnsson and Bodvarsson 1990, pp. 19 to 21) showed a correlation between permeability and temperature for various geothermal systems (Figure G-25). The values are scattered, but they indicate a trend toward decreasing permeability with increasing temperatures. Geochemical effects more likely cause the low permeability at temperatures around 300°C and above. Thermal-hydrologic-mechanical effects may be present at lower temperatures.



Source: BSC 2004b, Figure 7.8.4-1.

Figure G-25. Correlation between Permeability and Temperature for Geothermal Reservoirs Worldwide

G.4.3.8.5 Coupled Thermal-Hydrologic-Mechanical Analyses of the Drift Scale Test within DECOVALEX III

The thermal-mechanical and thermal-hydrologic-mechanical responses of the DST were independently analyzed by the participants of the DECOVALEX III project, which is an international research project for development of coupled models and their validation against experiments. The outcome of the analyses by the DECOVALEX participants, generally corroborative of the Yucca Mountain coupled thermal-hydrologic-mechanical-process models,

was presented in the GeoProc2003 conference held in Stockholm, Sweden, in October 2003 (Datta et al. 2003; Rutqvist, Tsang et al. 2004; Hsiung et al. 2003; Green and Painter 2003; Olivella et al. 2003; Millard and Rutqvist 2003).

Three independent analyses presented by Rutqvist, Tsang et al. (2004), Green and Painter (2003), and Olivella et al. (2003) show a good agreement in the results of moisture redistribution around the drift. The formation of a dryout zone and its extent at various times is consistent for these three independent analyses.

Millard and Rutqvist (2003) compare the predictions of mechanical displacement using the Yucca Mountain coupled thermal-hydrologic-mechanical process model to an independent model analysis conducted by a research team from the Commissariat à l'Énergie Atomique de Cadarache (CEA) in France. It was concluded that the displacement predicted by the two independent analyses compared reasonably well to the measured ones, both in trends and average magnitude. Both analyses showed that the in situ rock mass thermal expansion coefficient is appropriately represented by a temperature-dependent thermal-expansion coefficient derived from intact rock samples. Finally, the two analyses indicate that rock behavior is essentially elastic, although a few instances of inelastic behavior can be observed near the drift wall. The results of displacements presented by the two models described by Millard and Rutqvist (2003) also agree with the results of displacements calculated by a third model, presented by Hsiung et al. (2003).

Permeability changes calculated using the Yucca Mountain coupled thermal-hydrologic-mechanical-process model (Rutqvist, Tsang et al. 2004) are generally in agreement with permeability changes calculated with two other models (Olivella et al. 2003; Hsiung et al. 2003). The analyses by Rutqvist, Tsang et al. (2004) and Hsiung et al. (2003) consistently show that fracture aperture change caused by changes in stress normal to fractures is the dominating mechanism of permeability changes. Thus, permeability changes caused by shear slip appear to be small compared to changes by normal stress.

The papers from the GeoProc2003 conference will be published in Elsevier Sciences Book Series on Engineering Geology. Furthermore, the results of DECOVALEX III is to be published in an upcoming special issue of the *International Journal of Rock Mechanics and Mining Sciences*.

G.4.3.8.6 Validation by Publication in Peer-Reviewed Journals

The models have also been published in several international journals, undergoing scientific peer-review of the adopted concepts. The TOUGH2-FLAC3D simulator was presented in the *International Journal of Rock Mechanics and Mining Sciences* in 2002 (Rutqvist, Wu et al. 2002). This paper includes the fundamental theories and underlying conceptual models for the TOUGH2 code, the FLAC3D code, and the coupling functions between the two codes. An application of the simulator for a drift-scale thermal-hydrologic-mechanical analysis of the repository has been published in a special issue of the *Journal of Contaminant Hydrology* (Rutqvist and Tsang 2003). The result and the general conclusions of the published analysis are consistent with the results presented in *Drift Scale THM Model* (BSC 2004b). An application of the TOUGH2-FLAC3D code to problems related to hydrologic-mechanical processes in the geologic sequestration of greenhouse gases has been published (Rutqvist and Tsang 2002).

G.4.3.9 Discussion of Validation Activities

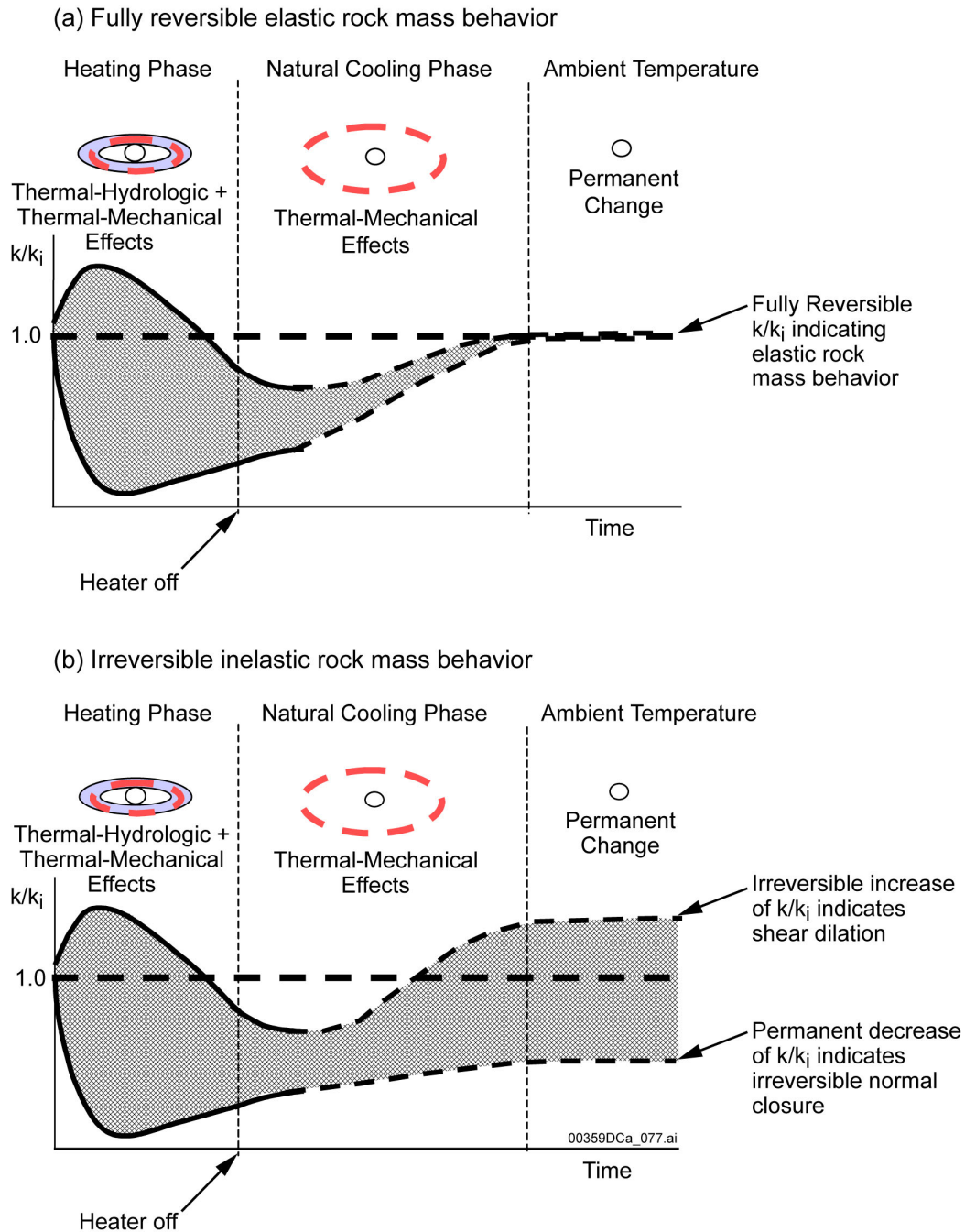
The comparison of the coupled thermal-hydrologic-mechanical model results against DST heating-phase data indicates that relevant processes are well represented by the model. In general, calculated responses are within the range of measurements and aspects that remain uncertain. The present analysis of the DST heating phase shows that the drift-scale thermal-hydrologic-mechanical model is valid for the analysis of coupled thermal-hydrologic-mechanical processes and that the underlying conceptual model is sound.

Furthermore, the analysis shows that the conceptual model for hydrologic-mechanical coupling is valid. This validation indicates that fracture opening and closing caused by changes in normal stress is the dominant mode of permeability changes. Mechanical responses in the DST indicate that no significant shear slip occurs, except possibly in isolated instances, such as the event in Anchor 1 of borehole 154 (discussed above). The measured change in air permeability at the DST does not show any widespread increase. Although a few increases in permeability have been observed, they appear to be isolated to one packed-off section, while no such increase can be noticed in neighboring sections. This observation provides further evidence that shear-induced permeability enhancement is not significant and that fracture opening or closure by changes in normal stress are the dominant modes of permeability changes.

The air-permeability measurement during the natural cooling phase of the DST will be extremely helpful for confirming the stress-aperture function and for observing potential irreversible (permanent) permeability changes. For an elastic rock mass, mechanical deformations and permeability changes would be fully reversible, meaning that after the temperature declined to ambient, MPBX displacements and air permeability would go back to their original values (see Figure G-26a). However, irreversible changes will almost certainly occur in permeability and displacement after the temperature has declined to ambient (Figure G-26b). Although rock mass behavior is essentially elastic, small irreversible inelastic changes are still expected. Trends in displacement and permeability changes at the DST so far indicate that the irreversible changes in permeability will be small, most certainly not larger than 1 order of magnitude.

The findings here are generally supported by studies of similar heater tests, such as tests at Stripa Mine, Fanay-Augères Mine, and Kamaishi Mine (Section G.4.3.5.3). In particular, the temperature field and the bulk thermal expansion of the rock can be predicted with confidence using a simple thermoelastic model. Analyses of Fanay-Augères and Kamaishi Mine experiments indicate that predicting the magnitude displacements at individual points of the rock mass and over individual fractures can be difficult. However, the rock mass characteristics at Yucca Mountain differ from those at these other heater tests: the rock mass of the repository units at Yucca Mountain is heavily fractured volcanic tuff, while the other experiments have been conducted in sparsely fractured granitic rock. In relation to other fractured rock sites, the rock mass at Yucca Mountain is relatively homogenous (ubiquitously fractured), with much less spatial variability in rock mass mechanical and hydrologic properties. This is especially evident for hydraulic permeability, which at sparsely fractured sites generally ranges over 6 orders of magnitude, whereas the permeability at each rock unit at Yucca Mountain generally spans less than 3 orders of magnitude. A continuum model approach is shown to be appropriate for the analysis of thermal-hydrologic-mechanical processes because the rock mass at Yucca Mountain is ubiquitously fractured, forming a dense, well-connected fracture network for fluid flow. This is

the main reason why the drift-scale thermal-hydrologic-mechanical model consistently captures relevant thermal-hydrologic-mechanical responses at Yucca Mountain.



Source: BSC 2004b, Figure 7.10-1.

NOTE: The shaded area between solid lines represents observed responses of most experimental data during the heating phase of the DST (e.g., Figure G-15). The shaded area between dashed lines represents possible responses during the ongoing cooling phase. Thus, these are not simulation results nor an exact representation of the field data.

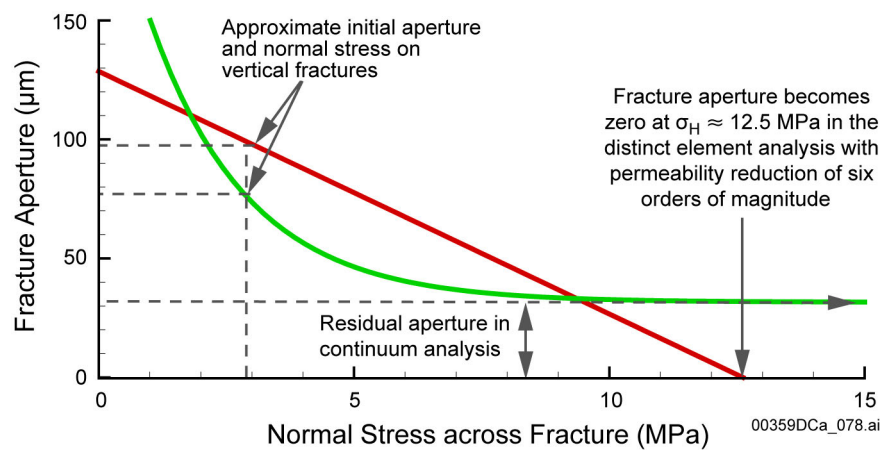
Figure G-26. Concepts of Possible Evolution of Air Permeability at the Drift Scale Test Showing the Expected Responses for the Case of (a) Elastic Fully Reversible Rock Mass Behavior and (b) Inelastic Irreversible Rock Mass Behavior

The comprehensive model validation provided in *Drift Scale THM Model* (BSC 2004b, Section 7) shows that the adopted continuum model can capture relevant thermal-hydrologic-mechanical processes and that the underlying conceptual model is sound. In particular, analysis of the DST shows that the conceptual model for stress versus permeability coupling is capable of capturing the observed changes in permeability. The fracture normal stress versus permeability relationship is the most important aspect of this analysis. This relationship (discussed in Section G.4.2.6) is the key to an accurate assessment of possible stress-induced changes in hydraulic properties at the repository. The relationship provides limits for how much permeability can decrease or increase from the impact of stresses. Other aspects or sources of uncertainties, such as conceptualization of the fracture network (BSC 2004b, Section 6.10.1), possible inelastic mechanical responses near the drift wall (BSC 2004b, Section 6.10.2), and even possible shear slip (BSC 2004b, Section 6.10.3), are of minor importance compared to the limits of the stress versus permeability relationship. If these limits are correctly determined, then an accurate prediction of the main coupled thermal-hydrologic-mechanical processes is expected. In this study, the upper and lower limits of the normal stress versus permeability function were determined and validated against field experiments at a relevant drift scale. The stress versus permeability function adopted for the predictive analysis of the drift-scale thermal-hydrologic-mechanical model (BSC 2004b, Section 6) is a conservative one, in the sense that it tends to result in larger permeability changes and, hence, has a larger impact on the percolation flux. The comprehensive validation (BSC 2004b, Section 7) establishes a sound technical basis for parameters used to assess thermal-mechanical effects on hydrologic properties and flow fields at Yucca Mountain.

G.4.4 GEN 1.01 (Comment 83): Comparison of Distinct Element and Continuum Modeling Analysis (1)

As mentioned above, a 6-order-of-magnitude decrease in permeability was estimated for most vertical fractures from 55 years to more than 1,000 years in the distinct element analysis presented in *FY 01 Supplemental Science and Performance Analyses, Volume 1: Scientific Bases and Analyses* (BSC 2001a, Section 4.3.7). In GEN 1.01 (Comment 83), NRC remarked that it is not obvious how this amount of change would be included in the original distribution of permeability. However, as pointed out above, the 6 order-of-magnitude decrease in fracture permeability calculated from the earlier distinct element analysis originally calculated in *Coupled Thermal-Hydrologic-Mechanical Effects on Permeability Analysis and Models Report* (BSC 2001b, Section 6.3.3) is an artifact of an unsubstantiated assumed relationship between normal stress and fracture permeability. The relationship between normal stress and fracture permeability adopted for the distinct element analysis resulted in overstating the fracture permeability because it did not consider residual fracture permeability at high fracture normal stress. It is well known, from numerous laboratory and field experiments, that even if fractures are compressed with a high stress across the fracture planes, the fractures are still open to conduct water flow in voids between fracture surface contacts (Rutqvist and Stephansson 2003, p. 15). According to the most recent analysis documented in *Drift Scale THM Model* (BSC 2004b, Sections 6.5.5, 6.6.2, and 6.7.3), the permeability decreases in vertical fractures within the repository units are limited to a change of within 2 orders of magnitude of their original values. Observations and model validation against the DST show that thermal-mechanical-induced reductions in permeability during heating are limited to within 1 order of magnitude of the original (preheating) values.

Figure G-27 shows a comparison of the relationship between normal stress and aperture used for fractures in the distinct element analysis (BSC 2001b) and the relationship adopted in the most recent continuum analysis (BSC 2004b). It is shown that the linear relationship between normal stress and aperture used in the distinct element analysis of *Coupled Thermal-Hydrologic-Mechanical Effects on Permeability Analysis and Models Report* (BSC 2001b) results in a complete fracture closure and zero permeability at a normal stress of about 12.5 MPa. Such a relationship between normal stress and aperture is unrealistic and cannot be used to reproduce permeability changes observed in the DST. On the other hand, in the continuum analysis (BSC 2004b), a residual aperture is defined into the normal stress versus aperture relationship of fractures that ensures that water flows along fractures even at a high normal stress. The stress versus aperture relationship and the resulting stress versus permeability function used in the continuum analysis have been extensively validated against air-permeability measurements at the DST (BSC 2004b, Section 7).



Source: Rutqvist 2004, Figure 103.

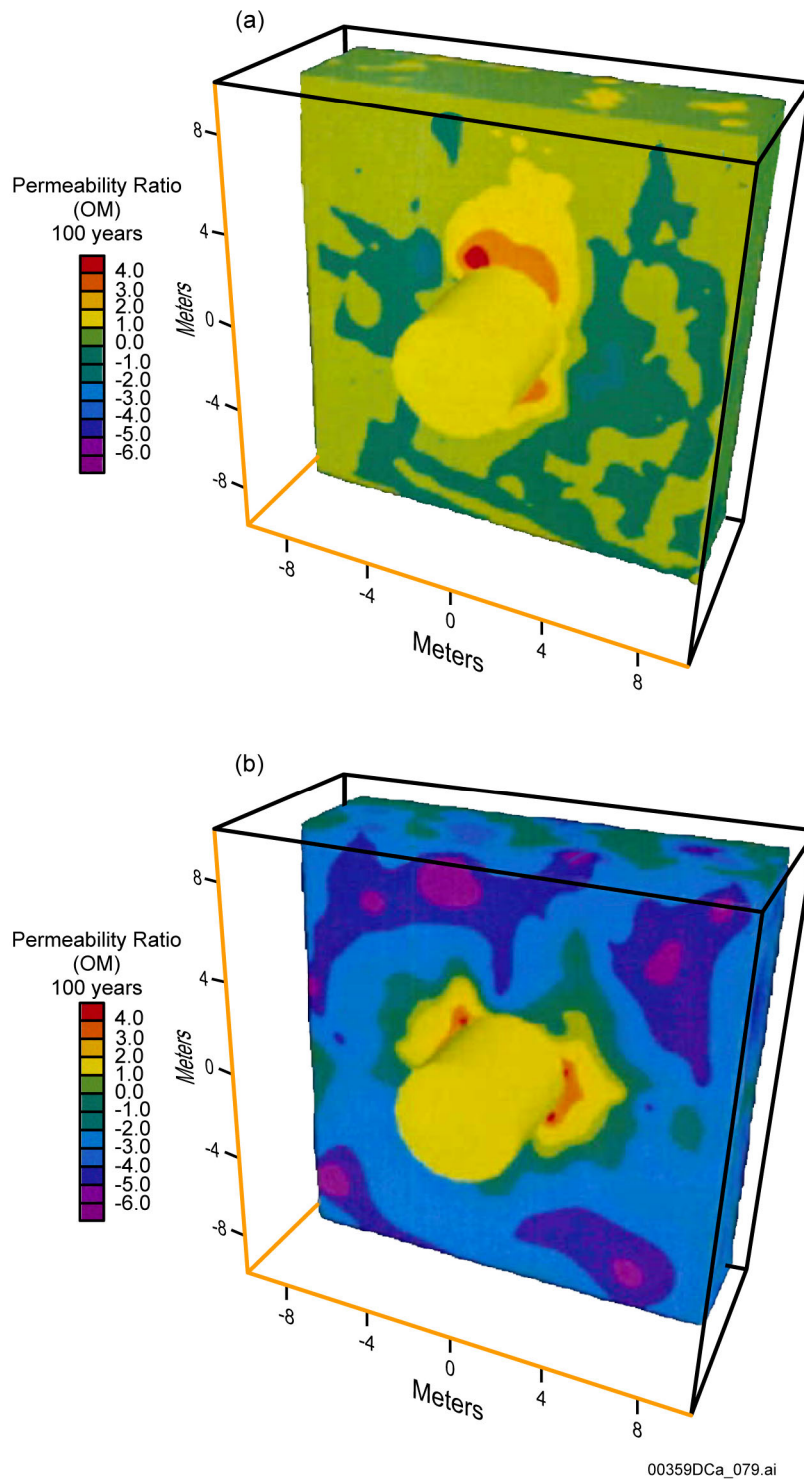
Figure G-27. Comparison of Stress Versus Aperture Relationship Used in the Distinct Element Analysis and the Recent Continuum Analysis

In summary, the discrepancy in calculated permeability between the discrete element and continuum analyses in *FY 01 Supplemental Science and Performance Analyses, Volume 1: Scientific Bases and Analyses* (BSC 2001a, Section 4.3.7) was not a result of using different modeling approaches but rather a result of different relationships between stress and fracture aperture used in the two analyses. In fact, the two analyses consistently predict a reduction in permeability for vertical fractures (except near the side wall of the drift, where both analyses predict increased permeability for vertical fractures) and essentially no change in permeability for horizontal fractures (except near the crown of the drift, where both analyses predict increased permeability for horizontal fractures). The comparison of the two analyses for permeability changes at the drift wall (at the side wall and the crown of the drift) is discussed in more detail in Section G.4.5.

G.4.5 GEN 1.01 (Comment 97): Comparison of Distinct Element and Continuum Modeling Analysis (2)

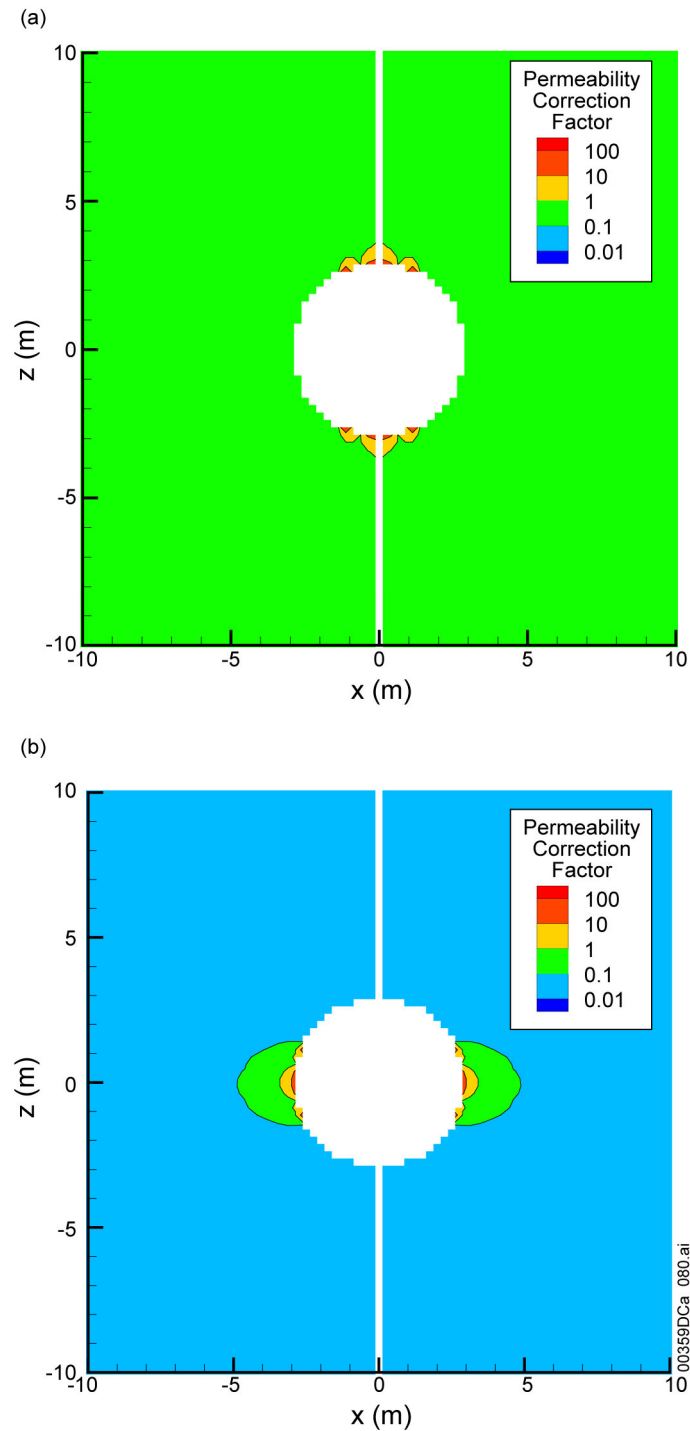
As mentioned above, in *FY 01 Supplemental Science and Performance Analyses, Volume 1: Scientific Bases and Analyses* (BSC 2001a) there was an apparent disagreement between results from the distinct element analysis and the continuum analysis regarding predicted permeability changes near the drift wall. In GEN 1.01 (Comment 97), NRC remarked that this appears to be the area of the problem that should cause the most concern, due to its influence on seepage. The apparent disagreement was observed by comparing the permeability ratio at 55 years in the distinct element analysis (BSC 2001a, Figure 4.3.7-1) with the permeability changes at 10 and 1,000 years in the continuum analysis (BSC 2001a, Figures 4.3.7-12 to 4.3.7-15). However, the comparison of these figures is not very clear, because the figures are at different scales and do not show the same parameters. One figure (BSC 2001a, Figure 4.3.7-1) shows an overall mean permeability change, while others (BSC 2001a, Figures 4.3.7-12 to 4.3.7-15) show changes partitioned as permeability in horizontal and vertical fractures. In the most recent revision of *Coupled Thermal-Hydrologic-Mechanical Effects on Permeability Analysis and Models Report* (BSC 2001b), the output results of the distinct element analysis are partitioned into permeability changes in horizontal and vertical fractures. Figures G-28 and G-29 present results of estimated permeability changes in the distinct element analysis and in the recent TOUGH-FLAC continuum analysis (BSC 2004b), respectively. Both figures present changes in permeability of vertical and horizontal fractures at 100 years. These figures show that both analyses consistently predict a reduction in permeability of vertical fractures on top of the drift and an increase in vertical permeability in the sidewall of the drift. Furthermore, both analyses consistently predict an increased permeability of horizontal fractures on the top of the drift and a decreased permeability of horizontal fractures in the sidewall of the drift. As noted in Section G.4.4, the distinct element analysis predicts a larger magnitude of permeability changes as an artifact of an unsubstantiated assumed relationship between normal stress and fracture permeability. The relationship between normal stress and fracture permeability adopted for the distinct element analysis resulted in overstating the fracture permeability because it did not consider residual fracture permeability at high fracture normal stress. However, the basic responses of fracture opening and fracture closure at different locations around the drift wall is consistent between the two analyses. The only exception might be cases in which the distinct element analysis produces large displacements in loose rock block near the drift wall. Such loose blocks were predicted in the distinct element analysis at the sidewall of the drift. This is shown in Figure G-28 as local zones of red contours with an additional increase in permeability.

The comparison of thermal-mechanical-induced permeability changes, with potential influence on seepage, calculated with the distinct element analysis and the continuum analysis is summarized in Figure G-30. For seepage of water into the drift, permeability changes on top of the drift are most relevant. It is clear that both approaches predict a decrease in vertical permeability and an increase in horizontal permeability on top of the drift. Generally, a decrease in vertical permeability and an increase in horizontal permeability indicate that water will be more easily diverted around the drift and, thus, be less likely to enter the drift. The reduced potential for seepage as a result of such thermally induced changes in vertical and horizontal permeability has also been shown in *Seepage Model for PA Including Drift Collapse* (BSC 2003a, Section 6.7).



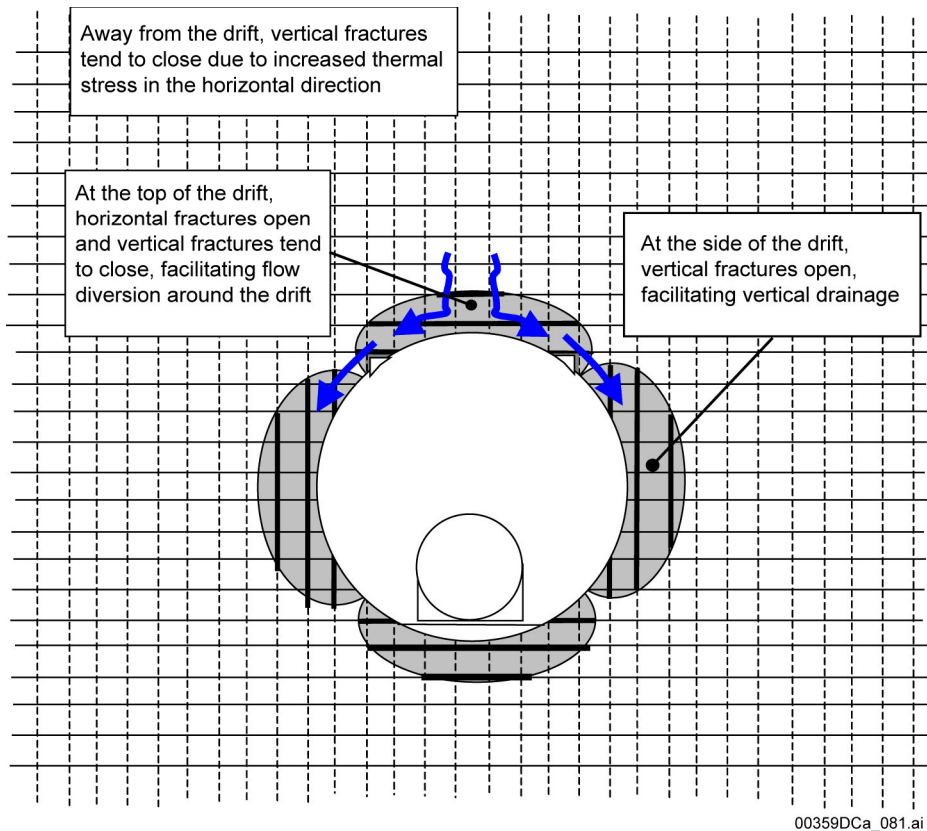
Source: BSC 2001b, Figures 6.3.3-14 and 6.3.3-15.

Figure G-28. Results of Distinct Element Thermal-Hydrologic-Mechanical Analysis Showing Order-of-Magnitude for Permeability Correction Factor Relative to Preexcavation Permeability around an Emplacement Drift in the Tptpmn Unit for Permeability Ratios for (a) Horizontal and (b) Vertical Fractures at 100 years after Waste Emplacement



Source: Rutqvist 2004, Figure 104.

Figure G-29. Results of a TOUGH-FLAC Continuum Thermal-Hydrologic-Mechanical Analysis Showing Permeability Correction Factor to Preexcavation Permeability around an Emplacement Drift in the Tptpmn Unit for (a) Permeability of Horizontal Fractures and (b) Permeability of Vertical Fractures at 100 years after Waste Emplacement



00359DCa_081.ai

Figure G-30. Summary of Estimated Changes in Fracture Permeability around a Drift in the Tptpmn Unit as a Result of Distinct Element and Continuum Analyses

G.4.6 Summary

This appendix provides responses for KTI agreements RDTME 3.20, RDTME 3.21, and GEN 1.01 (Comments 83 and 97). These agreements are concerned with providing analyses related to thermal-mechanical effects on fracture permeability. Since these agreements were made in 2001, a significant amount of additional work has been performed and documented in other reports that address these issues. The responses to each agreement are summarized as follows:

- **RDTME 3.20:** Sensitivity analyses have been performed and concerns about boundary conditions and flow diversion from the pillar region toward the drift have been resolved as a result of recent revisions and enhancements to the coupled thermal-hydrologic-mechanical-processes analysis at Yucca Mountain. A bounding analysis shows that effects of thermal-mechanically induced changes in permeability on the unsaturated zone flow field are small and observable only near the emplacement drifts. The predicted changes in permeability (one to 2 orders of magnitude) are within the permeability range (4 orders of magnitude) already considered in the seepage analysis (BSC 2003a, Figure 6-4).
- **RDTME 3.21:** The additional agreed-upon validation has been conducted for recent revisions to, and enhancements of, the coupled thermal-hydrologic-mechanical process

analysis at Yucca Mountain. The comprehensive model validation provided in *Drift Scale THM Model* (BSC 2004b, Section 7) shows that the current coupled thermal-hydrologic-mechanical models developed for the repository at Yucca Mountain can capture relevant thermal-hydrologic-mechanical processes and that the underlying conceptual model is sound.

- **GEN 1.01 (Comment 83):** The 6-order-of-magnitude decrease in fracture permeability calculated from the earlier distinct element analysis is an artifact of an unsubstantiated assumed relationship between normal stress and fracture permeability. The relationship between normal stress and fracture permeability adopted for the distinct element analysis resulted in overstating the fracture permeability because it did not consider residual fracture permeability at high fracture normal stress. Current estimates show that permeability will not decrease more than 2 orders of magnitude and is unlikely to decrease more than 1 order of magnitude. Again, the current estimates of thermal-mechanically induced permeability changes (one to 2 orders of magnitude) are within the permeability range (4 orders of magnitude) already considered in the seepage analysis (BSC 2003a, Figure 6-4).
- **GEN 1.01 (Comment 97):** The apparent contradictory results between the distinct element analysis and continuum analysis regarding calculated permeability at the drift wall is partly caused by a misconception stemming from a comparison of two different types of permeability changes. A closer examination shows that, in general, the distinct element and continuum analyses produce consistent results regarding permeability changes around an emplacement drift. The fact that the current model produces results that are consistent with an alternative conceptual model provides additional confidence that the current coupled thermal-hydrologic-mechanical model is appropriate for evaluating the impact of thermal-mechanical effects on permeability and the flow field at Yucca Mountain.

The information in this appendix is responsive to agreements RDTME 3.20, RDTME 3.21, and GEN 1.01 (Comments 83 and 97) made between DOE and NRC. The report contains the information that DOE considers necessary for NRC review for closure of these agreements.

G.5 REFERENCES

- Björnsson, G. and Bodvarsson, G. 1990. "A Survey of Geothermal Reservoir Properties." *Geothermics*, 19, (1), 17–27. New York, New York: Pergamon Press. TIC: 249741.
- Bodvarsson, G., MacKinnon, R., Hardin, E. and Blair, S. 2001. *Subissue 3, Thermal-Mechanical Effects on Underground Facility Design and Performance – Component 3, Thermal Effects on Flow into Emplacement Drifts*. Presentation at U.S. Nuclear Regulatory Commission/U.S. Department of Energy Technical Exchange and Management Meeting on Repository Design and Thermal-Mechanical Effects, February 6 through 8, 2001. ACC: MOL.20010307.0520.

BSC (Bechtel SAIC Company) 2001a. *FY 01 Supplemental Science and Performance Analyses, Volume 1: Scientific Bases and Analyses*. TDR-MGR-MD-000007 REV 00 ICN 01. Las Vegas, Nevada: Bechtel SAIC Company. ACC: MOL.20010801.0404; MOL.20010712.0062; MOL.20010815.0001.

BSC 2001b. *Coupled Thermal-Hydrologic-Mechanical Effects on Permeability Analysis and Models Report*. ANL-NBS-HS-000037 REV 00. Las Vegas, Nevada: Bechtel SAIC Company. ACC: MOL.20010822.0092.

BSC 2001c. *Thermal Tests Thermal-Hydrological Analyses/Model Report*. ANL-NBS-TH-000001 REV 00 ICN 02. Las Vegas, Nevada: Bechtel SAIC Company. ACC: MOL.20011116.0025.

BSC 2002. *Thermal Testing Measurements Report*. ANL-NBS-HS-000041 REV 00. Las Vegas, Nevada: Bechtel SAIC Company. ACC: MOL.20021004.0314.

BSC 2003a. *Seepage Model for PA Including Drift Collapse*. MDL-NBS-HS-000002 REV 02. Las Vegas, Nevada: Bechtel SAIC Company. ACC: DOC.20030709.0001.

BSC 2003b. *In Situ Field Testing of Processes*. ANL-NBS-HS-000005 REV 02. Las Vegas, Nevada: Bechtel SAIC Company. ACC: DOC.20031208.0001.

BSC 2003c. *Drift-Scale Coupled Processes (DST and TH Seepage) Models*. MDL-NBS-HS-000015 REV 00C. Las Vegas, Nevada: Bechtel SAIC Company. ACC: MOL.20030910.0160.

BSC 2004a. *Abstraction of Drift Seepage*. MDL-NBS-HS-000019 REV 00 ICN 01, with errata. Las Vegas, Nevada: Bechtel SAIC Company. ACC: DOC.20031112.0002; DOC.20040223.0001.

BSC 2004b. *Drift Scale THM Model*. MDL-NBS-HS-000017 REV 00 ICN 01, with errata. Las Vegas, Nevada: Bechtel SAIC Company. ACC: DOC.20031014.0009; DOC.20040223.0002.

BSC 2004c. *Mountain-Scale Coupled Processes (TH/THC/THM)*. MDL-NBS-HS-000007 REV 01, with errata. Las Vegas, Nevada: Bechtel SAIC Company. ACC: DOC.20031216.0003; DOC.20040211.0006.

BSC 2004d. *Drift Degradation Analysis*. ANL-EBS-MD-000027 REV 02, with errata. Las Vegas, Nevada: Bechtel SAIC Company. ACC: DOC.20040325.0002; DOC.20030709.0003.

BSC 2004e. *Drift-Scale Coupled Processes (DST and THC Seepage) Models*. MDL-NBS-HS-000001 REV 02, with errata. Las Vegas, Nevada: Bechtel SAIC Company. ACC: DOC.20030804.0004; DOC.20040219.0002.

Chan, T.; Binnall, E.; Nelson, P.; Stolzman, R.; Wan, O.; Weaver, C.; Ang, K.; Braley, J.; and McEvoy, M. 1980. *Thermal and Thermomechanical Data from In Situ Heater Experiments at Stripa, Sweden*. LBL-11477. Berkeley, California: Lawrence Berkeley Laboratory. TIC: 211543.

CRWMS M&O 1997a. *Drift Scale Test Design and Forecast Results*. BAB000000-01717-4600-00007 REV 01. Las Vegas, Nevada: CRWMS M&O. ACC: MOL.19980710.0155.

CRWMS M&O 1997b. *Ambient Characterization of the Drift Scale Test Block*. BADD00000-01717-5705-00001 REV 01. Las Vegas, Nevada: CRWMS M&O. ACC: MOL.19980416.0689.

CRWMS M&O 1997c. *Yucca Mountain Site Geotechnical Report*. B00000000-01717-5705-00043 REV 01. Two volumes. Las Vegas, Nevada: CRWMS M&O. ACC: MOL.19971017.0736; MOL.19971017.0737.

CRWMS M&O 1998a. *Geology of the Exploratory Studies Facility Topopah Spring Loop*. BAB000000-01717-0200-00002 REV 01. Las Vegas, Nevada: CRWMS M&O. ACC: MOL.19980415.0283.

CRWMS M&O 1998b. *Drift Scale Test As-Built Report*. BAB000000-01717-5700-00003 REV 01. Las Vegas, Nevada: CRWMS M&O. ACC: MOL.19990107.0223.

CRWMS M&O 1999. *Single Heater Test Final Report*. BAB000000-01717-5700-00005 REV 00 ICN 1. Las Vegas, Nevada: CRWMS M&O. ACC: MOL.20000103.0634.

Datta, R.; Barr, D.; and Boyle, W. 2003. "Measuring Thermal, Hydrologic, Mechanical and Chemical Responses in the Yucca Mountain Drift Scale Test." *GeoProc 2003, International Conference on Coupled T-H-M-C Processes in Geo-Systems: Fundamentals, Modelling, Experiments & Applications, Stockholm, Sweden, October 13–15, 2003*. Stephansson, O.; Hudson, J.A.; and Jing, L., eds. Part I, 141–146. Stockholm, Sweden: Royal Institute of Technology. TIC: 256086.

Green, R.T. and Painter, S. 2003. "Numerical Simulation of Thermal-Hydrologic Processes Observed at the Drift-Scale Heater Test at Yucca Mountain, Nevada." *GeoProc 2003, International Conference on Coupled T-H-M-C Processes in Geo-Systems: Fundamentals, Modelling, Experiments & Applications, Stockholm, Sweden, October 13–15, 2003*. Stephansson, O.; Hudson, J.A.; and Jing, L., eds. Part I, 161–166. Stockholm, Sweden: Royal Institute of Technology. TIC: 256088.

Hardin, E.L. and Chesnut, D.A. 1997. *Synthesis Report on Thermally Driven Coupled Processes*. Milestone SPL8BM4. Livermore, California: Lawrence Livermore National Laboratory. ACC: MOL.19980113.0395.

Hsiung, S.M.; Chowdhury, A.H.; and Nataraja, M.S. 2003. "Thermal-Mechanical Modeling of a Large-Scale Heater Test." *GeoProc 2003, International Conference on Coupled T-H-M-C Processes in Geo-Systems: Fundamentals, Modelling, Experiments & Applications, Stockholm, Sweden, October 13–15, 2003*. Stephansson, O.; Hudson, J.A.; and Jing, L., eds. Part I, 153–159. Stockholm, Sweden: Royal Institute of Technology. TIC: 256090.

Jackson, C.P.; Hoch, A.R.; and Todman, S. 2000. "Self-Consistency of a Heterogeneous Continuum Porous Medium Representation of a Fractured Medium." *Water Resources Research*, 36, (1), 189–202. Washington, D.C.: American Geophysical Union. TIC: 247466.

- Millard, A. and Rutqvist, J. 2003. “Comparative Analyses of Predicted and Measured Displacements during the Heating Phase of the Yucca Mountain Drift Scale Test.” *GeoProc 2003, International Conference on Coupled T-H-M-C Processes in Geo-Systems: Fundamentals, Modelling, Experiments & Applications, Stockholm, Sweden, October 13–15, 2003*. Stephansson, O.; Hudson, J.A.; and Jing, L., eds. Part I, 147–152. Stockholm, Sweden: Royal Institute of Technology. TIC: 256089.
- Nelson, P.H.; Rachiele, R.; Remer, J.S.; and Carlsson, H. 1981. *Water Inflow into Boreholes During the Stripa Heater Experiments*. LBL-12574. Berkeley, California: Lawrence Berkeley Laboratory. TIC: 228851.
- NRC (U.S. Nuclear Regulatory Commission) 2002. *Integrated Issue Resolution Status Report*. NUREG-1762. Washington, D.C.: U.S. Nuclear Regulatory Commission, Office of Nuclear Material Safety and Safeguards. TIC: 253064.
- Olivella, S.; Gens, A.; and Gonzales, C. 2003. “THM Analysis of a Heater Test in a Fractured Tuff.” *GeoProc 2003, International Conference on Coupled T-H-M-C Processes in Geo-Systems: Fundamentals, Modelling, Experiments & Applications, Stockholm, Sweden, October 13–15, 2003*. Stephansson, O.; Hudson, J.A.; and Jing, L., eds. Part I, 167–172. Stockholm, Sweden: Royal Institute of Technology. TIC: 256091.
- Paulsson, B.N.P.; King, M.S.; and Rachiele, R. 1980. *Ultrasonic and Acoustic Emission Results from the Stripa Heater Experiments*. Parts I & II. LBL-10975. Berkeley, California: Lawrence Berkeley National Laboratory. TIC: 211547.
- Reamer, C.W. 2001a. *U.S. Nuclear Regulatory Commission/U.S. Department of Energy Technical Exchange and Management Meeting on Repository Design and Thermal-Mechanical Effects, February 6 through 8, 2001*. Letter from C.W. Reamer (NRC) to S. Brocoum (DOE/YMSCO), February 28, 2001, with enclosure. ACC: MOL.20010814.0172.
- Reamer, C.W. 2001b. *U.S. Nuclear Regulatory Commission/U.S. Department of Energy Technical Exchange and Management Meeting on Range of Operating Temperatures (September 18-19, 2001)*. Letter from C.W. Reamer (NRC) to S. Brocoum (DOE) October 2, 2001, 1018010176, with enclosures. ACC: MOL.20020102.0138.
- Rejeb, A. 1996. “Mathematical Simulations of Coupled THM Processes of Fanay-Augères Field Test by Distinct Element and Discrete Finite Element Methods.” *Developments in Geotechnical Engineering*, 79, 341–368. New York, New York: Elsevier. TIC: 254247.
- Rutqvist, J. 2002. UZ AMRs for SR - Thermal-Hydrological-Mechanical Effects (YMP-LBNL-JR-1). Scientific Notebook SN-LBNL-SCI-204-V1. ACC: MOL.20020701.0135; MOL.20020724.0607.
- Rutqvist, J. 2004. UZ AMRs - Thermal-Hydrological-Mechanical Effects (YMP-LBNL-JR-2). Scientific Notebook SN-LBNL-SCI-204-V2. ACC: MOL.20040513.0119.

Rutqvist, J.; Börgesson, L.; Chijimatsu, M.; Nguyen, T.S.; Jing, L.; Noorishad, J.; and Tsang, C.-F. 2001. “Coupled Thermo-Hydro-Mechanical Analysis of a Heater Test in Fractured Rock and Bentonite at Kamaishi Mine—Comparison of Field Results to Predictions of Four Finite Element Codes.” *International Journal of Rock Mechanics and Mining Sciences*, 38, (1), 129–142. New York, New York: Pergamon. TIC: 254246.

Rutqvist, J. and Stephansson, O. 2003. “The Role of Hydromechanical Coupling in Fractured Rock Engineering.” *Hydrogeology Journal*, 11, (1), 7-40. New York, New York: Springer-Verlag. TIC: 254245.

Rutqvist, J. and Tsang, C.-F. 2002. “A Study of Caprock Hydromechanical Changes Associated with CO₂-Injection into a Brine Formation.” *Environmental Geology*, 42, (2–3), 296–305. New York, New York: Springer-Verlag. TIC: 254244.

Rutqvist, J. and Tsang, C.-F. 2003. “Analysis of Thermal-Hydrologic-Mechanical Behavior Near an Emplacement Drift at Yucca Mountain.” *Journal of Contaminant Hydrology*, 62–63, 637–652. New York, New York: Elsevier. TIC: 254205.

Rutqvist, J.; Tsang, C.-F.; and Tsang, Y. 2004. “Analysis of Stress- and Moisture-Induced Changes in Fractured Rock Permeability at the Yucca Mountain Drift Scale Test.” *GeoProc 2003, International Conference on Coupled T-H-M-C Processes in Geo-Systems: Fundamentals, Modelling, Experiments & Applications, Stockholm, Sweden, October 13–15, 2003*. Stephansson, O.; Hudson, J.A.; and Jing, L., eds. Part I, 147–152. Stockholm, Sweden: Royal Institute of Technology. TIC: 256087

Rutqvist, J.; Wu, Y.-S.; Tsang, C.-F.; and Bodvarsson, G. 2002. “A Modeling Approach for Analysis of Coupled Multiphase Fluid Flow, Heat Transfer, and Deformation in Fractured Porous Rock.” *International Journal of Rock Mechanics and Mining Sciences*, 39, (4), 429–442. New York, New York: Pergamon. TIC: 253953.

Sobolik, S.R.; Finley, R.E.; and Ballard, S. 1999. “Thermal-Mechanical Measurements in the Drift Scale Test, Yucca Mountain, Nevada.” *Rock Mechanics for Industry, Proceedings of the 37th U.S. Rock Mechanics Symposium, Vail, Colorado, USA, 6-9 June, 1999*. Amadei, B.; Kranz, R.L.; Scott, G.A.; and Smeallie, P.H.; eds. 2, 735–742. Brookfield, Vermont: A.A. Balkema. TIC: 245246.

Wagner, R.A.; Ballard, S.; Blair, S.C.; and Mukhopadhyay, S. 2001. “A Methodology for Validation of Process Models Used to Simulate Thermal Tests at Yucca Mountain.” *Rock Mechanics in the National Interest, Proceedings of the 38th U.S. Rock Mechanics Symposium, DC Rocks 2001, Washington, D.C., USA, 7-10 July 2001*. Elsworth, D.; Tinucci, J.P.; and Heasley, K.A.; eds. Volume 1. Pages 631–636. Exton, Pennsylvania: A.A. Balkema. TIC: 250864.

Wang, J.S. 2003. “Scientific Notebook Referenced in Model Report U0250, Drift Scale THM Model MDL-NBS-HS-000017 REV 00.” Correspondence from J.S. Wang (BSC) to File, April 28, 2003, with attachment. ACC: MOL.20030505.0160.

Zimmerman, R.M.; Blanford, M.L.; Holland, J.F.; Schuch, R.L.; and Barrett, W.H. 1986. *Final Report, G-Tunnel Small-Diameter Heater Experiments*. SAND84-2621. Albuquerque, New Mexico: Sandia National Laboratories. ACC: HQS.19880517.2365.

INTENTIONALLY LEFT BLANK